ELECTROMAGNETIC RADIATION AND SCATTERING IN A PLASMA WITH AN AZIMUTHAL BIASING FIELD

Thesis by

Larry Warne

In Partial Fulfillment of the Requirements

for the Degree of

Doctor of Philosophy

California Institute of Technology

Pasadena, California

1984

(Submitted December 5, 1983)

ACKNOWLEDGEMENTS

I would like to express my sincere gratitude to my advisor, Professor Charles Herach Papas, for his guidance, encourgement and support during the course of this work. I would also like to thank Dr. Nader Engheta for many helpful discussions regarding the contents.

I would like to acknowledge and extend my thanks to Ms. Janice L. Tucker for her careful typing of the manuscript.

ABSTRACT

The problem of radiation from an electric line source in a homogeneous, cold, incompressible electron plasma is considered when a large static current is superposed. The static axial current gives rise to a magnetostatic biasing field which is oriented in the azimuthal direction and varies with radial distance. When the driving frequency is greater than the plasma frequency, and the medium is assumed to be unbounded, the presence of the static current reduces the amount of radiation. On the other hand, if the driving frequency is less than the plasma frequency and the medium is assumed to be bounded, the amount of radiation is increased.

The problem of scattering from an axial current in a plasma is also considered. The medium in this problem is taken to be a bounded column of plasma containing a radially distributed axial current. At normal incidence the scattered wave contains a cross polarized field component due to the gyrotropic nature of the column. The scattered cross polarized component vanishes in the incident direction as well as in the backward direction. This null is explained by considering the effect of Faraday rotation on various rays traversing the column. Solutions to the scattering problem when the axial current density varies inversely with radial distance are considered in some detail. This case is labeled "homogeneous" since the dielectric tensor does not vary with radial distance and the resulting field equations are thus simplified. The field behavior in the vicinity of the origin is also considered in detail since phenomena similar to those encountered in wedge type media (unbounded fields) occur.

TABLE OF CONTENTS

CHAPTER 1

INTRODUCTION

Investigations of the propagation of electromagnetic waves in the ionospheric plasma as well as other astrophysical plasmas have resulted in a great body of knowledge concerning propagation in plane stratified gyroelectric media [1,2]. Furthermore, interest in controlled thermonuclear fusion, particle beams, and bounded plasmas in general has resulted in numerous investigations of electromagnetic interaction with cylindrical plasmas containing axial biasing fields [3], including scattering at oblique incidence [4]. The added complication of radial stratification has also been treated [5,6]. The work presented here is concerned with the case when the direction of the biasing field does not coincide with a cartesian coordinate but instead is purely azimuthal. Such a situation arises when an axial static current is present.

Chapters 2, 3, and 4 discuss the radiation problem. The static current in this case is confined to a filamentary wire and a small dynamic component of current is superposed. Figure 1 depicts the radiation problem. The static current generates a magnetostatic field which varies inversely with radial distance. The presence of the static current thus influences the properties of the surrounding plasma medium. We take the plasma density to be constant and treat the plasma as being cold and incompressible. Since the dynamic current component is small we may treat the plasma in the usual linear approximation [7]. A dielectric tensor may therefore be determined to describe the electrical

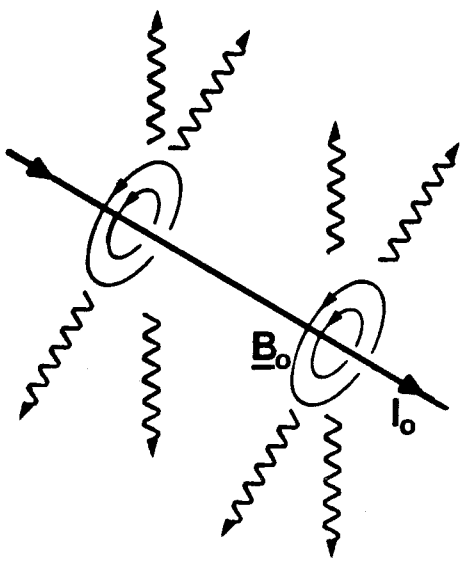

Fig. 1. A wire carrying a large static current, I_o, is immersed in a cold homogeneous plasma. A small dynamic current component is superposed and radiates into the resulting anisotropic medium.

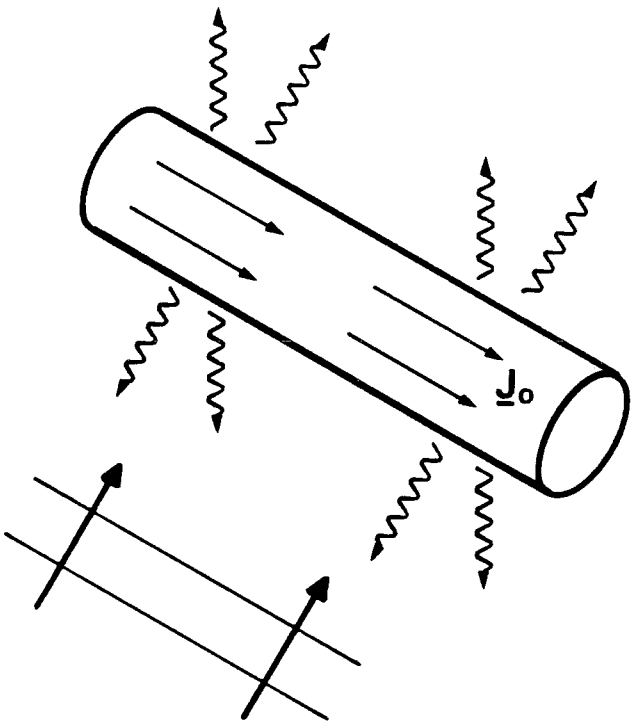

Fig. 2. A plane electromagnetic wave scattering off of a column of plasma carrying a strong axial static current, $\underline{J}_o$, which biases the plasma.

characteristics of the medium. The variation of the magnetostatic field results in a medium which becomes uniaxial in the vicinity of the wire, gyrotropic in the intermediate region, and isotropic at very large distances. The formulation of the radiation problem is given in Chapter 2. The dielectric tensor is determined and used in Maxwell's equations to yield an equation for the axial component of the dynamic electric field. The problem is one dimensional and the equation for the axial field is shown to be a confluent form of Heun's differential equation [8]. Heun's equation is also of current interest in planar inhomogeneous plasmas [9]. We define a transmission and reflection coefficient for the medium. The solution of the equation is given in Chapter 3 and is similar to that of the spheroidal wave equation [10]. This solution is compared to a direct numerical integration of the equation and the WKB approximate solution. Chapter 4 presents the results of the radiation problem. When the plasma is unbounded, as for example in the case of a long wire antenna in the ionosphere, and a large static current is induced, the radiation is reduced. When the plasma is bounded, such as the wake of a reentering space vehicle [11], and the driving frequency is below the plasma frequency a static current (or low frequency current) on a trailing wire antenna can increase the radiation.

Chapters 5, 6, and 7 discuss the scattering problem. The static current in this case is taken in general to be distributed radially. A plane electromagnetic wave is normally incident on a bounded column of plasma containing the axial currents. Figure 2 depicts the scattering problem. Such a medium resembles, for example, a portion of a lightning

stroke [12], or certain fusion devices [13]. The formulation of the scattering problem is given in Chapter 5. The dielectric tensor of Chapter 2 when substituted into Maxwell's equations leads to coupled equations. The problem is two dimensional since all quantities are independent of the axial coordinate. The field components are expanded in a Fourier series in the azimuthal variable reducing the problem to a coupled pair of ordinary differential equations in the axial electric and magnetic fields. A matrix reflection coefficient is defined which gives the fields in the external region. Chapter 6 considers the solution of the scattering problem. For general inhomogeneous columns, including variable plasma density, a matrix Riccati equation satisfied by the matrix reflection coefficient is determined. This equation is determined by the method of invariant imbedding [14], which has been used in cylindrical isotropic problems [15] and is extended to this gyrotropic case. The case of axial current density inversely proportional to radius gives rise to a uniform magnetostatic field. This case is labeled as "homogeneous" since the dielectric tensor becomes independent of radial distance. The solution of this "homogeneous" case is also considered in Chapter 6. Chapter 7 presents the results of the scattering problem. A cross polarized component of the scattered field exists which has a null on the axis defined by the incident wave. These results are explained in terms of Faraday rotation.

For the most part, the radiation problem, covered in Chapters 2, 3, and 4, and the scattering problem, covered in Chapters 5, 6, and 7, can be read independently. Chapter 8 gives some general conclusions.

CHAPTER 2

FORMULATION OF RADIATION PROBLEM

Section A determines the dielectric tensor for a plasma with azimuthal biasing field. When substituted into Maxwell's equations an ordinary differential equation of the second order is obtained for the axial electric field. Section B gives the relevant boundary conditions and defines the reflection and transmission coefficients of the surrounding medium.

2A. The Dielectric Tensor and Maxwell's Equations

An infinitely long wire is immersed in a cold incompressible electron plasma. The wire carries a large static current of amplitude I_0. A cylindrical coordinate system (ρ, ϕ, z) is aligned so that the z axis coincides with the wire, Fig. 3.

The static electric current generates a static magnetic field $\underline{B}_0$

$$\underline{B}_0 = \frac{I_0 \mu_0}{2\pi\rho} \underline{e}_\phi \tag{2A.1}$$

where μ_0 is the permeability of free space and $\underline{e}_\phi$ is a unit vector in the ϕ direction. Now we must determine the dielectric tensor pertaining to this medium with magnetic biasing field $\underline{B}_0$. Following the notation in [7] the velocity of the plasma electrons, $\underline{v}$, can be determined from the force law

$$-in_e m\omega_0 \underline{v} = -n_e e(\underline{E} + \underline{v}\times\underline{B}_0) \tag{2A.2}$$

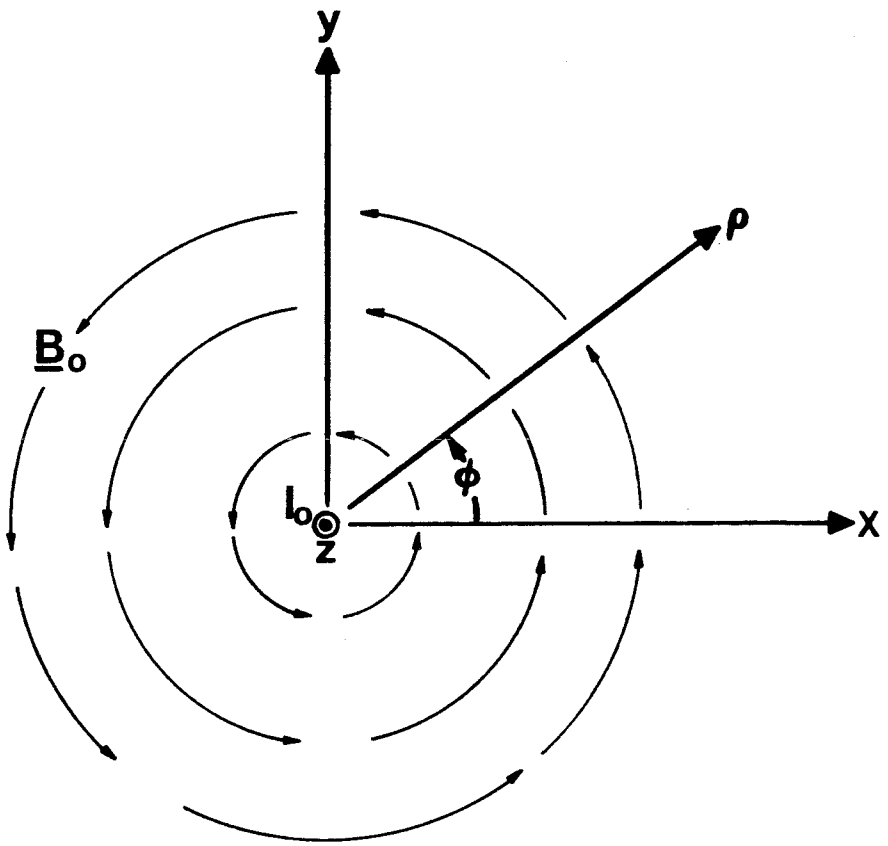

Fig. 3. A wire immersed in a plasma is coincident with the z axis and carries a large static current, I_o.

where i is the imaginary unit, n_e is the electron number density, e is the magnitude of the electron charge, m is the electron mass, $\underline{E}$ is the dynamic electric field of the wave;

$$\omega_o = \omega + i\omega_{eff} \tag{2A.3}$$

where ω is the dynamic temporal frequency; and ω_{eff}, is the effective collision frequency. All dynamic quantities are assumed time harmonic with variation $e^{-i\omega t}$. We have dropped nonlinear terms in the above force law since the dynamic fields are assumed weak. The current density is equal to

$$\underline{J} = - n_e e \underline{v} \tag{2A.4}$$

or using the above expression for $\underline{v}$

$$\underline{J} = -i\omega_o \frac{\varepsilon_o \omega_p^2}{(\omega_g^2-\omega_o^2)} \underline{E} + \frac{\varepsilon_o \omega_p^2}{(\omega_g^2-\omega_o^2)} \underline{E} \times \underline{\omega}_g - \frac{1}{i\omega_o} \frac{\omega_p^2 \varepsilon_o}{(\omega_g^2-\omega_o^2)} (\underline{E} \cdot \underline{\omega}_g) \underline{\omega}_g \tag{2A.5}$$

where $\omega_p^2 = n_e e^2/m\varepsilon_o$ is the plasma frequency and $\underline{\omega}_g = - \frac{e}{m} \underline{B}_o$ with the amplitude ω_g (to conform to notation this will be a negative quantity for electrons) being the electron gyrofrequency, and ε_o the permittivity of free space. The dyadic quantity $\underline{\underline{\varepsilon}}$ representing the dielectric properties of the medium can now be found from Maxwell's equation

$$\nabla \times \underline{H} = \underline{J} - i\omega\varepsilon_o \underline{E} = - i\omega \underline{\underline{\varepsilon}} \cdot \underline{E} \tag{2A.6}$$

which yields

$$\underline{\underline{\varepsilon}} = \begin{pmatrix} a & 0 & ig \\ 0 & b & 0 \\ -ig & 0 & a \end{pmatrix} \tag{2A.7}$$

where $a = \varepsilon_o\left(1 - \frac{\frac{\omega_p^2}{\omega}\omega_o}{\omega_o^2 - \omega_g^2}\right)$, $b = \varepsilon_o\left(1 - \frac{\omega_p^2}{\omega\omega_o}\right)$, $g = \frac{\omega_g\omega_p^2\varepsilon_o}{\omega(\omega_o^2 - \omega_g^2)}$,

and the ordering of components follows that of the cylindrical system (ρ, ϕ, z). The collision frequency, ω_{eff}, will be taken as a very small positive quantity in what follows. Indeed it is used only for mathematical purposes and will be allowed to approach zero in all results. Physical considerations will thus be limited to the collisionless case.

Using this dyadic description of the medium, Maxwell's equations become

$$\nabla x \underline{E} = i\omega\mu_o \underline{H} \tag{2A.8}$$

$$\nabla x \underline{H} = -i\omega \underline{\underline{\varepsilon}} \cdot \underline{E} \tag{2A.9}$$

which upon elimination of $\underline{H}$ becomes

$$\nabla x \nabla x \underline{E} = \omega^2 \mu_o \underline{\underline{\varepsilon}} \cdot \underline{E} \tag{2A.10}$$

The radiation problem is independent of the coordinates ϕ, z. Furthermore, we may ignore the TE configuration (H mode) with components E_ϕ, H_z, H_ρ since these components are not excited by the infinite line source. The equations of interest are then

$$0 = \omega^2 \mu_o (aE_\rho + igE_z) \tag{2A.11}$$

$$\frac{d^2E_z}{d\rho^2} + \frac{1}{\rho}\frac{dE_z}{d\rho} = -\omega^2\mu_o(aE_z - igE_\rho) \tag{2A.12}$$

Eliminating E_ρ yields

$$\frac{d^2E_z}{d\rho^2} + \frac{1}{\rho}\frac{dE_z}{d\rho} + \omega^2\mu_o\frac{a^2 - g^2}{a}E_z = o \tag{2A.13}$$

The above definitions of a and g allow the coefficient of E_z to be written as

$$\omega^2\mu_o\frac{a^2 - g^2}{a} = k_o^2\frac{\omega_o^2\left(1 - \frac{\omega_p^2}{\omega\omega_o}\right)^2 - \omega_g^2}{\omega_o^2\left(1 - \frac{\omega_p^2}{\omega\omega_o}\right) - \omega_g^2} \tag{2A.14}$$

where $k_o^2 = \omega^2\mu_o\varepsilon_o$ is the free space wave number.

The gyrofrequency, ω_g, is the variable quantity in this problem so we define

$$\omega_g = -\frac{\eta}{\rho} \tag{2A.15}$$

$$\eta = \frac{eI_o\mu_o}{2\pi m} \tag{2A.16}$$

Use of (2A.15) results in the ordinary differential equation

$$\frac{d^2E_z}{d\rho^2} + \frac{1}{\rho}\frac{dE_z}{d\rho} + k_1^2 \frac{k_1^2\rho^2 - q^2}{k_1^2\rho^2 - p^2} E_z = 0 \tag{2A.17}$$

where

$$p^2 = \frac{\eta^2}{c^2}\frac{\omega^2}{\omega_o^2}\ , \quad q^2 = p^2\Big/\left(1 - \frac{\omega_p^2}{\omega\omega_o}\right), \quad k_1^2 = k_o^2\left(1 - \frac{\omega_p^2}{\omega\omega_o}\right)\ ,$$

and k_1 is the wave number of an unbiased isotropic plasma.

2B. Boundary Conditions and Definition of Reflection and Transmission Coefficients

The asymptotic behavior of solutions to Eq. (2A.17) together with the particular physical application will make clear the appropriate boundary conditions. Close to the wire we may approximate (2A.17) as

$$\frac{d^2E_z}{d\rho^2} + \frac{1}{\rho}\frac{dE_z}{d\rho} + k_o^2 E_z = 0, \quad k_1\rho \ll p, q \tag{2B.1}$$

which has solution

$$E_z = H_o^{(1)}(k_o\rho) + RH_o^{(2)}(k_o\rho) \tag{2B.2}$$

The Hankel function of the first kind represents the expanding cylindrical wave emitted by the line source. The Hankel function of the second kind represents the converging cylindrical wave reflected by the medium. This equation serves to define the reflection coefficient R which is one of the two quantities of interest in the problem. The arguments of the Hankel functions are $k_0\rho$ which shows that the medium behaves similar to free space in the vicinity of the wire. This is to be expected as a result of the very large magnetostatic field in this region. At large distances from the wire we may approximate (2A.17) as

$$\frac{d^2E_z}{d\rho^2} + \frac{1}{\rho}\frac{dE_z}{d\rho} + k_1^2 E_z = 0 \quad , \quad k_1\rho >> p, q \tag{2B.3}$$

which has solution

$$E_z = T\, H_0^{(1)}(k_1\rho) \tag{2B.4}$$

The single solution has been chosen to satisfy the radiation condition

$$\lim_{\rho \to \infty} \sqrt{\rho}\left(\frac{dE_z}{d\rho} - ik_1E_z\right) = 0 \tag{2B.5}$$

representing an expanding cylindrical wave at infinity. The quantity T defined by this equation represents the transmission coefficient. The argument of the Hankel function, $k_1\rho$, is indicative of an ordinary unbiased plasma and is expected since the magnetostatic field becomes negligible at large distances.

The solutions (2B.2) and (2B.4) are only leading order asymptotic solutions to equation (2A.17). We will however take them as definitions of R and T. This definition is equivalent to adjoining homogeneous media with propagation constant k_0 near the origin, and with propagation constant k_1 near infinity.

When the operating frequency, ω, is above the plasma frequency, ω_p, radiation exists at infinity and the transmission coefficient T is physically meaningful. However in the case where the operating frequency, ω, is below the plasma frequency, ω_p, the wave is evanescent at infinity. There is therefore no transmitted wave, the reflection coefficient has magnitude unity, and a standing wave exists in the vicinity of the wire. The physical applications mentioned in the introduction for the case $\omega < \omega_p$ involve a bounded plasma medium. So in this case we terminate the plasma at radius ρ_0 and replace the external region with free space. The solution in this region is therefore

$$E_z = T\, H_0^{(1)}(k_0\rho) \ , \quad \rho > \rho_0 \tag{2B.6}$$

The boundary conditions at the interface ρ_0 are then

$$E_z = T\, H_0^{(1)}(k_0\rho_0) \tag{2B.7}$$

$$i\omega\mu_0 H_\phi = -\frac{dE_z}{d\rho} = k_0 T\, H_1^{(1)}(k_0\rho_0) \tag{2B.8}$$

Therefore the solution of Eq. (2A.17) matched to condition (2B.2) near $\rho = 0$ and the appropriate condition either near infinity (2B.4) or at ρ_0 (2B.7) and (2B.8) will determine the reflection and transmission coefficients. These quantities are of primary interest since they give not only the amplitude of the radiated field but also the influence of the medium on the antenna.

CHAPTER 3

SOLUTION OF RADIATION PROBLEM

The differential equation (2A.17) is a confluent form of an equation with four regular singular points, Heun's equation [8]. The designation of the solution to Heun's equation is not standard but in terms of the notation in [16] we can write a solution to (2A.17) in the form

$$\lim \mathrm{Hu}\left(\ell_1\ell_2, \frac{q^2}{p^2}\,;\, -\ell_1\,\frac{p}{2}\,,\, \ell_2\,\frac{p}{2}\,,\, 1,\, 0;\, k_1^2\,\frac{\rho^2}{p^2}\right)$$

and the quantities ℓ_1 and ℓ_2 approach infinity. Useful solutions to confluent forms of Heun's equation such as the spheroidal wave equation can be obtained by use of a series of special functions [10]. The solution of the radiation problem is obtained by this method in Section A. Section B briefly discusses an alternative numerical solution of (2A.17). Section C presents the approximate solution for the reflection and transmission coefficients by the WKB method.

3A. Solution in Special Function Series

The differential equation (2A.17) involves three parameters, p, q, and k_1. The wave number k_1 can be removed by using the dimensionless independent variable

$$\xi = k_1\rho \tag{3A.1}$$

which transforms (2A.17) into

$$\frac{d^2E_z}{d\xi^2} + \frac{1}{\xi}\frac{dE_z}{d\xi} + \frac{\xi^2 - q^2}{\xi^2 - p^2}E_z = 0 \qquad (3A.2)$$

This equation has four singular points. The points 0, $\pm$ p are regular singular points and infinity is irregular.

The quadratic transformation

$$\frac{\xi^2}{p^2} = x \qquad (3A.3)$$

transforms (3A.2) into

$$x(1-x)\frac{d^2E_z}{dx^2} + (1-x)\frac{dE_z}{dx} + \frac{1}{4}(q^2-p^2x)E_z = 0 \qquad (3A.4)$$

an equation with regular singular points at 0, 1 and an irregular singular point at infinity. A useful means of solution of (3A.4) involves expansion of the solution in a series of special functions resulting in a larger region of convergence than simple power series [10,17]. This procedure is carried out in Appendix 1 using results from Appendices 2 and 3. The solutions to (3A.2) or (3A.4) can be written as

$$E_z = \sum_{m=-\infty}^{\infty} c_m \mathscr{E}_m \qquad (3A.5)$$

where c_m are constant coefficients and $\mathscr{E}_m$ are special functions. The solution which is analytic at the origin is designated as EF(p, q, x)

and $\mathscr{E}_m$ in this instance is a special case of the hypergeometric function. The solution which is analytic at unity is designated as EG(p, q, x) where $\mathscr{E}_m$ represents the linearly independent solution of the hypergeometric equation. The series (3A.5) converges for all finite x in the case of EF and EG. A second pair of solutions are designated as EJ(p, q, ξ) and EY(p, q, ξ). In this second case $\mathscr{E}_m$ is proportional to either the Bessel function of the first kind or the second kind, respectively. The series (3A.5) only converges when $|\xi| > p$ ($|x| > 1$) for EJ or EY. The connection between the pair of solutions EF, EG and EJ, EY is given in Appendix 1 and Appendix 3.

We may now apply these results to the "radiation" problem. The case where the operating frequency is above the plasma frequency is treated first.

The radiation condition at infinity (2B.5) requires use of the solution

$$EH(p, q, \xi) = EJ(p, q, \xi) + iEY(p, q, \xi) \tag{3A.6}$$

and provides a representation of the solution for $|\xi| > p$ ($|x| > 1$). The asymptotic form of this solution for large ξ, from Appendix 4, is given by

$$EH(p, q, \xi) \sim H_0^{(1)}(\xi)\, S_1\, e^{-i\pi\nu}, \quad |\xi| \to \infty \tag{3A.7}$$

where $S_1 = \sum_{m=-\infty}^{\infty} \frac{c_m}{\Omega} (-1)^m$, $\Omega = m + \nu$, ν = characteristic exponent

discussed in Appendix 1, and we have refrained from using the asymptotic form of the Hankel function simply to make (3A.7) identifiable with (2B.4). Comparison with the asymptotic form of the field at a large radius, (2B.4), shows that the electric field in the region $|\xi| > p$ is given by

$$E_z = e^{i\pi\nu} \frac{T}{S_1} EH(p, q, \xi) \tag{3A.8}$$

where T is the transmission coefficient. The analytic continuation to the inner region $|\xi| < p$ ($|x| < 1$) is accomplished by the connection to the solutions EF and EG

$$EH = [A\ EF(p, q, x) + B\ EG(p, q, x)]S_1\ e^{-i\pi\nu} \tag{3A.9}$$

The constants A and B are determined from the last two formulas in Appendix 1 to be

$$A = \frac{i(e^{-i\pi\nu}\ c^{(+)} - c^{(-)}\ e^{i\pi\nu})}{4\ \cos^2\pi\nu\ \sin\pi\nu\ S_1} \tag{3A.10}$$

$$B = -\frac{i}{4\pi\ \cos^2\pi\nu\ S_1}\ (c^{(+)} + c^{(-)}) \tag{3A.11}$$

where the connecting constants $c^{(\pm)}$ are given in Appendix 1. Therefore the field in the inner region can be determined from the expression

$$E_z = T[A\ EF(p, q, x) + B\ EG(p, q, x)] \tag{3A.12}$$

Finally this expression must be matched to the asymptotic form of the field near the origin, (2B.2), which in terms of x reads

$$E_z = H_o^{(1)} (qx^{\frac{1}{2}}) + R\, H_o^{(2)} (qx^{\frac{1}{2}}) \qquad (3A.13)$$

Expanding the Hankel functions for small x gives

$$E_z \sim \frac{i}{\pi} (1 - R)\, \ell n\, x + (1 + R) + i\, \frac{2}{\pi} [\, \ell n(q/2) + \gamma\,](1 - R) \qquad (3A.14)$$

where γ is Euler's constant. Appendix 4 shows that (3A.12) can be expanded as

$$E_z \sim T\left[- B\, S_2\, \ell n\, x + (A\, S_2 + B\, S_3)\right] \qquad (3A.15)$$

where $S_2 = \sum_{m=-\infty}^{\infty} c_m$

$$S_3 = - 2\, \gamma\, S_2 - \sum_{m=-\infty}^{\infty} c_m \left[\psi(\Omega) + \psi(-\Omega)\right]$$

and ψ is the digamma function. The matching of the log and constant terms in (3A.14) and (3A.15) determines R and T

$$R = \frac{C - 1}{C + 1} \qquad (3A.16)$$

$$T = - \frac{i}{\pi}\, \frac{1 - R}{S_2\, B} \qquad (3A.17)$$

where $C = -\frac{i}{\pi}\left[\frac{A}{B} + \frac{S_3}{S_2} + 2\,\ell n\,(q/2) + 2\,\gamma\right]$

Making use of equation (3A.10) and (3A.11) these become

$$R = \frac{1}{1 + i/D} \tag{3A.18}$$

$$T = \frac{N}{1 - i\,D} \tag{3A.19}$$

where $N = 4\cos^2 \pi\nu \frac{S_1}{S_2} / (c^{(+)} + c^{(-)})$

$$2\pi D = -\pi \cot \pi\nu \frac{c^{(+)} - c^{(-)}}{c^{(+)} + c^{(-)}} + \frac{S_3}{S_2} + 2\,\ell n\,\frac{q}{2} + 2\,\gamma$$

Therefore by calculation of several sums involving rational functions and the coefficients c_m we obtain the transmission and reflection coefficients.

The case where the driving frequency is below the plasma frequency differs simply by the fact that the outer boundary conditions are now (2B.7) and (2B.8) applied at $\xi_o = k_1 \rho_o$. If $|\xi_o| > p$ we may use the Bessel series solutions to match the boundary conditions (2B.7) and (2B.8) giving

$$E_z = T[P\,EJ(p, q, \xi) + Q\,EY(p, q, \xi)] \tag{3A.20}$$

where $P = \frac{\pi}{2} \frac{\xi_0}{S_0} \left[H_0^{(1)}\left(\frac{q}{p}\xi_0\right) EY'(p, q, \xi_0) + \frac{q}{p} H_1^{(1)}\left(\frac{q}{p}\xi_0\right) EY(p, q, \xi_0) \right]$

$$Q = -\frac{\pi}{2} \frac{\xi_0}{S_0} \left[H_0^{(1)}\left(\frac{q}{p}\xi_0\right) EJ'(p, q, \xi_0) + \frac{q}{p} H_1^{(1)}\left(\frac{q}{p}\xi_0\right) EJ(p, q, \xi_0) \right]$$

where the prime denotes differentiation with respect to ξ and

$$S_0 = \sum_{m=-\infty}^{\infty} \frac{c_m}{\Omega}$$

The analytic continuation to $|x| < 1$ is accomplished by using

$$E_z = T[A\ EF(p, q, x) + B\ EG(p, q, x)] \qquad (3A.21)$$

where in this case

$$A = \left[(P + Q \cot 2\pi\nu)\, c^{(+)} - Q \csc 2\pi\nu\, c^{(-)} \right] \frac{1}{2} \sec \pi\nu$$

$$B = -e^{i\pi\nu} \left[(P + Q \cot 2\pi\nu)\, c^{(+)} + Q \csc 2\pi\nu\, c^{(-)} \right] \frac{1}{2\pi} \sec \pi\nu$$

and the formulas (3A.16) and (3A.17) determine R and T.

If $|\xi_0| < p$ (or if $|\xi_0| > p$ but not too large) we use only the solutions EF and EG to match the outer boundary condition.

$$A = -\frac{x_o}{S_2}\left[H_o^{(1)}\left(\frac{q}{p}\xi_o\right)\quad \dot{EG}(p, q, x_o) + \frac{pq}{2\xi_o} H_1^{(1)}\left(\frac{q}{p}\xi_o\right)\quad EG(p, q, x_o)\right]$$

$$B = \frac{x_o}{S_2}\left[H_o^{(1)}\left(\frac{q}{p}\xi_o\right)\quad \dot{EF}(p, q, x_o) + \frac{pq}{2\xi_o} H_1^{(1)}\left(\frac{q}{p}\xi_o\right)\quad EF(p, q, x_o)\right]$$

where the dot denotes differentiation with respect to x and $x_o = \xi_o^2/p^2$. Equations (3A.16) and (3A.17) determine R and T once again.

3B. Numerical Treatment of Radiation Problem

There are several approaches to the numerical solution of problems involving wave propagation in one dimensional inhomogeneous media. If the reflection and transmission coefficients are the only quantities of interest, Ambarzumian's principle may be invoked to determine rate of change (Riccati) equations for these quantities (invariant imbedding). This method has had wide spread use in planar configurations and has also been applied to cylindrical and spherical problems [14], [15]. The cylindrical application requires the integration of a Riccati equation with Bessel function coefficients. Although this is a rather elegant method and perhaps the most well adapted to computation, for ease of programming we resort to integration of the second order equation (3A.2) in this section. The method of invariant imbedding will be applied to the solution of the scattering problem in Chapter 6. The integration method made use of a packaged program using a Runge-Kutta algorithm. The numerical scheme will not be discussed other than to note the initial conditions used and the means of handling singularities of the coefficients.

Equation (3A.2) has regular singular points at 0 and $\pm$ p. In the case where $\omega > \omega_p$ the physical values of the variable ξ lie along the positive real axis. Integration in this case would typically begin at a large distance from the origin, $\xi^{(\infty)}$, and proceed inward. The solution and its derivative would be matched at this initial point, $\xi^{(\infty)}$, to that of an expanding cylindrical wave, or Hankel function of the first kind of order zero

$$E_z = H_o^{(1)}(\xi^{(\infty)}) \tag{3B.1}$$

$$\frac{dE_z}{d\xi} = - H_1^{(1)}(\xi^{(\infty)}) \tag{3B.2}$$

However if we integrate inward the singularity +p will be encountered and special treatment required. This has been avoided by rotating the problem to the positive imaginary axis. The point +p is a branch point of the solution. The branch cut as shown in Appendix 3 is taken below the initial point $\xi^{(\infty)}$ and thus rotation to the positive imaginary axis does not involve crossing the cut. The initial conditions (3B.1) and (3B.2) now become modified Bessel functions K_o and K_1. It is permissible to rotate these asymptotic solutions onto the Stokes line at the imaginary axis since they are subdominant there [18] and Stokes phenomenon does not occur. Integration can now proceed toward the origin, near which, $\xi^{(o)}$, the solution and its derivative are matched to

$$E_z = \left[H_o^{(1)}\left(\frac{q}{p}\,\xi^{(o)}\right) + RH_o^{(2)}\left(\frac{q}{p}\,\xi^{(o)}\right)\right]/T \tag{3B.3}$$

$$\frac{dE_z}{d\xi} = -\frac{q}{p}\left[H_1^{(1)}\left(\frac{q}{p}\,\xi^{(o)}\right) + RH_1^{(2)}\left(\frac{q}{p}\,\xi^{(o)}\right)\right]/T \tag{3B.4}$$

which determines R and T.

The case where $\omega < \omega_p$ is simpler in that the physical values of ξ now actually lie along the positive imaginary axis to begin with as discussed in Appendix 3. The regular singular points $\pm$ p remain on the real axis and thus it is not necessary to deform around them. Integration proceeds inward from the boundary of the plasma to a region near the origin. The initial conditions are applied at ξ_o

$$E_z = H_o^{(1)}\left(\frac{q}{p}\,\xi_o\right) \tag{3B.5}$$

$$\frac{dE_z}{d\xi} = -\frac{q}{p}\,H_1^{(1)}\left(\frac{q}{p}\,\xi_o\right) \tag{3B.6}$$

where ξ_o is now positive imaginary and integration proceeds towards the origin where (3B.3) and (3B.4) are matched.

3C. WKB Solution

The WKB method is an approximate method of solving differential equations [19,20]. This method has been widely used in wave propagation problems involving both dielectric media [21] and plasmas. The method provides useful quantitative results as well as a qualitative understanding of the phenomena.

The method is useful when aside from several special points, transition points, the properties of the medium vary little within a wavelength. Equation (2A.17) shows that as the static current I_0 becomes large (equivalently the parameter p becomes large) the coefficient E_z varies slowly over distances of a wavelength. The square root of the coefficient of E_z divided by k_0 is often referred to as an index of refraction. Thus the medium properties vary slowly when the static current becomes large. Making use of a new variable

$$\xi' = \xi/p \tag{3C.1}$$

equation (3A.2) becomes

$$\frac{d^2E_z}{d\xi'^2} + \frac{1}{\xi'}\frac{dE_z}{d\xi'} + p^2\frac{\xi'^2 - \alpha^2}{\xi'^2 - 1}E_z = 0 \tag{3C.2}$$

where we assume $\alpha = q/p$ is an order one quantity and that p is a large parameter. Near the transition points, 0, 1, α local solutions must be found which can be matched to the exponential approximations on either side of these points, details are supplied in Appendix 5. The leading order WKB results in the case where $\omega > \omega_p$ are

$$R = \text{exponentially small} \tag{3C.3}$$

$$T = e^{-p\zeta_0} \tag{3C.4}$$

where

$$\zeta_o = \int_1^{\alpha} \sqrt{\frac{\alpha^2 - t^2}{t^2 - 1}}\, dt$$

$$= \alpha\left[K\left(\frac{\alpha^2 - 1}{\alpha^2}\right) - E\left(\frac{\alpha^2 - 1}{\alpha^2}\right)\right]$$

E, K being complete elliptic integrals [22]. The exponential factor in (3C.4) represents the exponential decay of the wave as it propagates through the region $1 < \xi' < \alpha$ where the wave is evanescent. The reflection coefficient (3C.3) represents the contribution from the turning point at $\xi' = \alpha$. The two way travel of the wave through the region $1 < \xi' < \alpha$ is responsible for the exponential smallness of R.

The definition of reflection coefficient, (2B.2), has several useful features. This definition relates the inhomogeneous problem to a homogeneous cylindrical problem by use of the Hankel functions. The value of R is also identical to that which would be determined by integration of the Riccati equation which R satisfies (the invariant imbedding method). We should, however, keep in mind that R cannot be uniquely defined in an inhomogeneous media [23]. It is known that the reflection coefficient in smooth media, without turning points, becomes exponentially small as the characteristic length to wavelength ratio becomes large [21]. However if discontinuities in the medium electrical properties or their derivative appear, then R decays like a power of this large parameter [21]. The definition (2B.2) as noted in Chapter 2 is equivalent to adjoining a homogeneous medium in the vicinity of the origin. It thus introduces a

discontinuity in the second derivative of the refractive index giving an R which decays as the inverse square of p [21]. This discontinuity will therefore contribute to the value of R, particularly in the large current limit. The next order WKB solution will yield such a behavior in R.

The $\omega < \omega_p$ problem involves positive imaginary ξ' and negative imaginary α as can be shown from the results in Appendix 3. We can therefore write (3C.2) in the form

$$\frac{d^2E_z}{d\tilde{\xi}^2} + \frac{1}{\tilde{\xi}} \frac{dE_z}{d\tilde{\xi}} - p^2 \frac{\tilde{\xi}^2 - \tilde{\alpha}^2}{\tilde{\xi}^2 + 1} E_z = 0 \qquad (3C.5)$$

where $\tilde{\alpha} = i\alpha$ and $\tilde{\xi} = -i\xi'$ are positive real quantities. Transition points are 0 and $\tilde{\alpha}$. A larger reflection may result in this case since the turning point at $\tilde{\alpha}$ is not shielded by an evanescent region as it was in (3C.2). The plasma is bounded in this case with limit

$$\tilde{\xi}_o = -i\xi_o/p = -ik_1\rho_o/p \qquad (3C.6)$$

where $\tilde{\xi}_o$ is real and positive. We assume that $\tilde{\alpha}$ is an order one quantity and that the boundary is placed at a large distance $\tilde{\alpha}\ p\ \tilde{\xi}_o >> 1$. The uniformly valid solution for R and T is given in Appendix 5. We note that if $\tilde{\xi}_o < \tilde{\alpha}$ (boundary inside turning point) we can approximate these results as

$$R = -i \frac{Q_2(\tilde{\xi}_0) - \tilde{\alpha}}{Q_2(\tilde{\xi}_0) + \tilde{\alpha}} e^{i2p\zeta_2} \tag{3C.7}$$

$$T = \frac{2\tilde{\alpha}^{\frac{1}{2}} Q_2^{\frac{1}{2}}(\tilde{\xi}_0)}{Q_2(\tilde{\xi}_0) + \tilde{\alpha}} e^{ip(\zeta_2 - \tilde{\alpha}\tilde{\xi}_0)} \tag{3C.8}$$

where $\zeta_2 = \int_0^{\tilde{\xi}_0} Q_2(t)dt$

$$Q_2^2(t) = \frac{\tilde{\alpha}^2 - t^2}{t^2 + 1}$$

and if $\tilde{\xi}_0 > \tilde{\alpha}$ (boundary outside turning point) we can approximate these results as

$$R = - \frac{i2[Q_1(\tilde{\xi}_0) - i\tilde{\alpha}] - [Q_1(\tilde{\xi}_0) + i\tilde{\alpha}] e^{-2p\zeta_1}}{i2[Q_1(\tilde{\xi}_0) - i\tilde{\alpha}] + [Q_1(\tilde{\xi}_0) + i\tilde{\alpha}] e^{-2p\zeta_1}} e^{i2p\zeta_3} \tag{3C.9}$$

$$T = \frac{4\tilde{\alpha}^{-\frac{1}{2}} Q_1^{\frac{1}{2}}(\tilde{\xi}_0) e^{-p\zeta_1}}{i2[Q_1(\tilde{\xi}_0) - i\tilde{\alpha}] + [Q_1(\tilde{\xi}_0) + i\tilde{\alpha}] e^{-2p\zeta_1}} e^{i(p\zeta_3 - \tilde{\alpha}p\tilde{\xi}_0 + \pi/4)} \tag{3C.10}$$

where

$$\zeta_1 = \int_{\tilde{\alpha}}^{\tilde{\xi}_0} Q_1(t)dt = \frac{1}{\tilde{\xi}_0} \sqrt{(\tilde{\xi}_0^2+1)(\tilde{\xi}_0^2-\tilde{\alpha}^2)} - \sqrt{1+\tilde{\alpha}^2}\, E\left(\sqrt{1 - \frac{\tilde{\alpha}^2}{\tilde{\xi}_0^2}} \,\middle|\, \frac{1}{1+\tilde{\alpha}^2}\right)$$

$$Q_1^2(t) = \frac{t^2 - \tilde{\alpha}^2}{t^2 + 1}$$

$$\zeta_3 = \int_0^{\tilde{\alpha}} Q_2(t)dt$$

and E(|) is an elliptic integral of the second kind [22]. The results (3C.7) and (3C.8) are the expressions one would obtain for R and T in a planar medium with a refractive index discontinuity, at $\tilde{\xi}_0$, without turning points. The magnitude of R is simply the Fresnel reflection coefficient at the discontinuity.

The results (3C.9) and (3C.10) show the presence of a region where the wave is evanescent. The quantity ζ_1 represents the exponential attenuation of the wave in the region between the turning point $\tilde{\alpha}$ and the boundary $\tilde{\xi}_0$. The results obtained using the special function series (Section A), the numerical solution (Section B), and the WKB approximation (Section C) are plotted and compared in Chapter 4.

CHAPTER 4

RESULTS OF RADIATION PROBLEM

Section A presents the results of the unbounded case with $\omega > \omega_p$. Section B presents the results of the bounded case with $\omega < \omega_p$.

4A. Driving Frequency Greater than the Plasma Frequency

The behavior of the square of the refractive index n

$$n^2 = \frac{k_1^2}{k_o^2} \frac{k_1^2 \rho^2 - q^2}{k_1^2 \rho^2 - p^2} \qquad k_1^2 = k_o^2 \left(1 - \frac{\omega_p^2}{\omega^2}\right) \tag{4A.1}$$

is given in Fig. 4. The point $k_1\rho = p$ is known as a resonance. At this point the driving frequency is equal to the upper hybrid frequency ($\omega^2 = \omega_p^2 + \omega_g^2$). This is the natural frequency of electron oscillations perpendicular to a static magnetic field [24]. Thus at this radius there is a resonance between the applied field and the electron oscillations perpendicular to the magnetostatic field. Energy is transferred from the field to the kinetic energy of the electrons in this region. In the collisionless steady state, as treated here, the velocity of the electrons increases until the linear approximation breaks down. Therefore in reality the energy stored in this region will be dissipated as heat as well as being transferred by nonlinear effects to other modes. The linear approximation simply indicates that energy has been stored in this region and does not show up in the transmitted or reflected waves. This phenomenon of energy storage can be qualitatively understood by the fact

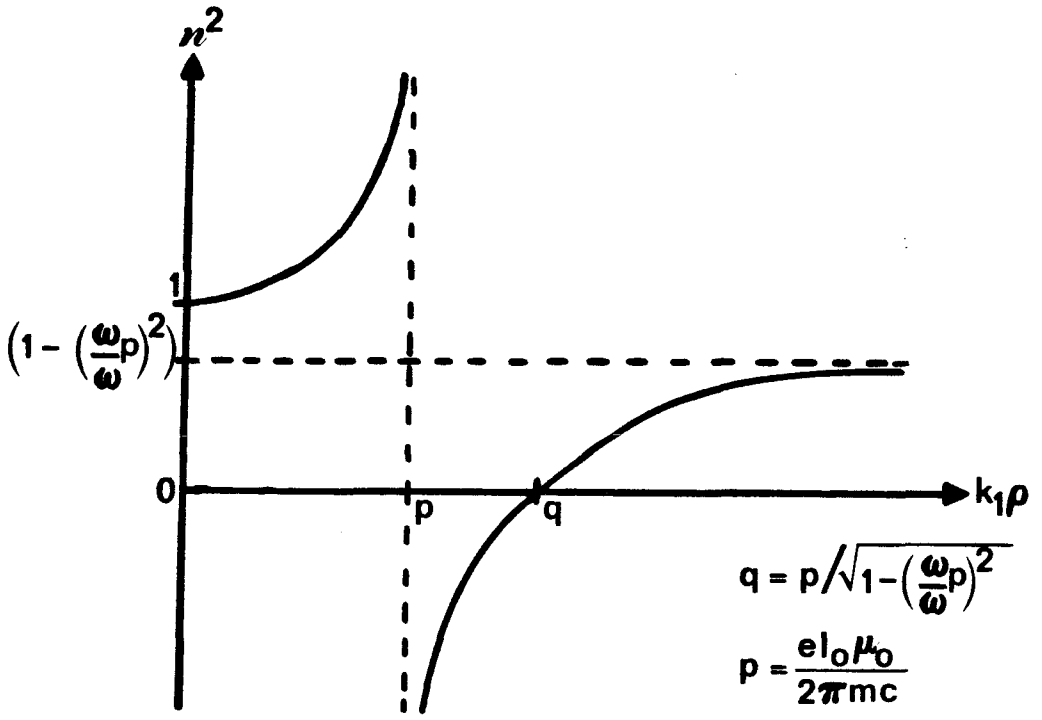

Fig. 4. The behavior of the refractive index in the case where $\omega > \omega_p$.

that the group velocity approaches zero at the point $k_1\rho = p$. By use of (4A.1) we may write

$$v_g \sim \frac{\text{const}}{(p - k_1\rho)^{3/2}} \qquad k_1\rho \to p \tag{4A.2}$$

which when inverted and integrated yields an infinite travel time as the resonance point is approached. The preceding qualitative argument is identical to the planar case [1].

Near the wire ($\rho \to 0$) the magnetostatic field is very large. The electrons are frozen to the field lines in this region and thus do not respond to the applied electric field. The medium therefore resembles free space with unit index of refraction as far as electric fields in the ρ - z plane are concerned.

At large distances from the wire the magnetostatic field is weak and the medium behaves similar to an unbiased isotropic plasma.

The results are presented as a function of the static current I_o. Instead of plotting the coefficients R and T themselves we plot the real quantities N and D related by

$$R = \frac{1}{1 + i/D} \tag{4A.3}$$

$$T = \frac{N}{1 - iD} \tag{4A.4}$$

Figure 5 gives the values of N and D for four different values of the ratio ω/ω_p. As a result of the small magnitude of D the

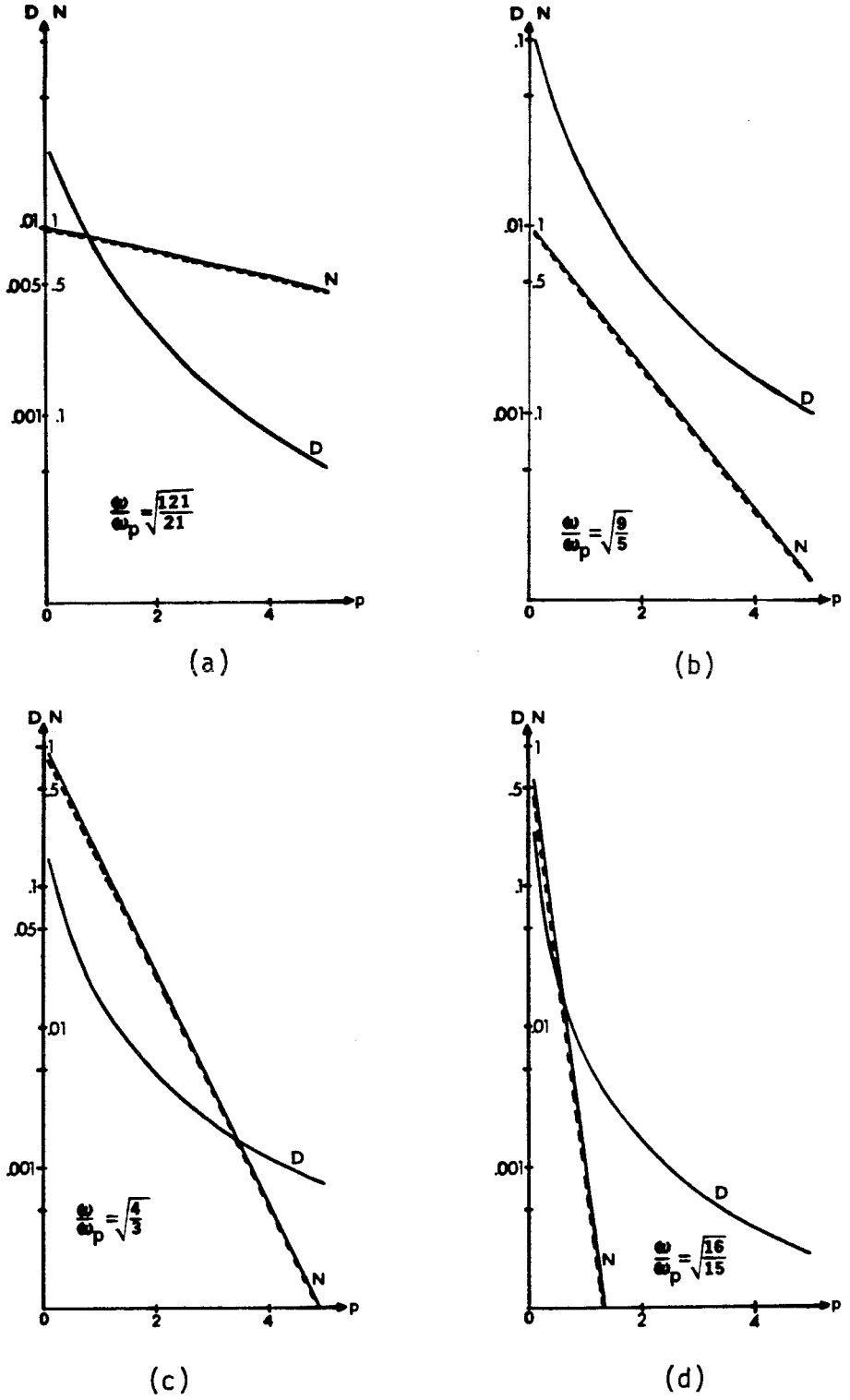

Fig. 5. The quantities N and D (approximately |T| and |R|) as functions of static current (note that p = 1 is equivalent to I_0 = 8.5 kA) for four ratios of ω to ω_p.

value of D is approximately equivalent to the magnitude of R. Furthermore the magnitude of T is approximately equivalent to the value of N. The WKB result (3C.4) for T is also plotted as the dashed curve. Note that although (3C.4) is the WKB result for T, due to the small values of D we can also associate this value with N as

$$N \sim e^{-p\zeta_o} \tag{4A.5}$$

These are the values plotted as dashed curves in Fig. 5. The solid curves represent the identical results derived from the special function series solution, Section 3A, and the direct numerical integration, Section 3B. The transmission coefficient decreases approximately exponentially with increasing static current and follows closely the WKB result. The reflection coefficient also decreases with increasing current. The fact that both R and T decrease with increasing static current means that the energy carried by the transmitted and reflected waves is smaller than the incident energy.

4B. Driving Frequency Less than the Plasma Frequency

The behavior of the square of the refractive index n is given in Fig. 6. The wave number k_1 and the parameter q are both imaginary in this case. The boundary of the plasma is placed at ρ_o. The wave is freely propagating in the region near the wire ($|k_1\rho| < |q|$). In the region between $|q|$ and the boundary, the wave is evanescent. Thus as the static current is increased the location of the point $|q|$ moves away from the wire. The amplitude of the transmitted wave will therefore

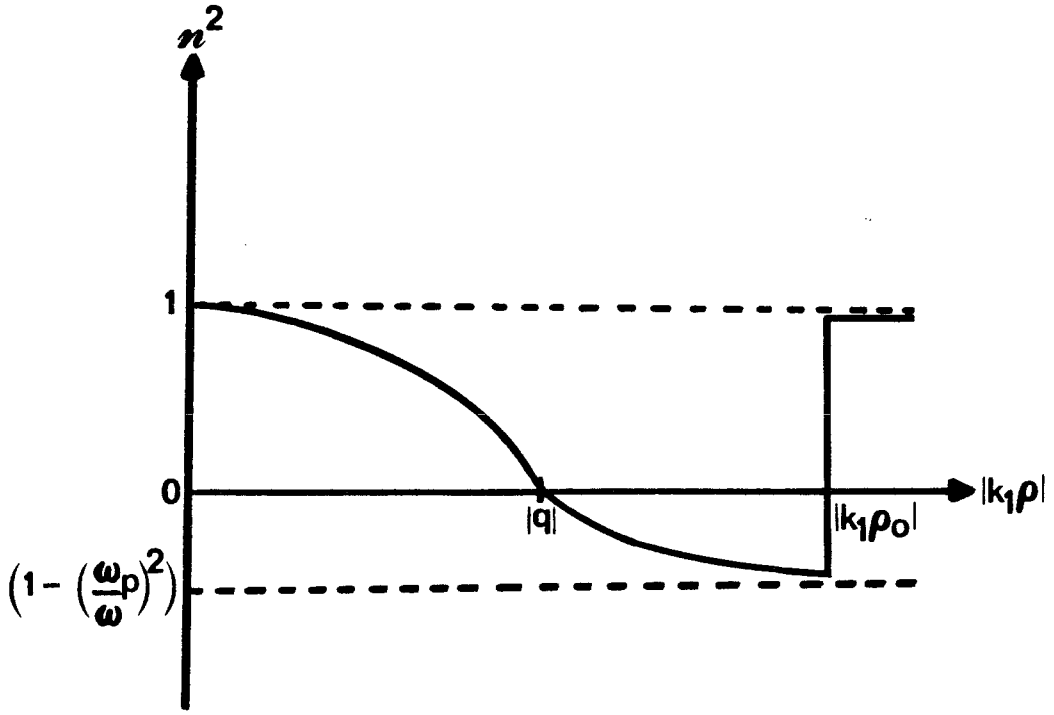

Fig. 6. The behavior of the refractive index in the case where $\omega < \omega_p$ and the medium is bounded by free space.

increase with increasing current since the width of the cutoff region shrinks.

Figure 7 gives the magnitude of R and T as functions of static current for three different positions of the column boundary $|k_1\rho|$. The solid curves represent the results of numerical integration and the dashed curves are the WKB results. The discrepancy between the WKB and numerical solutions in Fig. 7_a results from the fact that the boundary is close to the origin, violating the assumptions set forth in the derivation of the WKB solution (Appendix 5). The agreement is otherwise quite close except when the turning point $|q|$ lies near the boundary $|k_1\rho_0|$. The discrepancy in this region is simply due to the fact that we used the simpler equations (3C.7) through (3C.10) rather than the uniformly valid WKB solution, Appendix 5.

The results show that the presence of the static current does indeed increase the transmission coefficient provided the magnetic field influences a significant portion of the column (the value of the current must be very large to do so).

We have not mentioned the special function series in the above calculations. Since the outer boundary condition must be applied at a finite radius we must evaluate the special functions involved in this series at this radius. Although a relation exists between the hypergeometric functions and the Legendre functions, due to the lack of available programs for calculating these functions we dispensed with series solution.

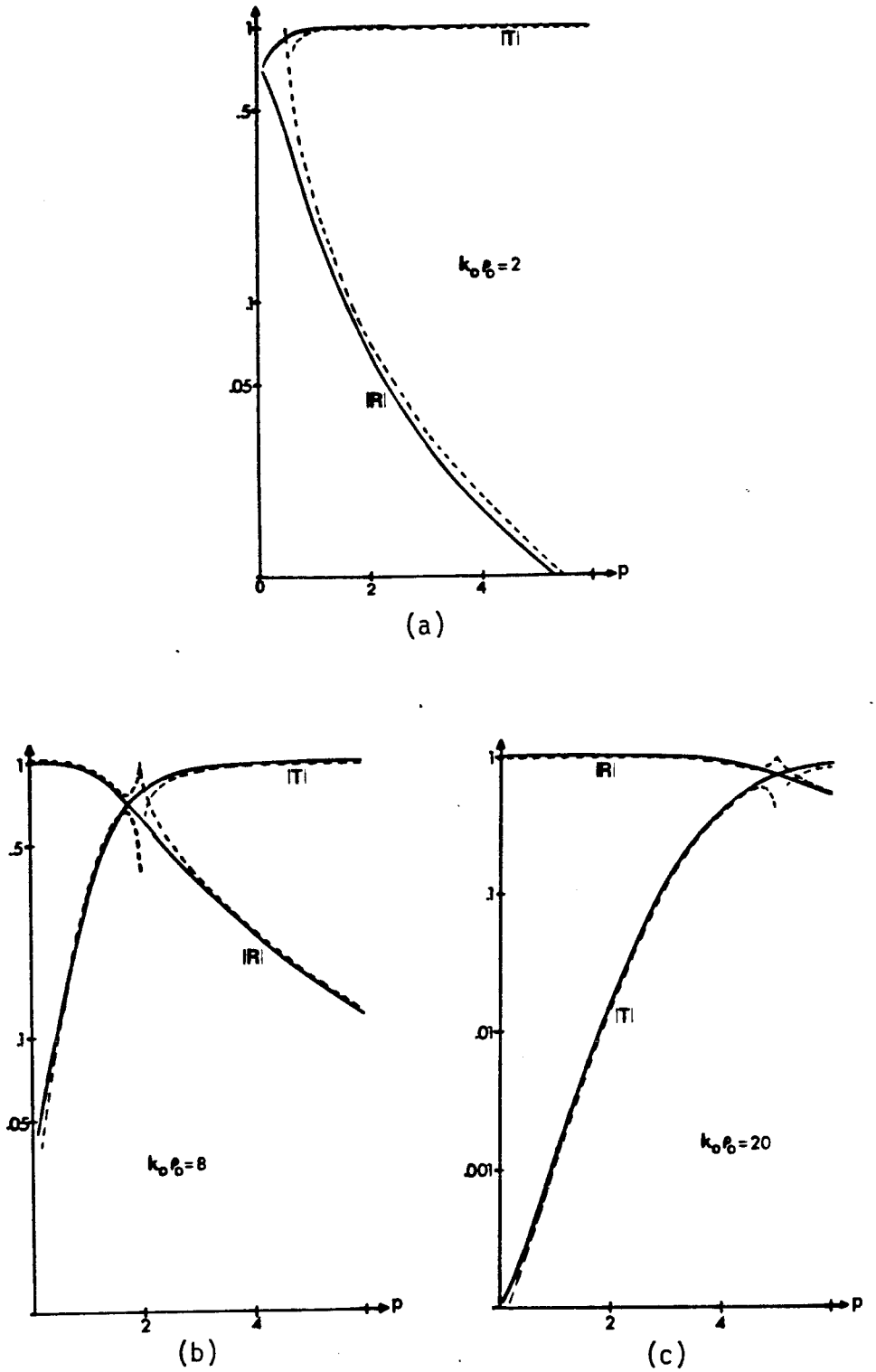

Fig. 7. The magnitudes of T and R for bounded columns of three different radii when $\omega_p/\omega = \sqrt{5/4}$ (note that p = 1 is equivalent to I_0 = 8.5 kA).

CHAPTER 5

FORMULATION OF SCATTERING PROBLEM

Chapters 5, 6, and 7 discuss the problem of a plane wave normally incident upon a bounded column of plasma. The plasma column contains a static axial current which gives rise to a static magnetic field. This static azimuthal magnetic field biases the plasma. The problem thus involves scattering from a gyroelectric cylindrical medium.

Section A sets up the equations for the modal fields. Section B gives the boundary conditions and defines the matrix reflection coefficient of the scattered fields. Section C considers the behavior of the fields in the vicinity of the origin.

5A. Coupled Equations in the Axial Fields

Instead of considering a single current carrying wire as we did in the radiation problem, we generalize the problem somewhat by allowing the axial current to be distributed radially. The static current is assumed to be independent of the azimuthal angle, ϕ, and of the axial distance, z. The static magnetic field is thus given by

$$\underline{B}_0 = \frac{I_0(\rho)\mu_0}{2\pi\rho}\,\underline{e}_\phi \tag{5A.1}$$

where μ_0 is the permeability of free space, $\underline{e}_\phi$ is a unit vector in the ϕ direction, ρ is the radial distance, and $I_0(\rho)$ is the "enclosed" current.

The "enclosed" current can be found by integrating the axial current density $J_{oz}(\rho)$ as

$$I_o(\rho) = 2\pi \int_0^\rho J_{oz}(\rho')\rho' d\rho' \tag{5A.2}$$

A current density distribution of interest in the following chapter for its mathematical simplicity is

$$J_{oz}(\rho) = \frac{J_o}{\rho} \tag{5A.3}$$

which yields a constant magnetic field

$$B_{o\phi} = \mu_o J_o \tag{5A.4}$$

This current distribution thus gives rise to a "homogeneous" medium in the sense that the dielectric tensor will be independent of ρ (this statement is of course contingent upon also having a uniform plasma density).

The dielectric tensor was shown in Chapter 2 to be

$$\underline{\underline{\varepsilon}} = \begin{pmatrix} a & 0 & ig \\ 0 & b & 0 \\ -ig & 0 & a \end{pmatrix} \tag{5A.5}$$

where $a = \varepsilon_o \left(1 - \frac{\frac{\omega_p^2}{\omega}\omega_o}{\omega_o^2 - \omega_g^2}\right)$, $b = \varepsilon_o \left(1 - \frac{\omega_p^2}{\omega\omega_o}\right)$, $g = \frac{\omega_g \omega_p^2 \varepsilon_o}{\omega(\omega_o^2 - \omega_g^2)}$,

$\omega_o = \omega + i\,\omega_{eff}$, ε_o is the permittivity of free space, ω is the temporal frequency, ω_{eff} is the collision frequency, which will be set to zero, ω_p is the plasma frequency, and ω_g is the gyro frequency.

The gyro frequency is dependent on the magnetic field through

$$\omega_g = -\frac{e}{m} B_{o\phi} \tag{5A.6}$$

where e is the magnitude of the electron charge and m is the electron mass. Maxwell's equations can be written as

$$\nabla \times \underline{E} = i\,\omega\,\mu_o\,\underline{H} \tag{5A.7}$$

$$\nabla \times \underline{H} = -i\,\omega\,\underline{\underline{\varepsilon}} \cdot \underline{E} \tag{5A.8}$$

The fields are periodic in the azimuthal angle ϕ, and therefore may be expanded as

$$\underline{E} = \sum_{n=-\infty}^{\infty} \underline{E}_n\, e^{in\phi} \tag{5A.9}$$

$$\underline{H} = \sum_{n=-\infty}^{\infty} \underline{H}_n\, e^{in\phi} \tag{5A.10}$$

Since the medium is linear and is itself independent of ϕ the solution of the field equations can be carried out individually for each angular mode. We assume that the fields are independent of the coordinate z. The equations (5A.7) and (5A.8) can be reduced to two coupled second

order equations in the axial magnetic and electric fields

$$\frac{d^2H_z}{d\rho^2} + \left(\frac{1}{\rho} - \frac{1}{b}\frac{db}{d\rho}\right)\frac{dH_z}{d\rho} + \left(\omega^2 \mu_o b - \frac{n^2}{\rho^2}\frac{b}{a}\right)H_z = i \frac{g}{a}\frac{n}{\rho} \omega b E_z \tag{5A.11}$$

$$\frac{d^2E_z}{d\rho^2} + \frac{1}{\rho}\frac{dE_z}{d\rho} + \left(\omega^2 \mu_o \frac{a^2 - g^2}{a} - \frac{n^2}{\rho^2}\right)E_z = -i \frac{g}{a}\frac{n}{\rho} \omega \mu_o H_z \tag{5A.12}$$

where we have suppressed the modal subscript n on all field components. The remaining field components may be derived from the axial ones through the relations

$$H_\phi = \frac{i}{\omega\mu_o}\frac{dE_z}{d\rho} \tag{5A.13}$$

$$E_\phi = -\frac{i}{\omega b}\frac{dH_z}{d\rho} \tag{5A.14}$$

$$H_\rho = \frac{n}{\omega\mu_o\rho} E_z \tag{5A.15}$$

$$E_\rho = -\frac{n}{a\omega\rho} H_z - i \frac{g}{a} E_z \tag{5A.16}$$

If the plasma density is constant, meaning that the quantity b is constant, equations (5A.11) and (5A.12) can be written as

$$\frac{d^2H_z}{d\rho^2} + \frac{1}{\rho}\frac{dH_z}{d\rho} + \left(k_1^2 - \frac{\nu^2}{\rho^2}\right) H_z = i\frac{\beta_1}{\rho} E_z \tag{5A.17}$$

$$\frac{d^2E_z}{d\rho^2} + \frac{1}{\rho}\frac{dE_z}{d\rho} + \left(k_2^2 - \frac{n^2}{\rho^2}\right) E_z = -i\frac{\beta_2}{\rho} H_z \tag{5A.18}$$

where $\nu^2 = n^2 \frac{b}{a}$, $k_1^2 = \omega^2\mu_o b$, $k_2^2 = \omega^2\mu_o \frac{a^2 - g^2}{a}$, $\beta_1 = n\frac{g}{a}\omega b$, $\beta_2 = n\frac{g}{a}\omega\mu_o$

and we have used the notation ν due to its familiarity as the order in Bessel's equation. This quantity should not be confused with the characteristic exponent in the radiation problem. When the current density profile (5A.3) is present, the parameters in (5A.17) and (5A.18) are independent of the coordinate ρ. These equations thus take the form of two coupled Bessel equations. The solution of this "homogeneous" case as well as the general inhomogeneous problem will be considered in Chapter 6.

5B. Definition of Incident and Scattered Field Components and Boundary Conditions

We are interested in the scattered field generated by a plane wave impinging on the column of plasma. The plasma boundary will therefore be placed at a finite distance ρ_c. The geometry is shown in Fig. 8. Outside of the column the fields can be written as

$$H_z = H_z^{inc} + H_z^{scatt} \tag{5B.1}$$

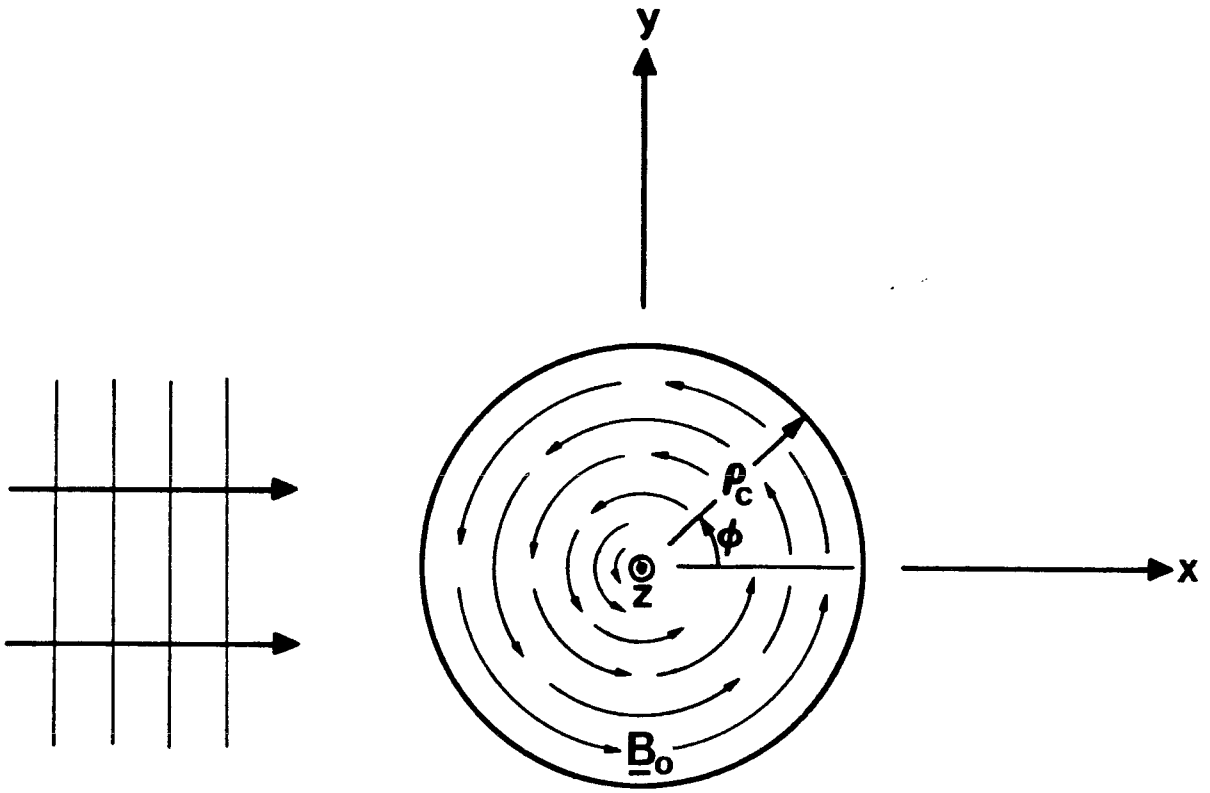

Fig. 8. The geometry of the scattering problem. A column of plasma biased by an azimuthal magnetostatic field is irradiated by a normally incident electromagnetic wave. The column is coincident with the z axis.

$$E_z = E_z^{inc} + E_z^{scatt} \tag{5B.2}$$

The incident wave is assumed to be propagating in the x direction and can be written as

$$H_z^{inc} = H_o\, e^{ik_o x} = H_o \sum_{n=-\infty}^{\infty} i^n J_n(k_o\rho)\, e^{in\phi} \tag{5B.3}$$

$$E_z^{inc} = E_o\, e^{ik_o x} = E_o \sum_{n=-\infty}^{\infty} i^n J_n(k_o\rho)\, e^{in\phi} \tag{5B.4}$$

where the wave amplitude is H_o, E_o, and ϕ is the angle measured from the x axis. We have included incident waves with general polarization in equations (5B.3) and (5B.4). However, due to the linearity of the problem, we may take sequentially $E_o = 0$ and then $H_o = 0$, these two polarization states providing the complete solution.

The scattered fields satisfying the radiation condition can be written

$$\sqrt{\frac{\mu_o}{\varepsilon_o}}\, H_z^{scatt} = \sum_{n=-\infty}^{\infty} i^n \left[\sqrt{\frac{\mu_o}{\varepsilon_o}}\, H_o\, R_n^{11} + E_o\, R_n^{21}\right] H_n^{(1)}(k_o\rho)\, e^{in\phi} \tag{5B.5}$$

$$E_z^{scatt} = \sum_{n=-\infty}^{\infty} i^n \left[\sqrt{\frac{\mu_o}{\varepsilon_o}}\, H_o\, R_n^{12} + E_o\, R_n^{22}\right] H_n^{(1)}(k_o\rho)\, e^{in\phi} \tag{5B.6}$$

where the quantity R_n

$$R_n = \begin{pmatrix} R_n^{11} & R_n^{12} \\ R_n^{21} & R_n^{22} \end{pmatrix} \tag{5B.7}$$

is the modal reflection coefficient matrix. The off diagonal elements of R_n represent the coupling due to the gyrotropic nature of the medium.

The expressions (5B.5) and (5B.6) can be simplified when the observation point is in the far zone yielding

$$\sqrt{\frac{\mu_o}{\varepsilon_o}}\, H_z^{scatt} \sim \sqrt{\frac{2}{\pi k_o \rho}}\, e^{i(k_o\rho - \pi/4)} \sum_{n=-\infty}^{\infty} \left[\sqrt{\frac{\mu_o}{\varepsilon_o}}\, H_o\, R_n^{11} + E_o\, R_n^{21}\right] e^{in\phi} \tag{5B.8}$$

$$E_z^{scatt} \sim \sqrt{\frac{2}{\pi k_o \rho}}\, e^{i(k_o\rho - \pi/4)} \sum_{n=-\infty}^{\infty} \left[\sqrt{\frac{\mu_o}{\varepsilon_o}}\, H_o\, R_n^{12} + E_o\, R_n^{22}\right] e^{in\phi} \tag{5B.9}$$

which make clear the meaning of the quantity

$$R(\phi) = \sum_{n=-\infty}^{\infty} R_n\, e^{in\phi} \tag{5B.10}$$

as being the scattering amplitude matrix in the far zone. (In this case it can be shown that the diagonal components of R_n are even in n and the off diagonal components are odd in n, so that only $n \geq 0$ need be calculated).

The modal reflection coefficients R_n are determined by matching the tangential field components at the column boundary, ρ_c. Therefore we require

H_z continuous at ρ_c

E_z continuous at ρ_c

$\frac{1}{b}\frac{\partial H_z}{\partial \rho}$ continuous at ρ_c

$\frac{\partial E_z}{\partial \rho}$ continuous at ρ_c (5B.11)

The modal fields inside the column must in general satisfy the equations (5A.11) and (5A.12). It is possible for solutions of these equations to become unbounded at the origin. However, we require the electric and magnetic energy densities [25]

$$\langle w_e \rangle = \frac{1}{4} \underline{E}^* \cdot \frac{\partial(\omega \underline{\underline{\varepsilon}})}{\partial \omega} \cdot \underline{E} \tag{5B.12}$$

$$\langle w_m \rangle = \frac{1}{4} \mu_o \underline{H}^* \cdot \underline{H} \tag{5B.13}$$

to be volume integrable in this region (the energy in any finite region being finite [26]). This in turn means that the axial fields, H_z and E_z, must be bounded at the origin. This condition completes the setup of the boundary value problem. We note in Section 5C that in certain cases, regarding the collisionless plasma as the limit of a lossy plasma, the solution will violate the intergrability of (5B.12).

Chapter 6 will consider the solution of the problem for the modal reflection coefficient matrix R_n. However, since in general, numerical methods will be required in solving (5A.11) and (5A.12) the method of invariant imbedding will be used to set up a rate of change equation for the quantity R_n. This matrix Riccati equation can then be integrated numerically to determine the scattered fields.

5C. Behavior of Fields Near the Origin

Before leaving this chapter, several interesting aspects of the field behavior near the origin will be considered. This will also serve as motivation for the types of solutions discussed in Chapter 6.

We consider here only cases where the plasma density is uniform allowing us to pass to the equations (5A.17) and (5A.18). For the moment let us take the magnetostatic field to be very large within the column of plasma. This means that

$$k_2^2 \to k_o^2$$

$$\beta_1 \to 0$$

$$\beta_2 \to 0$$

$$\nu^2 \to \left(1 - \frac{\omega_p^2}{\omega\omega_o}\right)n^2$$

resulting in the uncoupled equations

$$\frac{d^2H_z}{d\rho^2} + \frac{1}{\rho}\frac{dH_z}{d\rho} + \left(k_1^2 - \frac{\nu^2}{\rho^2}\right)H_z = 0 \tag{5C.1}$$

$$\frac{d^2E_z}{d\rho^2} + \frac{1}{\rho}\frac{dE_z}{d\rho} + \left(k_o^2 - \frac{n^2}{\rho^2}\right)E_z = 0 \tag{5C.2}$$

The solutions of (5C.1) and (5C.2) consistent with the finiteness condition at the origin are

$$H_z = J_\nu(k_1\rho) \tag{5C.3}$$

$$E_z = J_n(k_o\rho) \tag{5C.4}$$

The choice of the square root, ν, appearing in (5C.3) is obvious in the case ($\omega > \omega_p$), it being the positive branch. The collisionless case with ($\omega < \omega_p$) however results in a pure imaginary square root. The choice of the positive imaginary branch can be justified by allowing the collision frequency, ω_{eff}, to assume small positive values and performing analytic continuation [27], then allowing the medium to become lossless.

The solution (5C.4) is identical with the external free space solution and shows that there is no scattered wave for this polarization. The solution (5C.3) contains the isotropic plasma wave number k_1, as expected, however, the order of the Bessel function is not an integer. Very close to the origin we may expand the Bessel function to obtain

$$H_z \sim c_n\rho^{\nu} \tag{5C.5}$$

where c_n is a constant. The electric fields corresponding to this behavior are

$$E_\phi \sim -\frac{i\nu}{\omega b} c_n\rho^{\nu-1} \tag{5C.6}$$

$$E_\rho \sim -\frac{n}{\omega\varepsilon_o} c_n\rho^{\nu-1} \tag{5C.7}$$

Now when n is plus or minus one and ($\omega > \omega_p$) the quantity ν is real and lies between zero and one. (This can also be the case for greater values

of $|n|$). Equations (5C.6) and (5C.7) show that E_ϕ and E_ρ both become infinite at the origin. This fact is not too surprising if one considers further the characteristics of the medium. The dielectric tensor is given by

$$\underline{\underline{\varepsilon}} = \varepsilon_0 \begin{pmatrix} 1 & 0 & 0 \\ 0 & b/\varepsilon_0 & 0 \\ 0 & 0 & 1 \end{pmatrix} \tag{5C.8}$$

which describes a uniaxial medium. If instead of a plasma, we consider the construction of a medium with similar characteristics to those of (5C.8) made out of a laminated structure, we might be led to a medium such as that shown in Fig. 9. The wedges of alternating dielectric constant would be chosen to have thicknesses small compared to the wavelength. The structure shown in Fig. 9 would thus appear to have similar dielectric properties in the radial and axial directions, but quite different dielectric properties in the azimuthal direction. So qualitatively the characteristics of the medium shown in Fig. 9 resemble that of (5C.8). The singularity of fields near the tip of a dielectric wedge is well known [26]. A singularity in the E_ρ and E_ϕ field components near the origin of Fig. 9 would therefore be expected. Thus the behavior of E_ϕ and E_ρ given by (5C.6) and (5C.7) seems somewhat more reasonable. We can take this analogy a bit further by computing the form of the fields near the origin of Fig. 9. The H_z and E_ρ components in the m^{th} region can be written as [28]

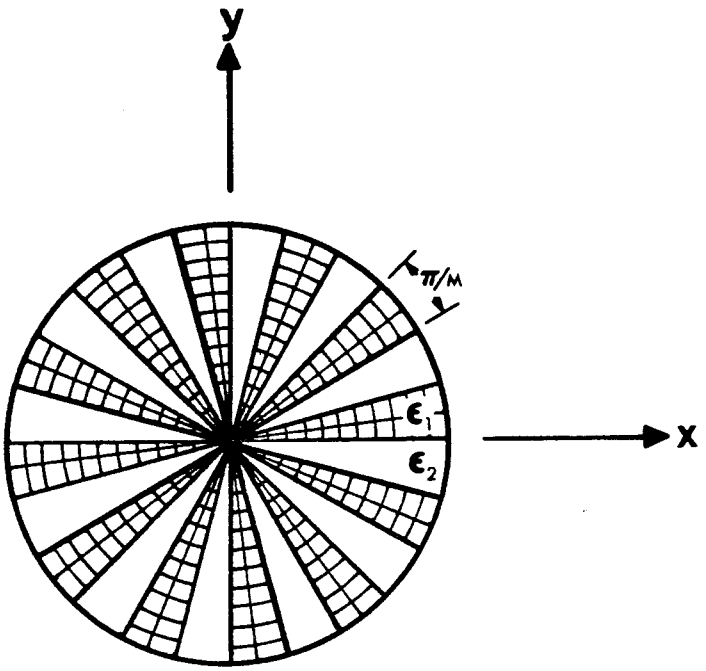

Fig. 9. A model for the magnetoactive plasma column consists of a series of wedges in contact with alternating dielectric properties, ε_1 and ε_2, each of thickness small compared to the wavelength.

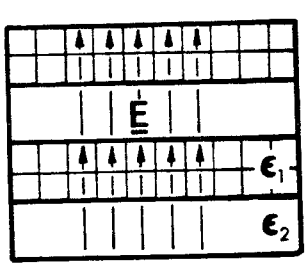

$$\epsilon_\perp = 2/(\epsilon_1^{-1} + \epsilon_2^{-1})$$

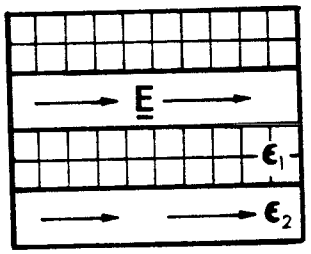

$$\epsilon_{||} = (\epsilon_1 + \epsilon_2)/2$$

Fig. 10. A planar stratified medium with alternating dielectric constants ε_1 and ε_2. Each layer is thin compared to the wavelength. The effective dielectric constants, $\varepsilon_\perp$ and $\varepsilon_{||}$, depend on the electric field orientation.

$$H_z = \rho^t (A_m \sin t\phi + B_m \cos t\phi) [1 + O(\rho)] \tag{5C.9}$$

$$E_\rho = \frac{i\, t\rho^{t-1}}{\omega} (A_m \cos t\phi - B_m \sin t\phi) [1 + O(\rho)] \tag{5C.10}$$

where A_m and B_m are unknown coefficients and t is an eigenvalue that determines the field behavior near the origin. The value of t is determined from the transcendental equation resulting from the enforcement of continuity of H_z and E_ρ at each interface. If we let the number of wedges, M, approach infinity, with alternating dielectric constants ε_1 and ε_2, the equation for t reduces to

$$\cos \pi t \sqrt{(\varepsilon_1 + \varepsilon_2)(\varepsilon_1^{-1} + \varepsilon_2^{-1})} = 1 \tag{5C.11}$$

which has solutions

$$t = 2j / \sqrt{(\varepsilon_1 + \varepsilon_2)(\varepsilon_1^{-1} + \varepsilon_2^{-1})}\ , \qquad j = 0, 1, 2, \ldots \tag{5C.12}$$

where we have neglected the negative solutions since H_z must be bounded. Fig. 10 shows two laminated slabs of material. When the wavelength of the electromagnetic wave is long compared to the thickness of each segment, a lumped circuit model can be used to determine the equivalent dielectric constant of the slab [29]. The dielectric constant thus depends on the orientation of the electric field as shown in Fig. 10. Assuming we can use these same equivalent parameters in the wedge geometry, (5C.12) becomes

$$t = j\sqrt{\varepsilon_{\perp}/\varepsilon_{||}} \tag{5C.13}$$

However in our problem we know

$$\varepsilon_{\perp} = b$$

$$\varepsilon_{||} = \varepsilon_o$$

which results in

$$t = j\sqrt{1 - \frac{\omega_p^2}{\omega^2}} \quad , \quad j = 0, 1, \ldots \tag{5C.14}$$

This equation gives values identical to the value of ν given above (5C.1). The order of the singularity can therefore also be predicted quantitatively by this wedge model.

Let us consider the case where ($\omega < \omega_p$) which makes ν become positive imaginary. The Poynting vector

$$\underline{S} = \frac{1}{2}\underline{E} \times \underline{H}^* \tag{5C.15}$$

computed for the fields (5C.5), (5C.6), and (5C.7) has two components S_ρ and S_ϕ. Let us consider at present the Poynting vector for only one angular mode.

The radial component of $\underline{S}$ near the origin is given by

$$S_\rho \sim - \left|c_n\right|^2 \frac{i\,\nu}{2\omega b}\, \rho^{\nu+\nu^*-1} \tag{5C.16}$$

and if we integrate over a cylindrical surface of unit length the radial power is

$$P_\rho \sim - \left|c_n\right|^2 \frac{i\nu\pi}{\omega b}\, \rho^{\nu+\nu^*} \tag{5C.17}$$

Now since ν is positive imaginary and b is negative this expression represents a time average flow of power inward.

$$P_\rho \sim - \left|c_n\right|^2 \left|\frac{\nu\pi}{\omega b}\right| \tag{5C.18}$$

The other angular modes can be taken into account simply by summing (5C.18) over the mode number n. We see from (5C.18) that there is a time average loss of power at the origin even though the medium is lossless. This effect resembles that which occurs near the tip of a conducting wedge immersed in a uniaxial plasma [30,31] where it has been referred to as intrinsic loss. The inward power flow (5C.18) vanishes sufficiently close to the origin if a small loss is allowed in the problem ($\omega_{eff} > 0$). However, in such a case large energy losses can be expected in the vicinity of the origin [32].

In summary, the problem involving infinite magnetostatic field thus gives rise to two rather interesting phenomena near the origin.

These phenomena are analogous to those found in wedge type problems.

The problem of finite (and possibly rho dependent) magnetostatic field results in the coupled equations (5A.17) and (5A.18). The solution of these equations is not so simple as (5C.3) and (5C.4). Nevertheless, the behavior of the field near the origin is similar to the solutions (5C.3) and (5C.4). For example, if a filamentary current exists at the origin, the magnetostatic field becomes large in the vicinity of the origin giving rise to the same type of behavior. The "homogeneous" problem (constant $B_{o\phi}$) also can result in singular behavior of the dynamic fields at the origin. (In this case if $\omega < \omega_p, -\omega_g$ then Im ν is taken to be positive, but if $\omega > \omega_p, -\omega_g$ and $\omega^2 < \omega_p^2 + \omega_g^2$ then Im ν is taken to be negative).

If the magnetostatic field vanishes at the origin, however, then all field components are finite there. The intrinsic loss phenomenon discussed by Hurd [30,31] is accompanied by infinite electric energy at the origin in the lossless limit. This is true here as well and in the resonance region of the radiation problem. In reality the energy will be finite as a result of various effects including losses, finite current density on the axis, and breakdown of the linear approximation.

CHAPTER 6

SOLUTION OF SCATTERING PROBLEM

The scattered fields resulting from a normally incident plane wave impinging on a gyroelectric plasma column will be determined. The external medium is assumed to be homogeneous and isotropic. The scattered fields can thus be described by the modal reflection coefficient matrix defined in Chapter 5. This quantity is shown to satisfy a matrix Riccati equation in Section 6A, which can be constructed by the method of invariant imbedding. This Riccati equation is not in general possible to solve analytically but can be integrated numerically. The determination of the reflection coefficient matrix is thus reduced to the solution of an initial value problem.

The invariant imbedding method allows us to build up the solution to a general inhomogeneous problem by considering the medium to consist of many thin annular shells. The material properties within each shell are usually assumed to be constant. The solution to Maxwell's equations must be known within each shell for the method to be useful. The assumption of constant properties within a shell forces us to consider the "homogeneous" problem described in Chapter 5. Section 6B discusses the solution to the "homogeneous" problem which is of considerable interest in itself. This solution however is not as readily calculable as the well known special functions. We therefore, as an alternative, allow the elements of the dielectric tensor to vary in a prescribed fashion within each shell. This variation is permitted solely to allow solution of the

resulting equations in terms of well known functions (Bessel functions). Section 6C discusses this alternative formulation of the invariant imbedding method.

6A. Invariant Imbedding Formulation

Chapter 5 showed that the scattering problem can be formulated in terms of the axial field components H_z and E_z. We therefore group these two field components into the row vector

$$W_i = \left(\sqrt{\frac{\mu_o}{\varepsilon_o}} H_{zi}^{inc} \quad E_{zi}^{inc} \right) \tag{6A.1}$$

$$i = 1, 2$$

where the subscript i denotes a particular solution to the field equations (5A.11) and (5A.12). Equations (5A.11) and (5A.12) being a coupled pair of second order equations have four linearly independent solutions. The two denoted by (6A.1) as W_i will be referred to as the "incident wave". The second pair of linearly independent solutions will be denoted by

$$V_i = \left(\sqrt{\frac{\mu_o}{\varepsilon_o}} H_{zi}^{scatt} \quad E_{zi}^{scatt} \right) \tag{6A.2}$$

$$i = 1, 2$$

and will be referred to as the "scattered wave". The choice of what constitutes the "incident wave" or the "scattered wave" is somewhat arbitrary. We will use two criterion for this selection. First we

require the "incident wave" to reduce to the Bessel functions of the first kind when the medium becomes homogeneous and isotropic. We further impose the condition that E_{z1}^{inc} and H_{z2}^{inc} vanish in this limit. The "incident wave" (6A.1) will also be required to have bounded axial field components at the origin of the coordinate system. Second we need the "scattered wave" to reduce to Hankel functions of the first kind when the medium becomes homogeneous and isotropic. We further impose the condition that E_{z1}^{scatt} and H_{z2}^{scatt} vanish in this limit. We will also only make use of solutions (6A.2) which represent outwardly moving waves.

The condition that the solutions (6A.1) and (6A.2) reduce to either Bessel or Hankel functions as the medium becomes homogeneous and isotropic will allow us to identify a multiplicative coefficient of (6A.2) in the external medium as the reflection coefficient. The boundedness of the incident solution (6A.1) at the origin will allow us to use the initial condition that the multiplier of the "scattered wave" (6A.2), the reflection coefficient, must vanish at the origin.

We group the solutions (6A.1) and (6A.2) into the two by two matrices

$$W = \begin{pmatrix} W_1 \\ \\ W_2 \end{pmatrix} \tag{6A.3}$$

$$V = \begin{pmatrix} V_1 \\ \\ V_2 \end{pmatrix} \tag{6A.4}$$

The formulation now follows that of Latham [15] except that we are dealing with matrices rather than scalars.

We must first consider the solution to two "elementary" problems which will define quantities needed in the formulation of the Riccati equation for the reflection coefficient. The first "elementary" problem consists of a modal wave impinging on a cylinder. The second consists of a source radiating at the axis of a cylinder.

The incoming elementary modal reflection coefficient matrix

$$\overleftarrow{r}(\rho_2, \rho_1)$$

is defined as the reflection coefficient when an n^{th} mode wave in an infinite medium, whose parameters are those of position ρ_2 in the final problem, is incident upon a uniform cylinder whose parameters correspond to position ρ_1 in the final problem, and is of radius ρ_1. Similarly, the incoming elementary transmission coefficient

$$\overrightarrow{t}(\rho_2, \rho_1)$$

is the amplitude of the wave in the interior of the cylinder. The total field U can therefore be written as

$$U = W(P(\rho_2), \rho) + \overleftarrow{r}(\rho_2, \rho_1) \quad V(P(\rho_2), \rho), \ \rho > \rho_1 \tag{6A.5}$$

$$U = \overrightarrow{t}(\rho_2, \rho_1) \ W(P(\rho_1), \rho), \ \rho < \rho_1 \tag{6A.6}$$

where the vector $P(\rho)$ indicates that the parameters of the medium are those at position ρ in the final problem. The matching of tangential field components at the boundary of the cylinder, ρ_1, gives

$$W(P(\rho_2), \rho_1) + \overleftarrow{r}(\rho_2, \rho_1)\, V(P(\rho_2), \rho_1) = \overrightarrow{t}(\rho_2, \rho_1)\, W(P(\rho_1), \rho_1) \tag{6A.7}$$

and

$$W'(P(\rho_2), \rho_1)\, S(P(\rho_2)) + \overleftarrow{r}(\rho_2, \rho_1)\, V'(P(\rho_2), \rho_1)\, S(P(\rho_2)) =$$

$$= \overrightarrow{t}(\rho_2, \rho_1)\, W'(P(\rho_1), \rho_1)\, S(P(\rho_1)) \tag{6A.8}$$

where the prime denotes differentiation with respect to ρ and $S(P(\rho))$ is the matrix

$$S = \begin{pmatrix} \frac{\epsilon_0}{b} & 0 \\ 0 & 1 \end{pmatrix} \tag{6A.9}$$

where b is the central element of the dielectric tensor (5A.5) evaluated at position ρ in the final problem. Solving (6A.7) and (6A.8) for $\overleftarrow{r}$ and $\overrightarrow{t}$ we obtain

$$\overleftarrow{r}(\rho_2, \rho_1) = \left[W(P(\rho_2), \rho_1)\, W^{-1}(P(\rho_1), \rho_1)\, W'(P(\rho_1), \rho_1)\, S(P(\rho_1))\right.$$

$$\left.-W'(P(\rho_2),\rho_1)\, S(P(\rho_2))\right]\left[V'(P(\rho_2), \rho_1)\, S(P(\rho_2)) - V(P(\rho_2), \rho_1)\, W^{-1}(P(\rho_1), \rho_1)\right.$$

$$\left.W'(P(\rho_1), \rho_1)\, S(P(\rho_1))\right]^{-1} \qquad (6A.10)$$

$$\overrightarrow{t}(\rho_2, \rho_1) = W(P(\rho_2), \rho_1)\, W^{-1}(P(\rho_1), \rho_1) + \overleftarrow{r}(\rho_2, \rho_1)\, V(P(\rho_2), \rho_1)$$

$$W^{-1}(P(\rho_1), \rho_1) \qquad (6A.11)$$

Expressions (6A.10) and (6A.11) will be used only when discontinuities occur in the dielectric profile of the final problem, taking $\rho_2 = \rho_1 + 0$. When the medium is continuous we let $\rho_2 = \rho_1 + \Delta$ and approximate (6A.10) and (6A.11) to first order in Δ as

$$\overleftarrow{r}(\rho_1 + \Delta, \rho_1) = \Delta\, D_1 + o(\Delta^2) \qquad (6A.12)$$

$$\overrightarrow{t}(\rho_1 + \Delta, \rho_1) = 1 + \Delta\, D_2 + o(\Delta^2) \qquad (6A.13)$$

where o is the conventional order symbol.
The matrices D_1 and D_2 are given by

$$D_1 = \left(\dot{W}\, W^{-1}\, W' - \dot{W}' - W'\, \dot{S}\, S^{-1}\right)\left(V' - V\, W^{-1}\, W'\right)^{-1} \qquad (6A.14)$$

$$D_2 = (\dot{W} + D_1 V) W^{-1} \tag{6A.15}$$

where the dot denotes

$$\dot{W}(P(\rho_1), \rho_1) = \sum_i \frac{\partial W}{\partial P_i} P_i'(\rho_1) \tag{6A.16}$$

$$\dot{W}'(P(\rho_1), \rho_1) = \sum \frac{\partial W'}{\partial P_i} P_i'(\rho_1) \tag{6A.17}$$

$$\dot{S}(P(\rho_1)) = \frac{\partial S}{\partial b} b' \tag{6A.18}$$

and $P_i(\rho_1)$ represents the elements of the medium parameter vector $P(\rho_1)$. All quantities in (6A.14) and (6A.15) are evaluated at position ρ_1 with medium parameters corresponding to position ρ_1 in the final problem.

We must also determine the elementary modal coefficients when a source coincides with the axis of the cylinder. The parameters of the cylinder are those of position ρ_1 in the final problem and those of the external medium are those of position ρ_2 in the final problem. The total field is given by

$$U = V(P(\rho_1), \rho) + \vec{r}(\rho_2, \rho_1) W(P(\rho_1), \rho), \rho < \rho_1 \tag{6A.19}$$

$$U = \overleftarrow{t}\,(\rho_2, \rho_1)\, V(P(\rho_2), \rho) \quad , \quad \rho > \rho_1 \tag{6A.20}$$

The boundary conditions at the boundary of the cylinder enable us to determine $\overrightarrow{r}$ and $\overleftarrow{t}$ as

$$\overrightarrow{r}\,(\rho_2, \rho_1) = \Big[V(P(\rho_1), \rho_1)V^{-1}(P(\rho_2), \rho_1)\, V'(P(\rho_2), \rho_1)\, S(P(\rho_2))$$

$$- V'(P(\rho_1), \rho_1)\, S(P(\rho_1))\Big]$$

$$\Big[W'(P(\rho_1), \rho_1)\, S(P(\rho_1)) - W(P(\rho_1), \rho_1)\, V^{-1}(P(\rho_2), \rho_1)\, V'(P(\rho_2), \rho_1)S(P(\rho_2))\Big]^{-1} \tag{6A.21}$$

$$\overleftarrow{t}\,(\rho_2, \rho_1) = V(P(\rho_1), \rho_1)\, V^{-1}(P(\rho_2), \rho_1)$$

$$+ \overrightarrow{r}\,(\rho_2, \rho_1)\, W(P(\rho_1), \rho_1)\, V^{-1}\,(P(\rho_2), \rho_1) \tag{6A.22}$$

we again take $\rho_2 = \rho_1 + \Delta$ and approximate these as

$$\overrightarrow{r}\,(\rho_1 + \Delta, \rho_1) = \Delta\, D_3 + O(\Delta^2) \tag{6A.23}$$

$$\overleftarrow{t}\,(\rho_1 + \Delta, \rho_1) = 1 + \Delta\, D_4 + O(\Delta^2) \tag{6A.24}$$

The matrices D_3 and D_4 are given by

$$D_3 = -(\dot{V} V^{-1} V' - \dot{V}' - V' \dot{S} S^{-1})(W' - W V^{-1} V')^{-1} \tag{6A.25}$$

$$D_4 = (-\dot{V} + D_3 W) V^{-1} \tag{6A.26}$$

where the dot denotes

$$\dot{V}(P(\rho_1), \rho_1) = \sum_i \frac{\partial V}{\partial P_i} P_i'(\rho_1) \tag{6A.27}$$

$$\dot{V}'(P(\rho_1), \rho_1) = \sum_i \frac{\partial V'}{\partial P_i} P_i'(\rho_1) \tag{6A.28}$$

Again all quantities in (6A.25) and (6A.26) are evaluated at position ρ_1 with medium parameters corresponding to position ρ_1 in final problem.

We are now in a position to determine the equation for the reflection coefficient matrix in the inhomogeneous problem. The geometry is shown in Fig. 11 which as been taken from Latham [15]. In the external medium the field can be written as

$$U = W(P(\rho_1 + \Delta), \rho) + R(\rho_1 + \Delta) V(P(\rho_1 + \Delta), \rho) \tag{6A.29}$$

We wish to determine an equation for the reflection coefficient matrix R by considering how it changes when a thin additional layer is added to the cylinder of radius ρ_1. Assuming the reflection coefficient of the original inhomogeneous cylinder of radius ρ_1 is $R(\rho_1)$ we may write

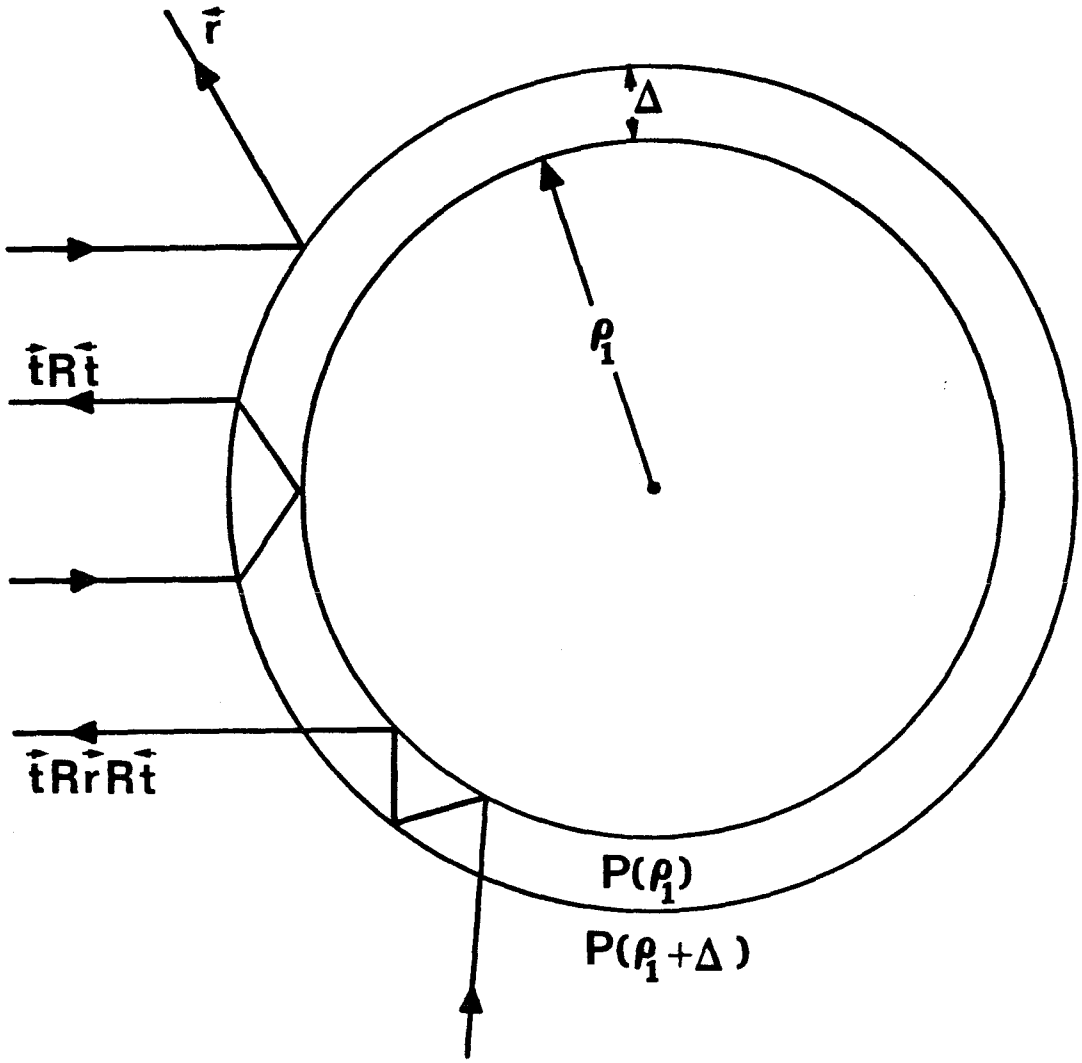

Fig. 11. A cylindrical shell of thickness Δ in which the material properties have the value of position ρ_1 in the inhomogeneous problem. The three rays shown are the ones that contribute to the change in reflection coefficient as Δ becomes small.

$$R(\rho_1 + \Delta) = \overleftarrow{r}\,(\rho_1 + \Delta, \rho_1) + \overrightarrow{t}\,(\rho_1 + \Delta, \rho_1)\, R(\rho_1)\, \overleftarrow{t}\,(\rho_1 + \Delta, \rho_1)$$

$$+ \overrightarrow{t}\,(\rho_1 + \Delta, \rho_1)\, R(\rho_1)\, \overrightarrow{r}\,(\rho_1 + \Delta, \rho_1)\, R(\rho_1)\, \overleftarrow{t}\,(\rho_1 + \Delta, \rho_1) + \ldots \quad (6A.30)$$

This series may be summed as

$$R(\rho_1 + \Delta) = \overleftarrow{r}\,(\rho_1 + \Delta, \rho_1) + \overrightarrow{t}\,(\rho_1 + \Delta, \rho_1)\left[1 - R(\rho_1)\, \overrightarrow{r}\,(\rho_1 + \Delta, \rho_1)\right]^{-1}$$

$$R(\rho_1)\, \overleftarrow{t}\,(\rho_1 + \Delta, \rho_1) \quad (6A.31)$$

However for small Δ we may approximate the right hand side of (6A.30) and obtain

$$R(\rho_1) + \Delta\, \dot{R}(\rho_1) = \Delta\, D_1 + R(\rho_1) + \Delta\, D_2\, R(\rho_1) + \Delta\, R(\rho_1)\, D_4 +$$

$$+ \Delta\, R(\rho_1)\, D_3\, R(\rho_1) + O(\Delta^2) \quad (6A.32)$$

where the dot denotes differentiation with respect to ρ_1. This equation gives us the equation for the reflection coefficient matrix $R(\rho_1)$

$$\dot{R}(\rho_1) = D_1 + D_2\, R(\rho_1) + R(\rho_1)\, D_4 + R(\rho_1)\, D_3\, R(\rho_1) \quad (6A.33)$$

which is a matrix Riccati equation. As described at the beginning of this section, the incident and scattered components of the field will be

chosen so that the initial condition associated with (6A.33) will be

$$R(0) = 0 \tag{6A.34}$$

Equations (6A.33) and (6A.34) thus together constitute an initial value problem for R. At any points of discontinuity in material properties we must use (6A.31) which can be written as

$$R(\rho_1 + 0) = \overleftarrow{r}\,(\rho_1 + 0, \rho_1) + \overrightarrow{t}\,(\rho_1 + 0, \rho_1)\left[1 - R(\rho_1)\,\overrightarrow{r}\,(\rho_1 + 0, \rho_1)\right]^{-1}$$

$$R(\rho_1)\,\overleftarrow{t}\,(\rho_1 + 0, \rho_1) \tag{6A.35}$$

The radius ρ_c represents the boundary of the inhomogeneous plasma cylinder. The incident and scattered components of the modal field reduce to Bessel and Hankel functions in the external medium. This makes it possible to identify $R(\rho_c)$ with the modal reflection coefficients R_n defined in Chapter 5 (5B.5), (5B.6), and (5B.7). The solution of this initial value problem thus provides us with the scattered fields in the external region.

The choice of the solutions (6A.1) and (6A.2) to the field equations, which appear in the coefficients of equation (6A.33), will be discussed in the following two sections.

6B. Solution to "Homogeneous" Modal Equations

The solutions (6A.1) and (6A.2) used to formulate the Riccati equation for the reflection coefficient are solutions to Maxwell's equations in a cylindrical shell with certain assumed variations in material properties. It is typically assumed that the material properties are constant within such a shell. The "homogeneous" problem described in Chapter 5 gives rise to constant material properties. Equations (5A.17) and (5A.18) with rho independent parameters must therefore be solved to determine the axial fields. We hasten to point out that the "homogeneous" problem is interesting in itself since it provides a tractable setting in which to view many aspects of the scattering problem. To effect a solution of (5A.17) and (5A.18) we first transform them into

$$\frac{d^2h}{d\xi^2} + \frac{1}{\xi}\frac{dh}{d\xi} + \left(1 - \frac{\nu^2}{\xi^2}\right) h = i\,\frac{\beta}{\xi}\,e \tag{6B.1}$$

$$\frac{d^2e}{d\xi^2} + \frac{1}{\xi}\frac{de}{d\xi} + \left(k^2 - \frac{n^2}{\xi^2}\right) e = -\,i\,\frac{\beta}{\xi}\,h \tag{6B.2}$$

where $\xi = k_1\rho$, $k^2 = k_2^2/k_1^2 = \dfrac{a^2 - g^2}{ab}$, $\beta = \sqrt{\beta_1\beta_2}/k_1 = ng/a$,

$e = \sqrt{\beta_1}\,E_z$, $h = \sqrt{\beta_2}\,H_z$

It is possible to obtain fourth order equations for each of the axial field components. The only singular points of the fourth order equations are at the origin (regular singular point) and infinity (irregular singular point).

A solution of (6B.1) and (6B.2) can be determined by the method of Frobenius [33]. Assuming that ν is not equal to an integer and that $n > 0$ with $\mathrm{Re}\ \nu > 0$ we write the four solutions as

$$h_{\pm}^{(1)} = \sum_{m=0}^{\infty} a_m^{(1)\pm}\, \xi^{2m \pm \nu} \tag{6B.3}$$

$$e_{\pm}^{(1)} = \sum_{m=0}^{\infty} b_m^{(1)\pm}\, \xi^{2m \pm \nu + 1} \tag{6B.4}$$

$$h_{\pm}^{(2)} = \sum_{m=0}^{\infty} a_m^{(2)\pm}\, \xi^{2m \pm n + 1} + \kappa^{\pm} h_{+}^{(2)}\, \ell n\, \xi \tag{6B.5}$$

$$e_{\pm}^{(2)} = \sum_{m=0}^{\infty} b_m^{(2)\pm}\, \xi^{2m \pm n} + \kappa^{\pm} e_{+}^{(2)}\, \ell n\, \xi \tag{6B.6}$$

which converge for $|\xi| < \infty$ and where the coefficients satisfy the recurrence relations

$$a_{m+1}^{(1)\pm}\left[(2m \pm \nu + 2)^2 - \nu^2\right] + a_m^{(1)\pm} = i\,\beta\, b_m^{(1)\pm}$$

$$b_m^{(1)\pm}\left[(2m \pm \nu + 1)^2 - n^2\right] + k^2\, b_{m-1}^{(1)\pm} = -\,i\,\beta\, a_m^{(1)\pm}$$

$$a_o^{(1)\pm} = 1$$

$$a_m^{(2)\pm}\left[(2m \pm n + 1)^2 - \nu^2\right] + a_{m-1}^{(2)\pm} = i\,\beta\, b_m^{(2)\pm} - 2(2m-n+1)\kappa^{\pm}\, a_{m-n}^{(2)+}$$

$$b_{m+1}^{(2)\pm}\left[(2m \pm n + 2)^2 - n^2\right] + k^2\, b_m^{(2)\pm} = -\,i\,\beta\, a_m^{(2)\pm} - 2(2m-n+2)\kappa^{\pm}\, b_{m-n}^{(2)+}$$

$$b_o^{(2)\pm} = 1$$

and

$$\kappa^{\pm} = \begin{pmatrix} 0 \\ \\ -\left(k^2\, b_{n-1}^{(2)-} + i\,\beta\, a_{n-1}^{(2)-}\right)/2n \end{pmatrix}$$

Coefficients with negative subscripts in the above recurrence relations are taken to be zero. The restriction $n > 0$ results in no loss of generality since the solutions for $n < 0$ can be obtained by using the above equations with n positive and Re ν positive, but taking $-\underline{e}_{\pm}^{(1)}$, $-\underline{h}_{\pm}^{(2)}$ instead of $\underline{e}_{\pm}^{(1)}$, $\underline{h}_{\pm}^{(2)}$ (since β is proportional to n and changes sign). The case $n = 0$ results in uncoupled Bessel equations with solutions

$$\underline{h}_{\pm}^{(1)} = \begin{pmatrix} J_0(\xi) \\ \\ Y_0(\xi) \end{pmatrix}$$

$$\underline{e}_{\pm}^{(1)} = 0 \qquad \text{(6B.7)}$$

$$\underline{h}_{\pm}^{(2)} = 0$$

$$\underline{e}_{\pm}^{(2)} = \begin{pmatrix} J_0(k\xi) \\ \\ Y_0(k\xi) \end{pmatrix}$$

The "homogeneous" scattering problem can now be solved by taking

$$W(P(\rho_1),\ \rho) = \begin{pmatrix} \sqrt{\frac{\mu_o}{\varepsilon_o \beta_2}}\, h_+^{(1)} & \frac{1}{\sqrt{\beta_1}}\, e_+^{(1)} \\ \sqrt{\frac{\mu_o}{\varepsilon_o \beta_2}}\, h_+^{(2)} & \frac{1}{\sqrt{\beta_1}}\, e_+^{(2)} \end{pmatrix} \tag{6B.8}$$

inside the plasma column and

$$W(P(\rho_2),\ \rho) = \begin{pmatrix} \sqrt{\frac{\mu_o}{\varepsilon_o}}\, J_n(k_o\rho) & 0 \\ 0 & J_n(k_o\rho) \end{pmatrix} \tag{6B.9}$$

$$V(P(\rho_2),\ \rho) = \begin{pmatrix} \sqrt{\frac{\mu_o}{\varepsilon_o}}\, H_n^{(1)}(k_o\rho) & 0 \\ 0 & H_n^{(1)}(k_o\rho) \end{pmatrix} \tag{6B.10}$$

in the external free space region.

These are then used in equation (6A.10) at the boundary of the column to find $\overleftarrow{r}$. The elementary reflection coefficient, $\overleftarrow{r}$, coincides with the total reflection coefficient, $R(\rho_1 + 0)$, as seen from (6A.35) since $R(\rho_1)$ is zero when the cylinder is "homogeneous". Examples of this "homogeneous" solution are given in Section 7A. The solution (6B.8) also can be used as the solution W in the inhomogeneous problem. The solution is rather simple because we have taken the magnetic field to be independent of radius

resulting in modal equations with only one finite singular point, at the origin.

The minus solutions were not needed in this case as a result of the required boundedness of the axial fields at the origin. These solutions will be required however to form the scattered field V in the invariant imbedding method.

An asymptotic solution to the modal equations (6B.1) and (6B.2) for large values of $|\xi|$ can be written as [34]

$$h_{\pm}^{(3)} \sim e^{\pm i\xi} \sum_{m=0}^{\infty} a_m^{(3)\pm} \xi^{-\frac{1}{2}-m} \tag{6B.11}$$

$$e_{\pm}^{(3)} \sim e^{\pm i\xi} \sum_{m=0}^{\infty} b_m^{(3)\pm} \xi^{-\frac{3}{2}-m} \tag{6B.12}$$

$$h_{\pm}^{(4)} \sim e^{\pm ik\xi} \sum_{m=0}^{\infty} a_m^{(4)\pm} \xi^{-\frac{3}{2}-m} \tag{6B.13}$$

$$e_{\pm}^{(4)} \sim e^{\pm ik\xi} \sum_{m=0}^{\infty} b_m^{(4)\pm} \xi^{-\frac{1}{2}-m} \tag{6B.14}$$

for $|\xi| \to \infty$

where the coefficients satisfy the recurrence relations

$$\mp i\, 2(m+1)\, a_{m+1}^{(3)\pm} + \left[\left(\tfrac{1}{2}+m\right)^2 - \nu^2\right] a_m^{(3)\pm} = i\,\beta\, b_m^{(3)\pm}$$

$$(k^2-1)\, b_{m+1}^{(3)\pm} \mp i\, 2(m+1)\, b_m^{(3)\pm} + \left[\left(\tfrac{1}{2}+m\right)^2 - n^2\right] b_{m-1}^{(3)\pm} =$$

$$= -i\,\beta\, a_{m+1}^{(3)\pm}$$

$$a_o^{(3)\pm} = 1$$

$$(1-k^2)\, a_{m+1}^{(4)\pm} \mp i\, 2\, k(m+1)\, a_m^{(4)\pm} + \left[\left(\tfrac{1}{2}+m\right)^2 - \nu^2\right] a_{m-1}^{(4)\pm} = i\,\beta\, b_{m+1}^{(4)\pm}$$

$$\mp i\, 2\, k(m+1)\, b_{m+1}^{(4)\pm} + \left[\left(\tfrac{1}{2}+m\right)^2 - n^2\right] b_m^{(4)\pm} = -\,i\,\beta\, a_m^{(4)\pm}$$

$$b_o^{(4)\pm} = 1$$

The physical values of ξ will be restricted to either entirely positive real or positive imaginary. It is therefore appropriate to take

$$V = \begin{pmatrix} \sqrt{\frac{\mu_o}{\varepsilon_o \beta_2}}\, h_+^{(3)} & \frac{1}{\sqrt{\beta_1}}\, e_+^{(3)} \\ \sqrt{\frac{\mu_o}{\varepsilon_o \beta_2}}\, h_+^{(4)} & \frac{1}{\sqrt{\beta_1}}\, e_+^{(4)} \end{pmatrix} \tag{6B.15}$$

since this will represent either an expanding cylindrical wave, when ξ is real, or an evanescent solution, when ξ is imaginary.

These asymptotic solutions have greater importance than merely defining the scattered wave (6B.15). For example, large "homogeneous" columns will require the evaluation of the solution to the modal equations with large arguments. It is far easier to evaluate such solutions by use of the asymptotic representations than the series representations.

Since the modal equations (6B.1) and (6B.2) are coupled second order differential equations there exist four linearly independent solution pairs (h e). It must therefore be possible to write each of the series solutions as an appropriate linear combination of the four asymptotic solutions and vice versa. The coefficients in these relations are known as connecting constants. These constants are not determined by the local analyses used to obtain (6B.3) through (6B.6) and (6B.11) through (6B.14). Their evaluation forms a much more complicated global problem. But their evaluation is necessary for the asymptotic expansions to be of use in calculating the modal solutions $h_{\pm}^{(1)}$, $e_{\pm}^{(1)}$, $h_{\pm}^{(2)}$, $e_{\pm}^{(2)}$ for large arguments, or for the series expansions to be of use in

calculating $h_{\pm}^{(3)}$, $e_{\pm}^{(3)}$, $h_{\pm}^{(4)}$, $e_{\pm}^{(4)}$ for small arguments.

The connection problem can be related to one which has been studied previously, namely, the second order equation with four regular singular points (Heun's equation). This can be shown by assuming a solution of (6B.1) and (6B.2) in the form of Hankel transforms. The procedure is carried out in Appendix 6. It is shown that the connection of (6B.3) through (6B.6) to (6B.11) through (6B.14) involves the connection constants of solutions to Heun's equation about the various singular points. The connection problem for Heun's equation has been studied. The connecting constants can be determined as the sum of factorial series [16,35].

We have thus shown that the functions which are solutions of the modal equations (6B.1) and (6B.2) can be determined by methods of local analysis in the form of Frobenius series and asymptotic series. Furthermore, the connection between these two forms can be accomplished in terms of the connection between solutions of Heun's equation, a problem which has been studied.

Section 7A presents the results of this "homogeneous" problem for moderate size columns. The modal solutions in this case were calculated by means of the Frobenius solutions.

6C. Bessel Function Solution to "Inhomogeneous" Modal Equations

Solutions to the modal equations (5A.11) and (5A.12) in the case when the dielectric tensor varies with rho in a prescribed fashion will now be discussed. The goal of the present section is to find what type of rho variation the dielectric tensor must possess such that the modal equations have solutions involving well known functions. This dielectric tensor must remain flexible enough, however, to form a close approximation to the actual inhomogeneous dielectric profile over a thin annular region.

Since we are dealing with cylindrical geometry we expect Bessel functions to play some role in these solutions. The synthesis of a dielectric profile which gives rise to solutions in the form of well known functions is not a unique process. But in this discussion we limit ourselves to two different types of rho variation. To accomplish our goal the dielectric tensor must first be generalized to the form

$$\underline{\underline{\varepsilon}} = \begin{pmatrix} a_1 & 0 & ig \\ 0 & b & 0 \\ -ig & 0 & a_2 \end{pmatrix} \tag{6C.1}$$

which when inserted into Maxwell's equations leads to

$$\frac{d^2H_z}{d\rho^2} + \left(\frac{1}{\rho} - \frac{1}{b}\frac{db}{d\rho}\right)\frac{dH_z}{d\rho} + \left(\omega^2\mu_o b - \frac{n^2}{\rho^2}\frac{b}{a_1}\right)H_z = i\frac{g}{a_1}\frac{n}{\rho}\omega b\, E_z \tag{6C.2}$$

$$\frac{d^2E_z}{d\rho^2} + \frac{1}{\rho}\frac{dE_z}{d\rho} + \left[\omega^2\mu_o\left(a_2 - \frac{g^2}{a_1}\right) - \frac{n^2}{\rho^2}\right]E_z = -i\frac{g}{a_1}\frac{n}{\rho}\omega\mu_o H_z \qquad (6C.3)$$

we now choose a particular form for the functions a_1, a_2, b, and g. A useful choice is

$$\underline{\underline{\varepsilon}} = \begin{pmatrix} \hat{a} & 0 & i\frac{\hat{g}}{\rho} \\ 0 & \hat{b} & 0 \\ -i\frac{\hat{g}}{\rho} & 0 & \hat{b} - \frac{\hat{\delta}^2}{\rho^2} \end{pmatrix} \qquad (6C.4)$$

where $\hat{a}$, $\hat{b}$, $\hat{g}$, and $\hat{\delta}$ are constants. Equations (6C.2) and (6C.3) become

$$\frac{d^2H_z}{d\rho^2} + \frac{1}{\rho}\frac{dH_z}{d\rho} + \left(\hat{k}_1^2 - \frac{\hat{\nu}^2}{\rho^2}\right)H_z = i\frac{\hat{\beta}_1}{\rho^2}E_z \qquad (6C.5)$$

$$\frac{d^2E_z}{d\rho^2} + \frac{1}{\rho}\frac{dE_z}{d\rho} + \left(\hat{k}_1^2 - \frac{\hat{\mu}^2}{\rho^2}\right)E_z = -i\frac{\hat{\beta}_2}{\rho^2}H_z \qquad (6C.6)$$

where $\hat{k}_1^2 = \omega^2 \mu_o \hat{b}$, $\hat{\nu}^2 = n^2 \frac{\hat{b}}{\hat{a}}$, $\hat{\beta}_1 = \frac{\hat{g}}{\hat{a}} n\omega\hat{b}$, $\hat{\beta}_2 = \frac{\hat{g}}{\hat{a}} n\omega\mu_o$,

$$\hat{\mu}^2 = n^2 + \left(\frac{\hat{g}^2}{\hat{a}} + \hat{\delta}^2 \right) \omega^2 \mu_o$$

The solution to (6C.5) and (6C.6) can be obtained by substituting

$$H_z = x \mathscr{C}_\lambda (\hat{k}_1 \rho) \tag{6C.7}$$

$$E_z = y \mathscr{C}_\lambda (\hat{k}_1 \rho) \tag{6C.8}$$

where $\mathscr{C}_\lambda (\hat{k}_1 \rho)$ is a cylinder function of order λ, and x, y, and λ are constants to be determined. Substitution of this trial solution results in the equations

$$(\lambda^2 - \hat{\nu}^2)\, x = i\hat{\beta}_1\, y \tag{6C.9}$$

$$(\lambda^2 - \hat{\mu}^2)\, y = - i\hat{\beta}_2\, x \tag{6C.10}$$

Equations (6C.9) and (6C.10) constitute an eigenvalue problem. The eigenvalue λ^2 can be determined by the requirement that the determinant vanish yielding

$$(\lambda^2 - \hat{\nu}^2)\, (\lambda^2 - \hat{\mu}^2) - \hat{\beta}_1\, \hat{\beta}_2 = 0 \tag{6C.11}$$

Denoting by λ_1 and λ_2 the two solutions of (6C.11) with

positive real parts, the solutions of the modal equations can now be written in the form

$$W = \begin{pmatrix} \sqrt{\frac{\mu_o}{\varepsilon_o}}\, x_1 J_{\lambda_1}(\hat{k}_1\rho) & y_1 J_{\lambda_1}(\hat{k}_1\rho) \\ \sqrt{\frac{\mu_o}{\varepsilon_o}}\, x_2 J_{\lambda_2}(\hat{k}_1\rho) & y_2 J_{\lambda_2}(\hat{k}_1\rho) \end{pmatrix} \tag{6C.12}$$

$$V = \begin{pmatrix} \sqrt{\frac{\mu_o}{\varepsilon_o}}\, x_1 H^{(1)}_{\lambda_1}(\hat{k}_1\rho) & y_1 H^{(1)}_{\lambda_1}(\hat{k}_1\rho) \\ \sqrt{\frac{\mu_o}{\varepsilon_o}}\, x_2 H^{(1)}_{\lambda_2}(\hat{k}_1\rho) & y_2 H^{(1)}_{\lambda_2}(\hat{k}_1\rho) \end{pmatrix} \tag{6C.13}$$

W and V are the "incident" and "scattered" solutions described in Section 6A, and the ratios of x_1 to y_1 or x_2 to y_2 are determined from (6C.9) or (6C.10) using λ_1^2 or λ_2^2, respectively. The matrices (6C.12) and (6C.13) thus form the set of solutions required in the formulation of the Riccati equation for the reflection coefficient R. The values of the parameters entering equations (6C.5) and (6C.6) are varied to make the dielectric tensor (6C.4) fit the actual tensor (5A.5). This means we must have

$$\hat{k}_1^2 = k_1^2$$

$$\hat{\nu}^2 = \nu^2$$

$$\hat{\beta}_1 = \rho\beta_1$$

$$\hat{\beta}_2 = \rho\beta_2$$

$$\hat{\mu}^2 = n^2 + \rho^2 (k_1^2 - k_2^2)$$

The solutions (6C.12) and (6C.13) provide a rather flexible model, namely dielectric tensor (6C.4), for building up arbitrary profiles via the invariant imbedding method. This fact can be illustrated by considering two limits. When the plasma density vanishes near the boundary of the column, the order, λ, becomes an integer, n, reducing (6C.12) and (6C.13) to free space solutions (note that k_1 becomes k_0 in this limit). Secondly, near the origin the incident solution, (6C.12), is flexible enough to take on the various types of field behavior discussed in Section 5C. Therefore, although in themselves (6C.12) and (6C.13) do not represent solutions of interest in the context of the medium described by the dielectric tensor (5A.5), they are useful in building up such a solution. The invariant imbedding method thus treats the actual profile as consisting of many thin annular slabs of this inhomogeneous anisotropic medium.

There is a drawback to using solutions W and V, defined by (6C.12) and (6C.13), in the invariant imbedding scheme. The derivative

$$\dot{W} = \sum_i \frac{\partial W}{\partial P_i} P_i'$$

and similarly

$$\dot{V},\ W',\ V'$$

required in Section 6A are taken with respect to parameters of the medium which vary with radial distance. This means that derivatives of W and V must be taken with respect to λ. However the derivatives of Bessel functions with respect to order are not included in standard numerical libraries. For this reason a second choice of the functions a_1, a_2, g, b will be considered. The second choice of the tensor is

$$\underline{\underline{\varepsilon}} = \begin{pmatrix} a_1 & 0 & i\hat{g}\rho a_1 \\ 0 & \hat{b} & 0 \\ -i\hat{g}\rho a_1 & 0 & a_2+\hat{g}^2\rho^2 a_1 \end{pmatrix} \tag{6C.14}$$

where $a_1 = 1/(1/\hat{b} + \hat{a}_1\rho^2)$, and $\hat{a}_1$, $\hat{a}_2$, $\hat{g}$, $\hat{b}$ are constants. The modal equations (6C.2) and (6C.3) thus become

$$\frac{d^2H_z}{d\rho^2} + \frac{1}{\rho}\frac{dH_z}{d\rho} + \left(\hat{k}_1^2 - \frac{n^2}{\rho^2}\right)H_z = i\hat{\beta}_1 E_z \tag{6C.15}$$

$$\frac{d^2E_z}{d\rho^2} + \frac{1}{\rho}\frac{dE_z}{d\rho} + \left(\hat{k}_2^2 - \frac{n^2}{\rho^2}\right)E_z = -i\hat{\beta}_2 H_z \tag{6C.16}$$

where $\hat{k}_1^2 = (\omega^2\mu_o - n^2\hat{a}_1)\hat{b}$

$$\hat{k}_2^2 = \omega^2 \mu_o \hat{a}_2$$

$$\hat{\beta}_1 = \hat{g} n \omega \hat{b}$$

$$\hat{\beta}_2 = \hat{g} n \omega \mu_o$$

The solution to (6C.15) and (6C.16) can be obtained by substituting

$$H_z = x \mathscr{C}_n (\gamma \rho) \tag{6C.17}$$

$$E_z = y \mathscr{C}_n (\gamma \rho) \tag{6C.18}$$

where x, y, and γ are constants to be determined. This yields the equations

$$(\hat{k}_1^2 - \gamma^2)\, x = i\hat{\beta}_1\, y \tag{6C.19}$$

$$(\hat{k}_2^2 - \gamma^2)\, y = - i\hat{\beta}_2\, x \tag{6C.20}$$

Equations (6C.19) and (6C.20) have non trivial solutions provided the determinant vanishes or

$$(\hat{k}_1^2 - \gamma^2)\,(\hat{k}_2^2 - \gamma^2) - \hat{\beta}_1 \hat{\beta}_2 = 0 \tag{6C.21}$$

which has solutions

$$\gamma^2 = \frac{1}{2}(\hat{k}_1^2 + \hat{k}_2^2) \pm \frac{1}{2}\sqrt{(\hat{k}_1^2 - \hat{k}_2^2)^2 + 4\hat{\beta}_1\hat{\beta}_2} \tag{6C.22}$$

where by γ_1^2 we will denote the + sign value, and by γ_2^2 the - sign value. The solutions of the modal equations may therefore be written as

$$W = \begin{pmatrix} \sqrt{\frac{\mu_o}{\varepsilon_o}}\, x_1 J_n(\gamma_1\rho) & y_1 J_n(\gamma_1\rho) \\ \sqrt{\frac{\mu_o}{\varepsilon_o}}\, x_2 J_n(\gamma_2\rho) & y_2 J_n(\gamma_2\rho) \end{pmatrix} \tag{6C.23}$$

$$V = \begin{pmatrix} \sqrt{\frac{\mu_o}{\varepsilon_o}}\, x_1 H_n^{(1)}(\gamma_1\rho) & y_1 H_n^{(1)}(\gamma_1\rho) \\ \sqrt{\frac{\mu_o}{\varepsilon_o}}\, x_2 H_n^{(1)}(\gamma_2\rho) & y_2 H_n^{(1)}(\gamma_2\rho) \end{pmatrix} \tag{6C.24}$$

where $(\hat{k}_1^2 - \gamma_1^2)x_1 = i\hat{\beta}_1 y_1$

$$(\hat{k}_2^2 - \gamma_2^2)y_2 = -i\hat{\beta}_2 x_2$$

The values of the parameters entering equations (6C.15) and (6C.16) are varied to make the dielectric tensor (6C.14) fit the actual tensor (5A.5). This determines these parameters as

$$\hat{k}_1^2 = k_1^2 - (\nu^2 - n^2)/\rho^2$$

$$\hat{k}_2^2 = k_2^2$$

$$\hat{\beta}_1 = \beta_1/\rho$$

$$\hat{\beta}_2 = \beta_2/\rho$$

The solutions (6C.23) and (6C.24) reduce to the free space solutions when the plasma density vanishes (γ^2 becomes k_0^2). However, the type of field behavior near the origin modeled by these solutions is somewhat restricted. This fact is evident from inspection of the "incident" solution (6C.23). The ϕ component of the electric field, which is the derivative of H_z with respect to ρ, remains bounded at the origin. As noted in Section 5C bounded fields result when the magnetostatic field vanishes at the origin. Therefore the solutions (6C.23) and (6C.24) are most useful in solving problems where this condition is actually met at the origin.

The solutions (6C.23) and (6C.24) were used to set up a computer program to determine the reflection coefficient matrix via the Riccati equation of Section 6A. A slightly modified form of (6C.23) and (6C.24) were actually implemented in the program. These modifications are required for certain numerical purposes as well as to make the off diagonal elements vanish as the external region is approached. They are discussed briefly in Appendix 7. Chapter 7 presents solutions obtained using this program.

CHAPTER 7

RESULTS OF SCATTERING PROBLEM

This chapter presents the results of the scattering problem. Section 7A discusses the "homogeneous" case whose solution was given in Section 6B. A qualitative interpretation of the results is given by considering Faraday rotation in a magnetized plasma (with plane biasing field). Section 7B presents several examples of inhomogeneous columns. The solutions in Section 7B were calculated by numerical integration of the matrix Riccati equation for the reflection coefficient.

7A. "Homogeneous" Plasma Column

We present in this section several examples of scattering from a "homogeneous" plasma column. The results were calculated through use of the series expansions of the modal equations described in Section 6B.

Since the exterior medium is reciprocal there exists a simple relation among the four entries of the reflection coefficient matrix [36]. Indeed, in conformity with its definition, in Section 5B, we must have

$$R^{12} = - R^{21} \tag{7A.1}$$

Figure 12 comprises a sequence of scattering results for various plasma column radii. Three magntiudes and phases, θ, are given on each plot. The curves labeled H represent the magnitude and phase of R^{11} and correspond to an incident plane wave with the H field in the axial

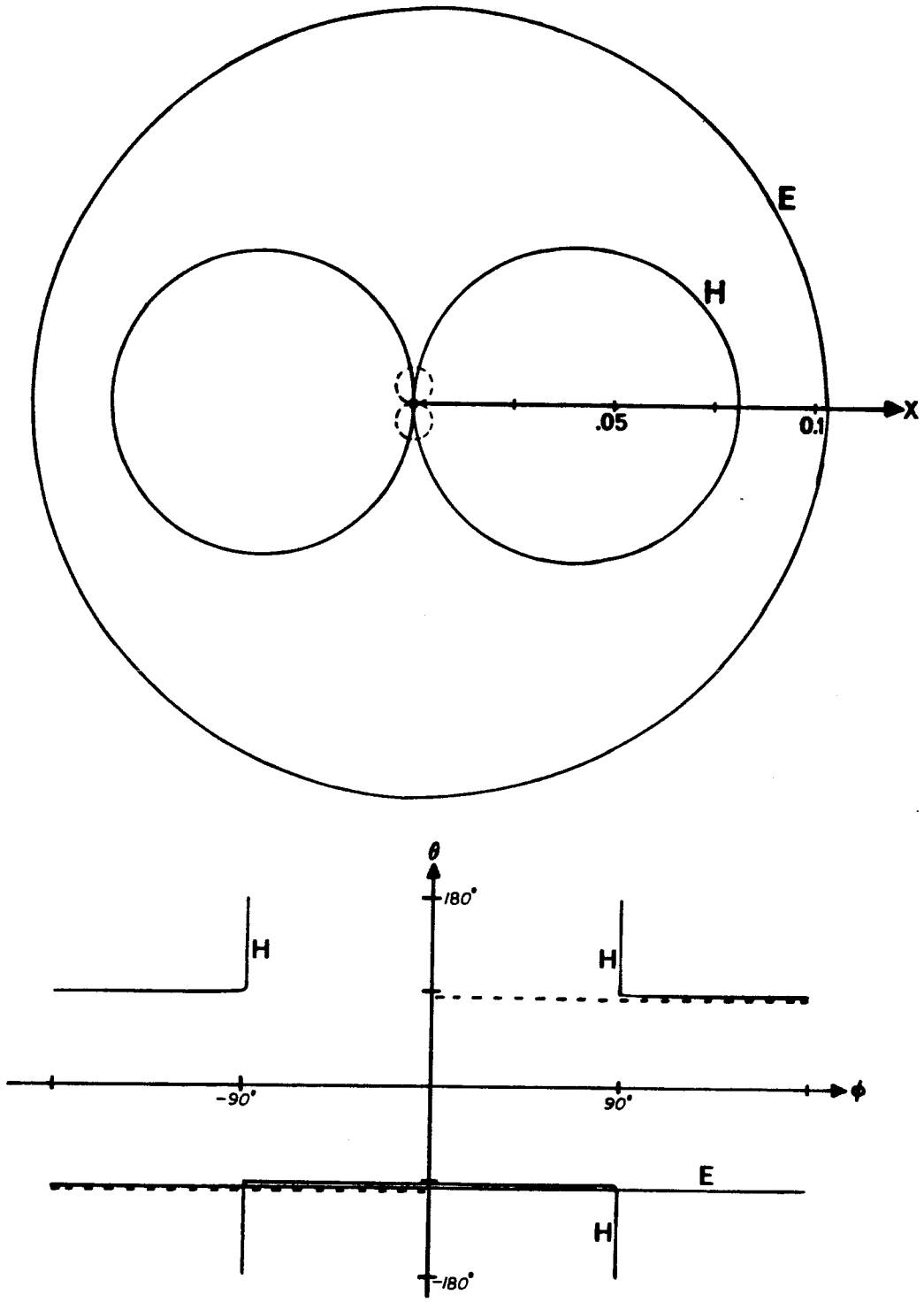

Fig. 12. A sequence of scattering patterns are shown. The plasma parameters are $\omega_p/\omega = 3/5$ and $-\omega_g/\omega = 3/5$. Both for zone field amplitude and phase are included.

(a) $k_o\rho_c = \frac{5}{12}$

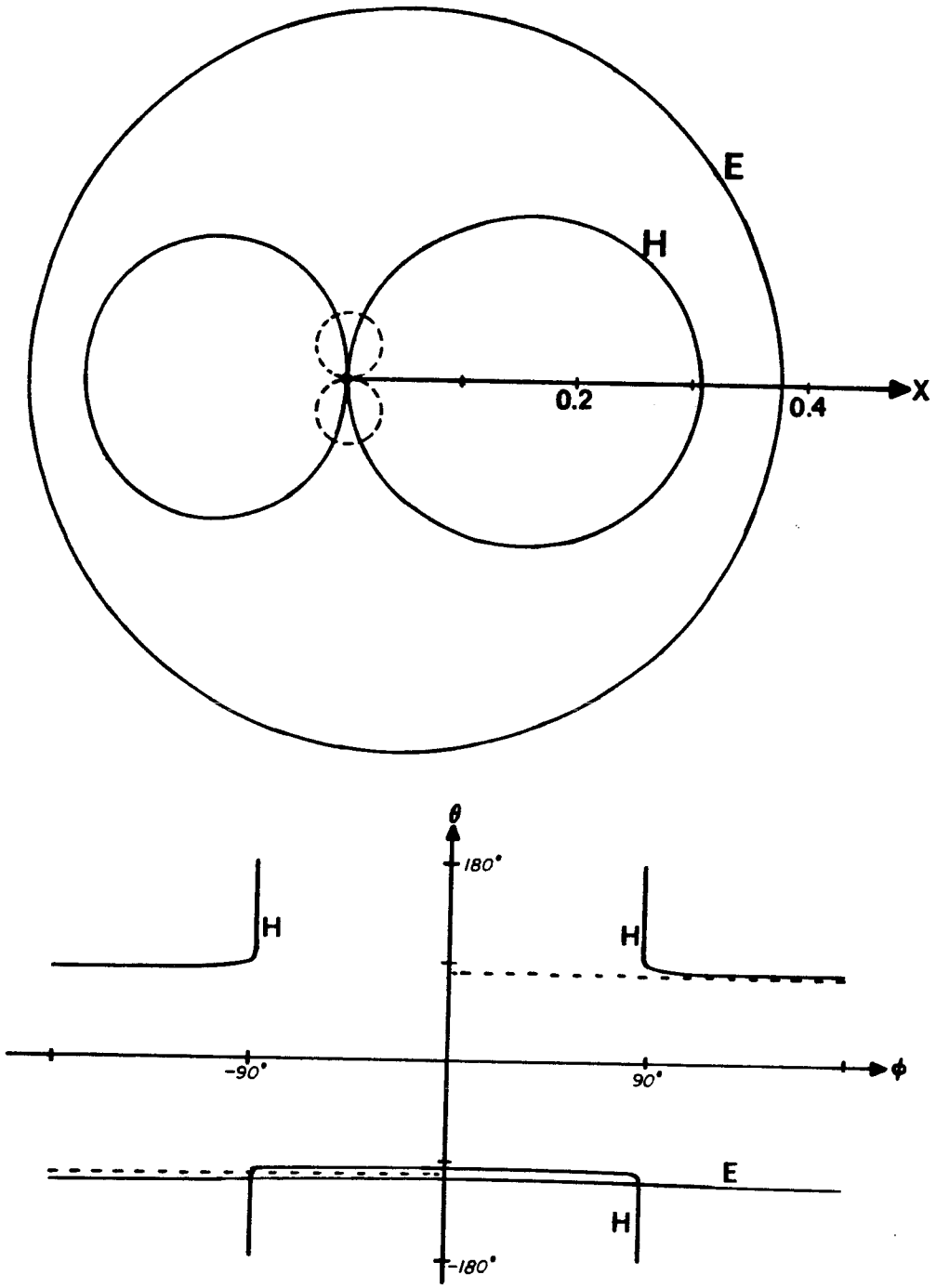

Fig. 12. (b) $k_o\rho_c = \frac{5}{6}$

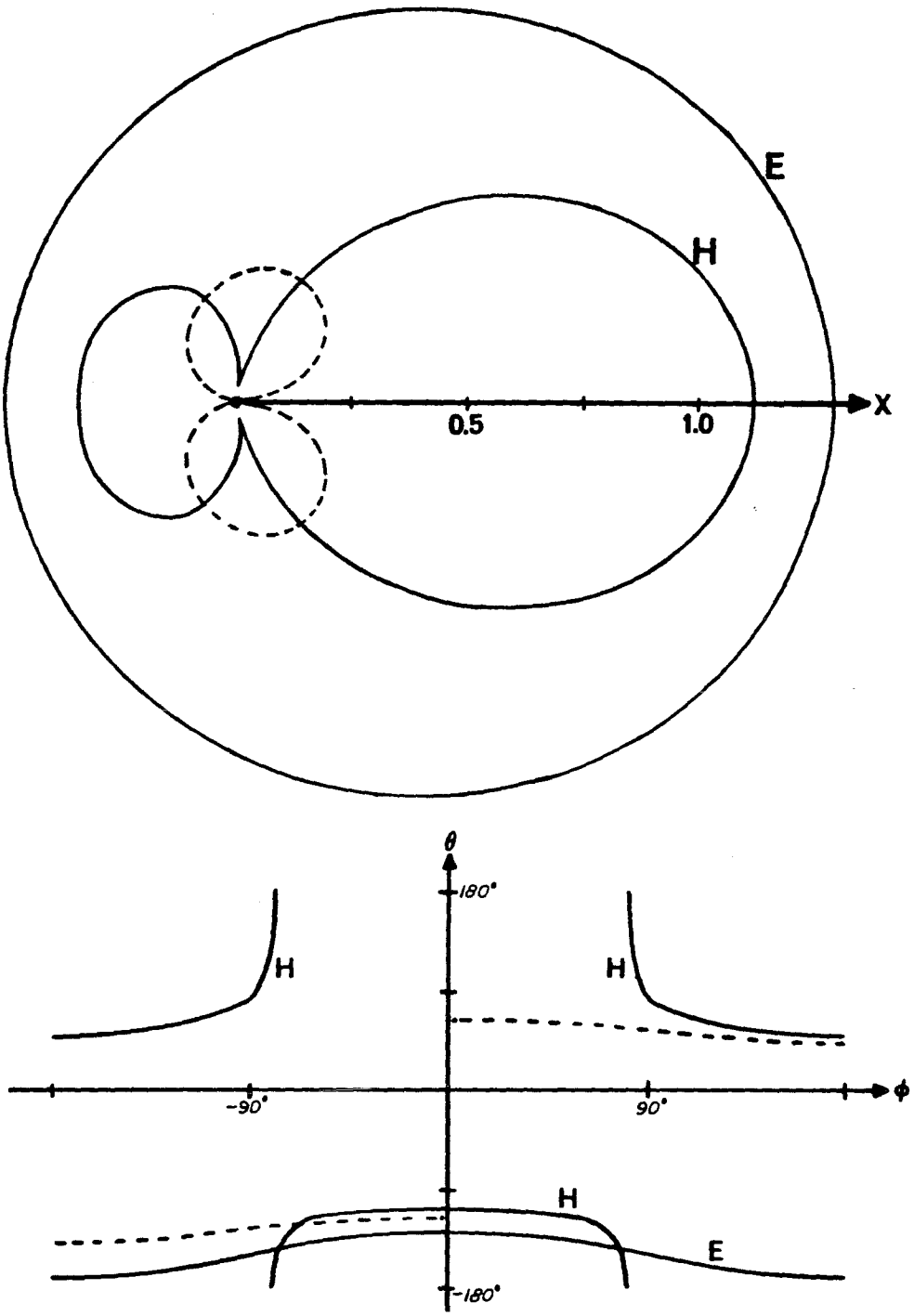

Fig. 12. (c) $k_0\rho_c = \frac{5}{3}$

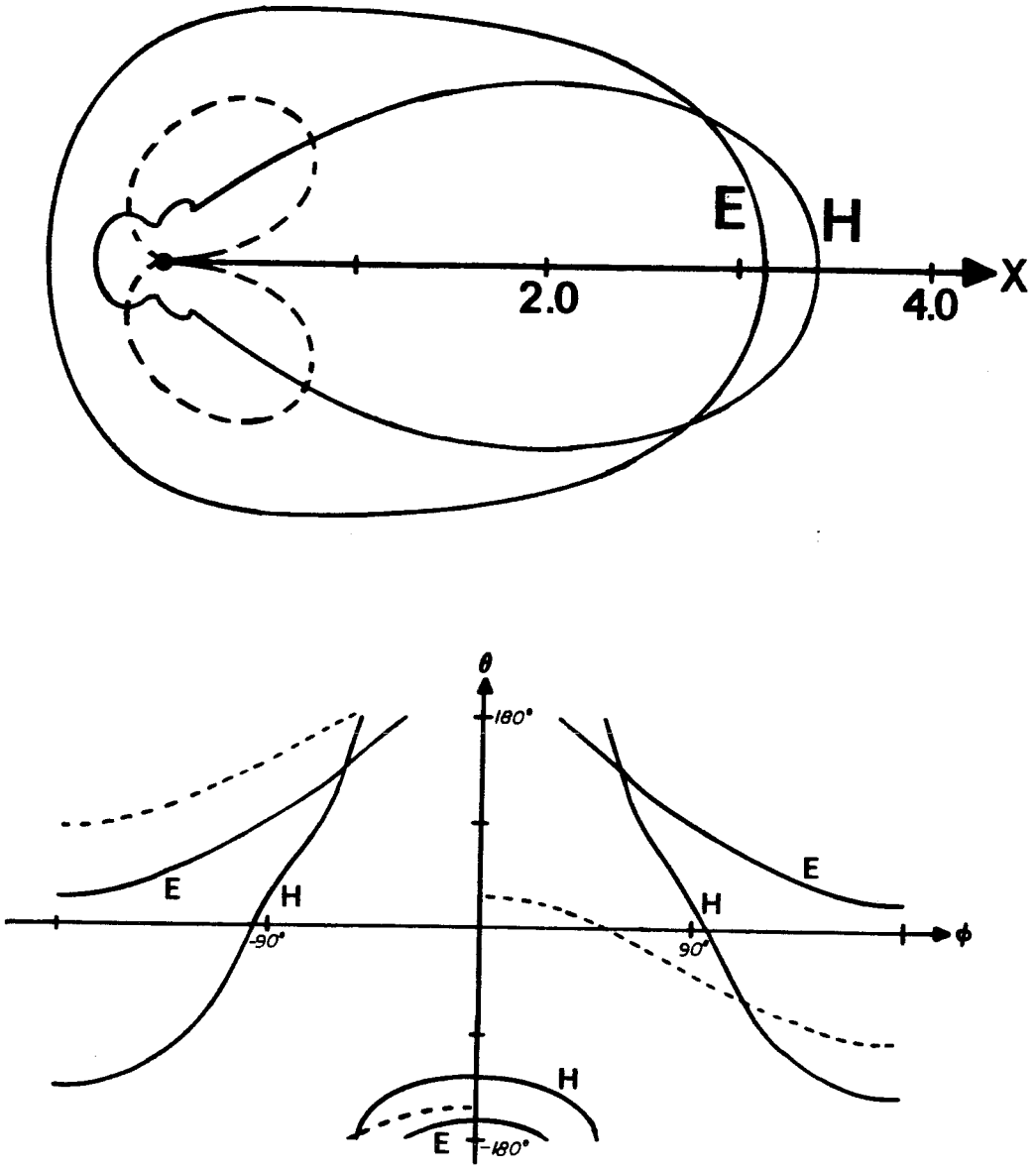

Fig. 12. (d) $k_o\rho_c = \frac{10}{3}$

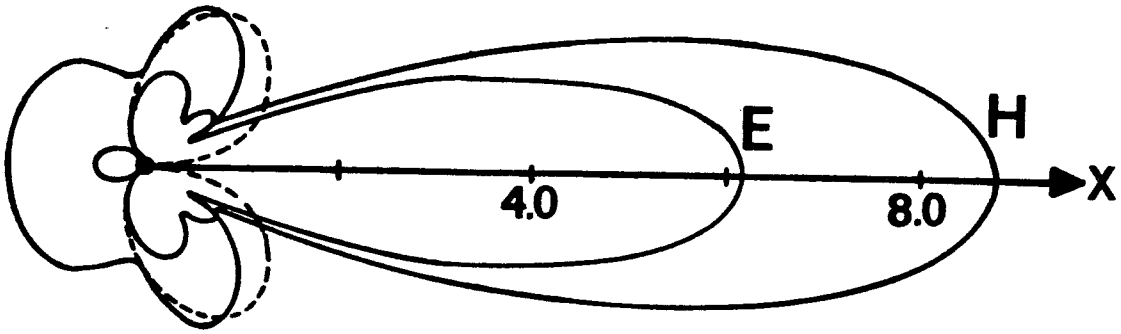

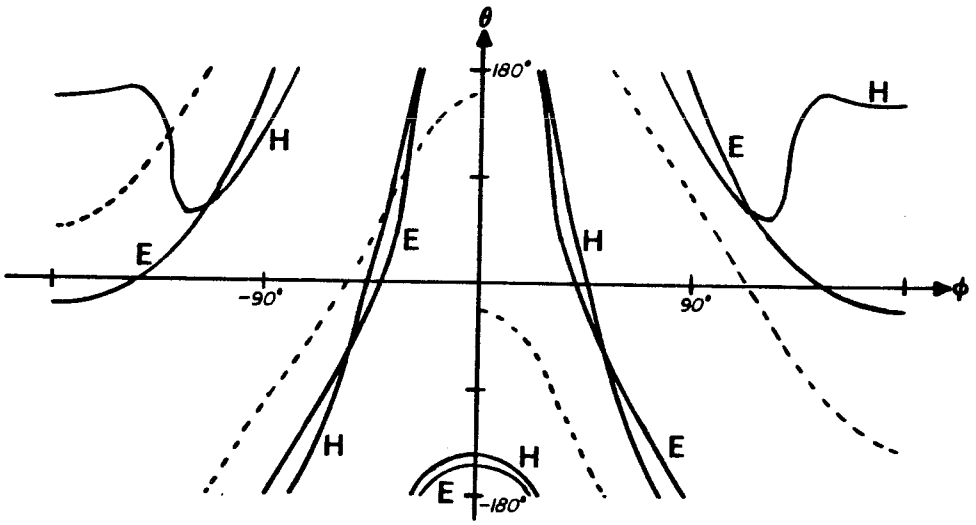

Fig. 12. (e) $k_o\rho_c = \frac{20}{3}$

direction. The curves labeled E represent the magnitude and phase of R^{22} and correspond to an incident plane wave with the E field in the axial direction. The unlabeled dashed curves represent the magnitude and phase of R^{12} and correspond to the cross polarized component of the scattered field. We have restricted the phase to lie between $\pm 180^0$.

We notice that when the column radius is small compared to the wavelength the magnitude curves take on well known shapes. The E polarization curve represents the radiation pattern of an electric dipole perpendicular to the plane of the paper. The H polarization curve represents the radiation pattern of an electric dipole in the plane of the paper oriented perpendicular to the direction of the incident wave. These two patterns are similar to those resulting from scattering off an isotropic column. The cross polarized pattern however is not so familiar. We see that its relative magnitude decreases rapidly with column size. If we take as an approximation a uniform exciting field within the column we see that in the case of E polarization charges are accelerated in the axial direction. This axial current is responsible for the symmetric E pattern on the figure. However an interaction of this current with the magnetostatic field also results in radial charge motion. But such a symmetric current does not radiate. Similarly for the H polarization charges are accelerated perpendicular to the axis giving rise to the dipole H pattern. The interaction with the magnetostatic field accelerates charges axially. However, in the top half of the column the axial current flows in one direction, while in the bottom half of the column it flows in the opposite direction. The two dipole moments cancel when the column radius is small. The generation of the cross polarized components

therefore results from the phase change of the field within the column and explains why its relative magnitude diminishes as the column becomes small.

The null of the cross polarized component along the direction of the incident wave persists throughout all these figures. This can be qualitatively understood by the following ray optical model. Figure 13 shows two rays traversing the column. Ray A propagating antiparallel to the static magnetic field undergoes Faraday rotation in the counterclockwise direction. Ray B propagating parallel to the static field undergoes Faraday rotation in the clockwise direction. On the symmetry line of the figure the rotations are equal in magnitude but opposite in sense. The cross polarized field components generated by the Faraday rotation therefore exactly cancel on the symmetry line.

The predominantly forward direction (in the direction of the incident wave) of the scattered fields when the column becomes larger, resembles that of a phased linear array of dipoles. The phasing is retarded due to the propagation delay of the incident wave.

The H and E phase curves are even in ϕ while the cross polarized curves are odd in ϕ. This fact follows from the evenness of the diagonal components of R_n with respect to n, and the oddness of the off diagonal components of R_n.

Figure 14 shows the two limiting cases, small magnetostatic field resulting in a nearly isotropic column, and large magnetostatic field resulting in a nearly uniaxial column. The cross polarized components become small in both cases. The E polarization also becomes small in the uniaxial case since the electrons are frozen to the magnetostatic field

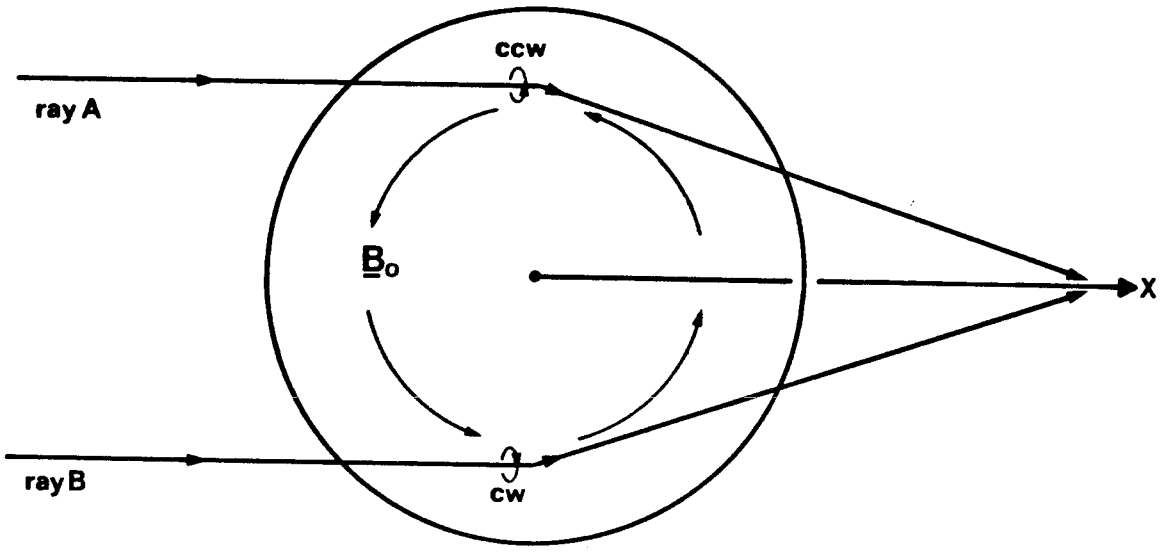

Fig. 13. A ray optical picture of the generation of the cross polarized component of the scattered field. The Faraday rotations cancel on the symmetry line.

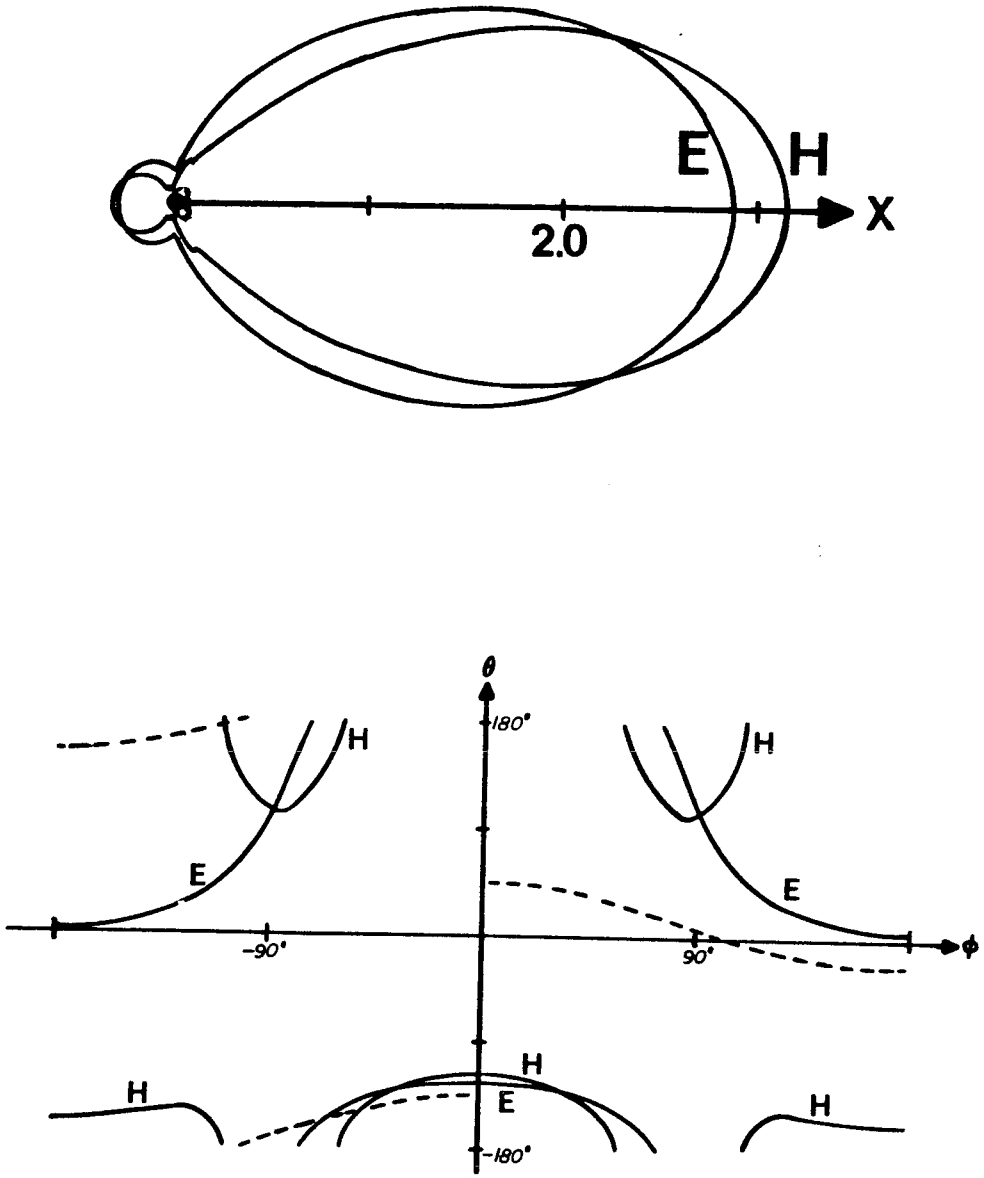

Fig. 14. Cases of small magnetostatic field and large magnetostatic field are shown. The plasma frequency is $\omega_p/\omega = 3/5$ and the column radius is $k_0\rho_c = 10/3$.

(a) $-\frac{\omega_g}{\omega} = \frac{1}{25}$

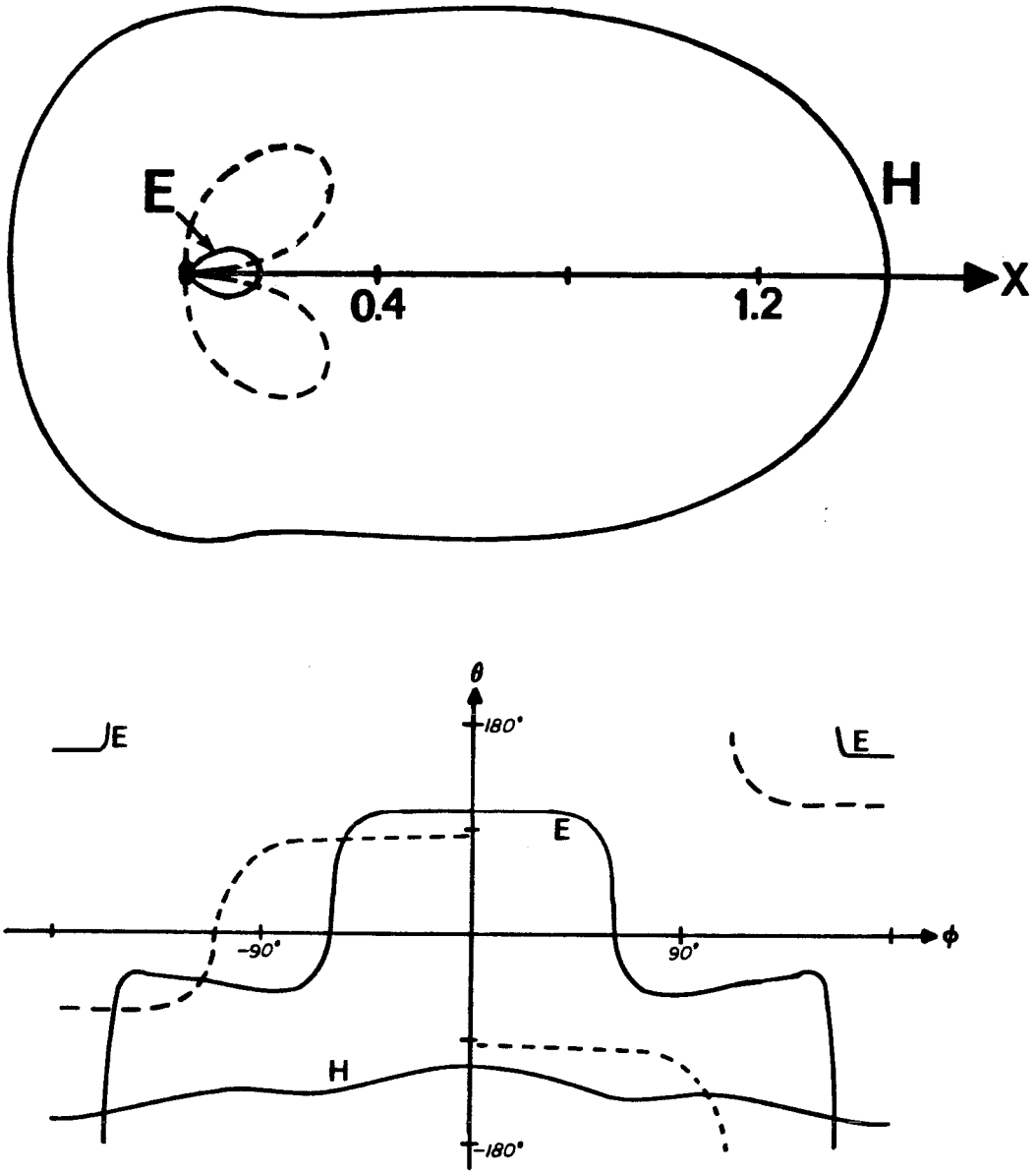

Fig. 14. (b) $-\frac{\omega_g}{\omega} = 4$

lines and cannot respond to the applied field.

Figure 15 illustrates the case where the wave number k_2 is imaginary.

Figure 16 illustrates the case where the quantity ν defined in Section 5B is imaginary. This results in intrinsic loss at the axis as described in Section 5C.

The next section presents examples when the column is inhomogeneous. More "homogeneous" patterns will also be given there as a comparison.

7B. Inhomogeneous Plasma Column

We now give two examples of scattering from an inhomogeneous plasma column. The matrix reflection coefficient was calculated by numerical integration of the Riccati equation of Section 6A. Figure 17a represents a column of plasma containing a uniform axial current density. The magnetostatic field thus varies linearly from zero at the axis to a maximum at the boundary of the cylinder. The vanishing of the magnetic field at the axis makes this example well suited to computation as discussed in Section 6C. Figure 17b gives the result for a "homogeneous" column with an intermediate strength magnetostatic field as a comparison.

The second example, Fig. 18a, represents a column of plasma containing a uniform axial current density in its central portion and zero axial current in the surrounding annular region. The magnetostatic field thus varies linearly from zero at the axis to a maximum at the edge of the current carrying portion, and then decreases inversely with distance. Figure 18b gives the result for a "homogeneous" column with an intermediate strength magnetostatic field as a comparison.

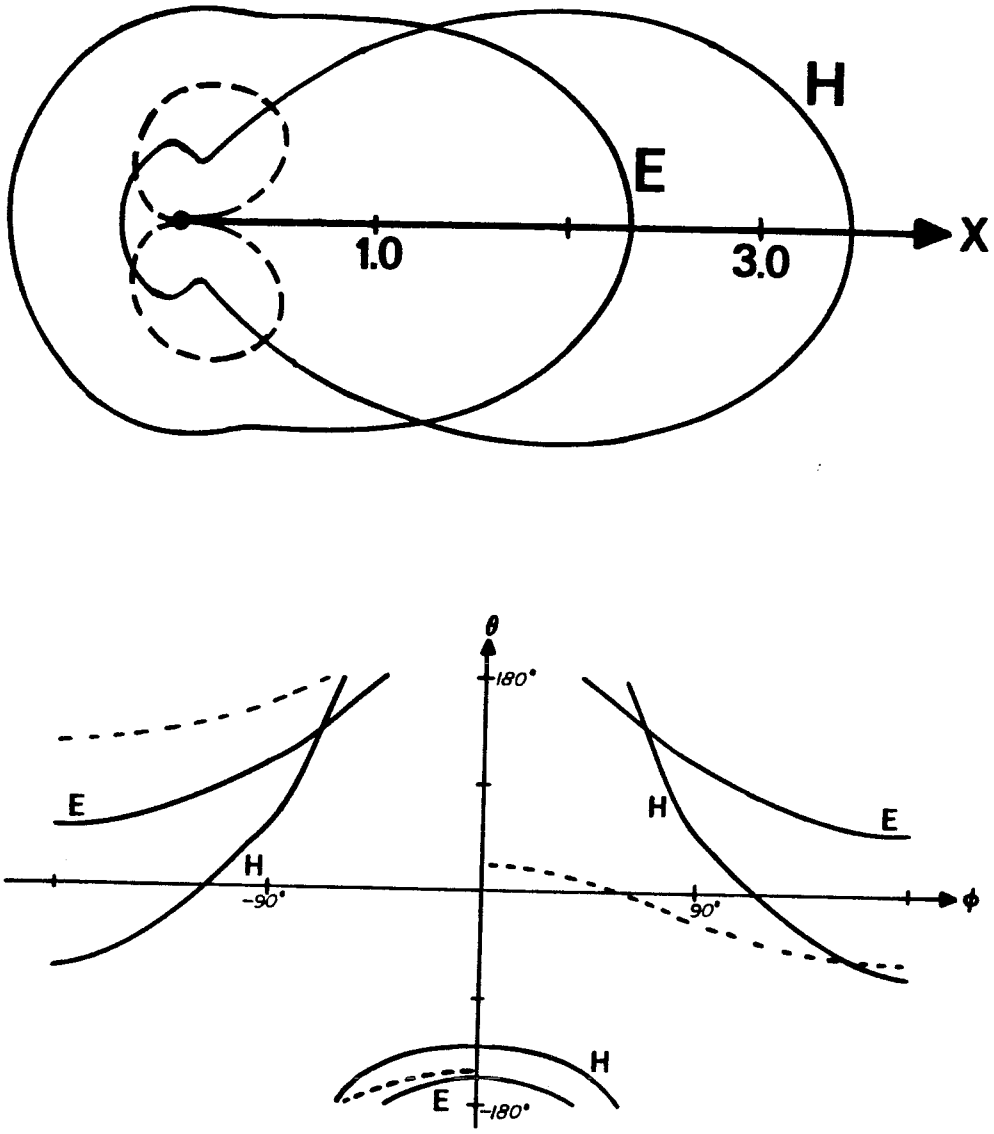

Fig. 15. The wave number k_2 is imaginary in this case. The parameters are $\omega_p/\omega = 3/4$, $-\omega_g/\omega = 1/2$, and $k_0\rho_c = 10/3$.

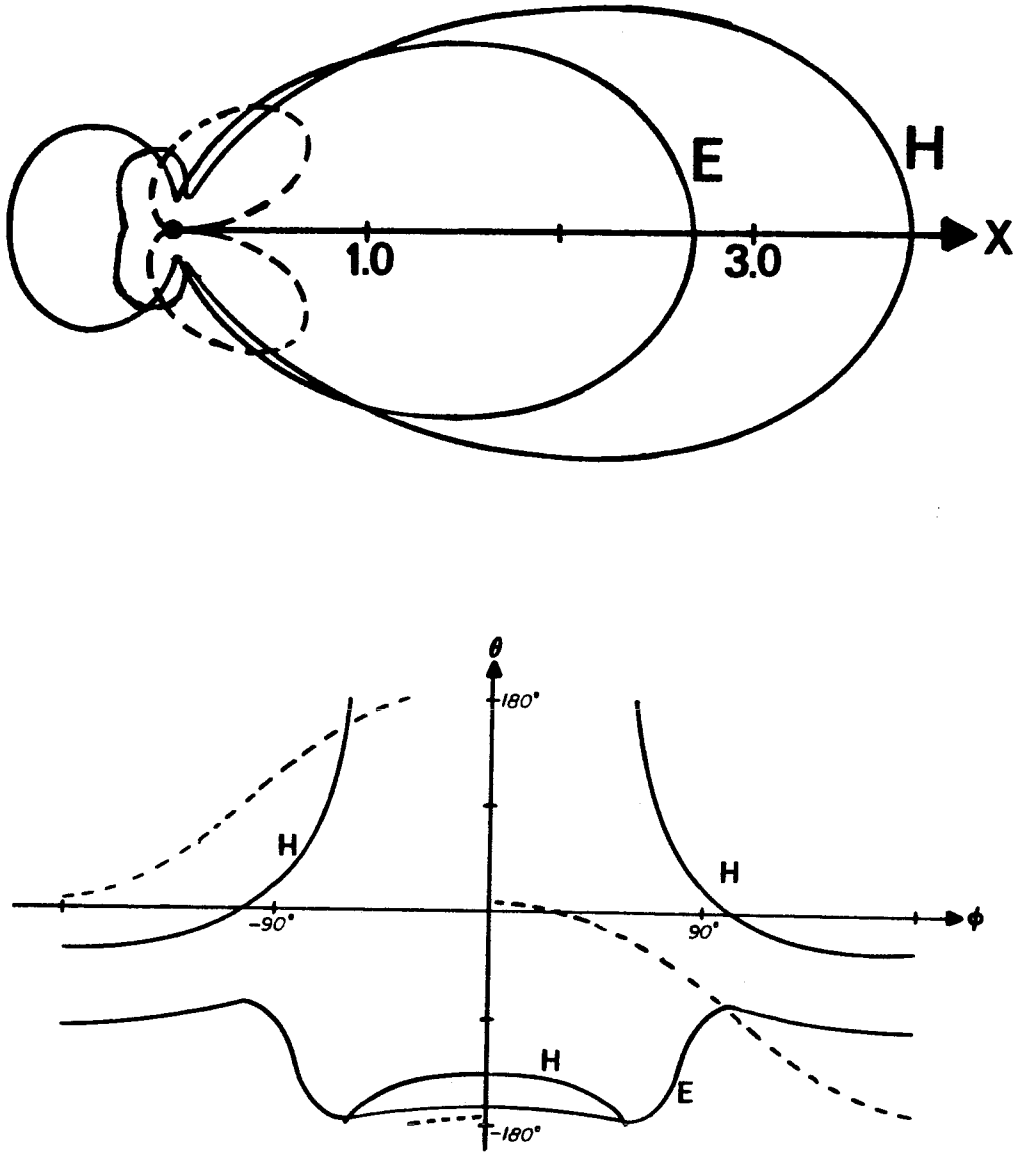

Fig. 16. The quantity ν is imaginary in this case resulting in intrinsic loss at the origin. The parameters are $\omega_p/\omega = 3/4$, $-\omega_g/\omega = 3/4$, and $k_o\rho_c = 10/3$.

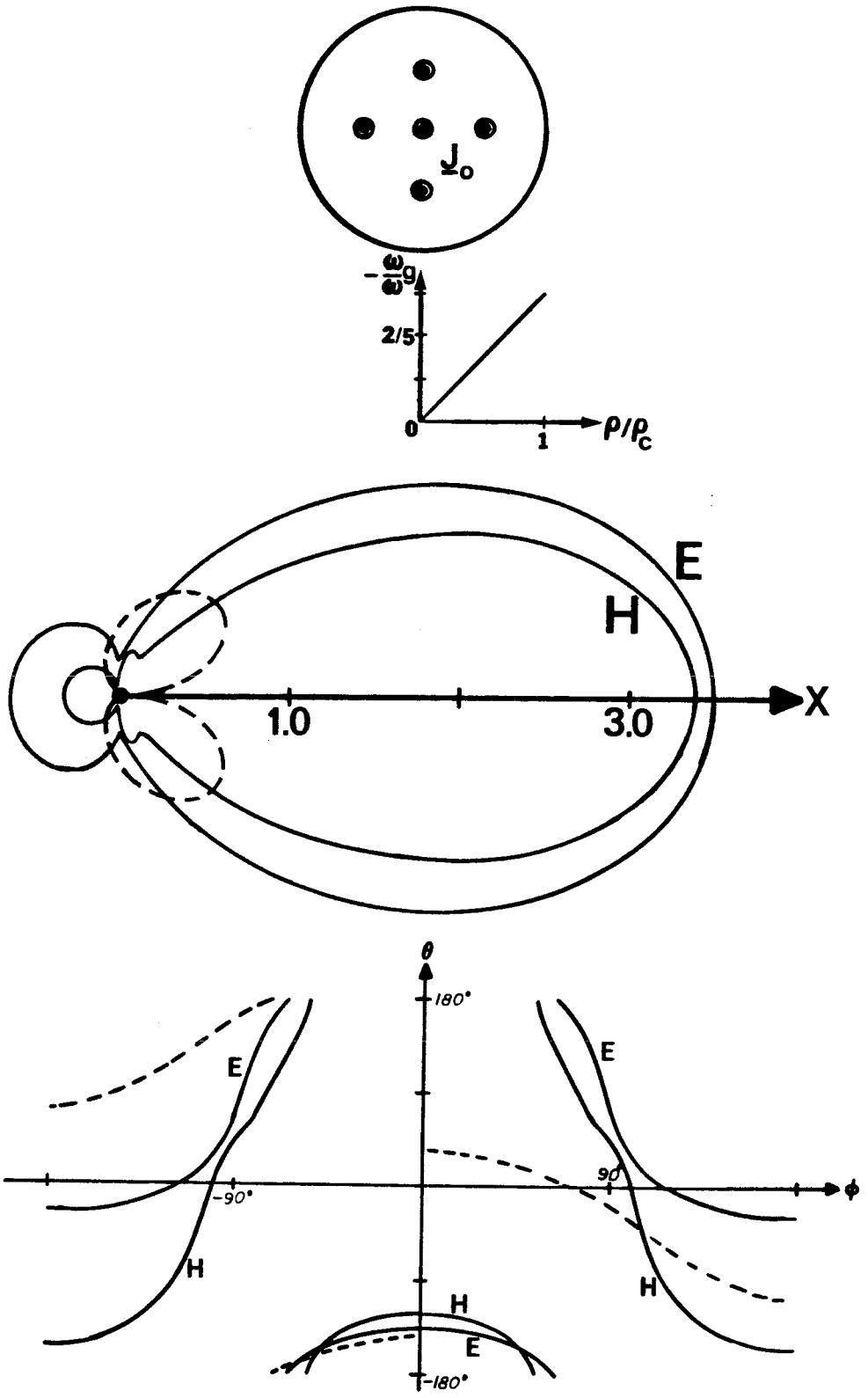

Fig. 17. A case of uniform current density is compared with a "homogeneous" case. The behavior of $-\omega_g/\omega$ is shown. The other parameters are $\omega_p/\omega = 3/5$, $k_o\rho_c = 10/3$.

(a) Inhomogeneous

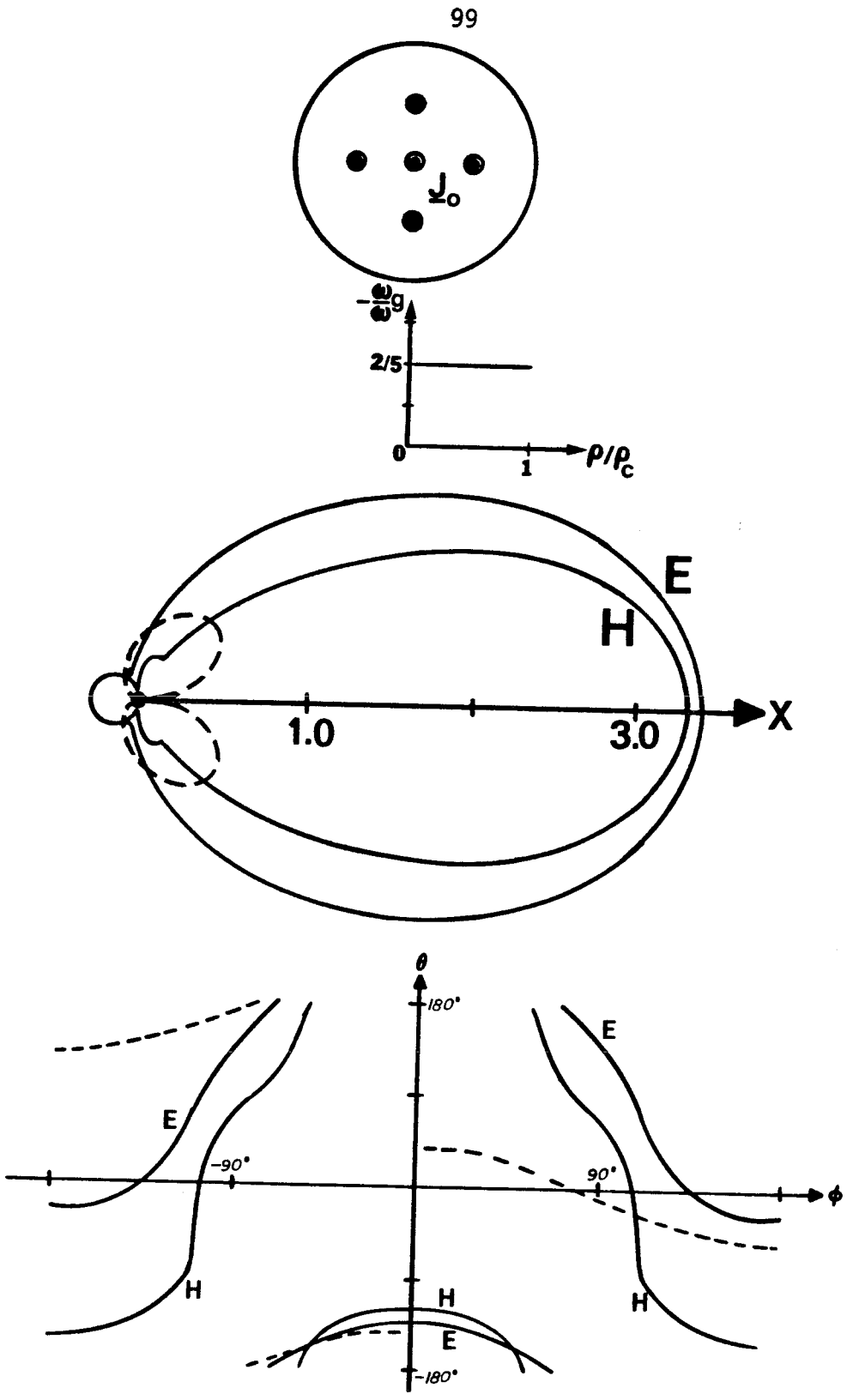

Fig. 17. (b) "Homogeneous"

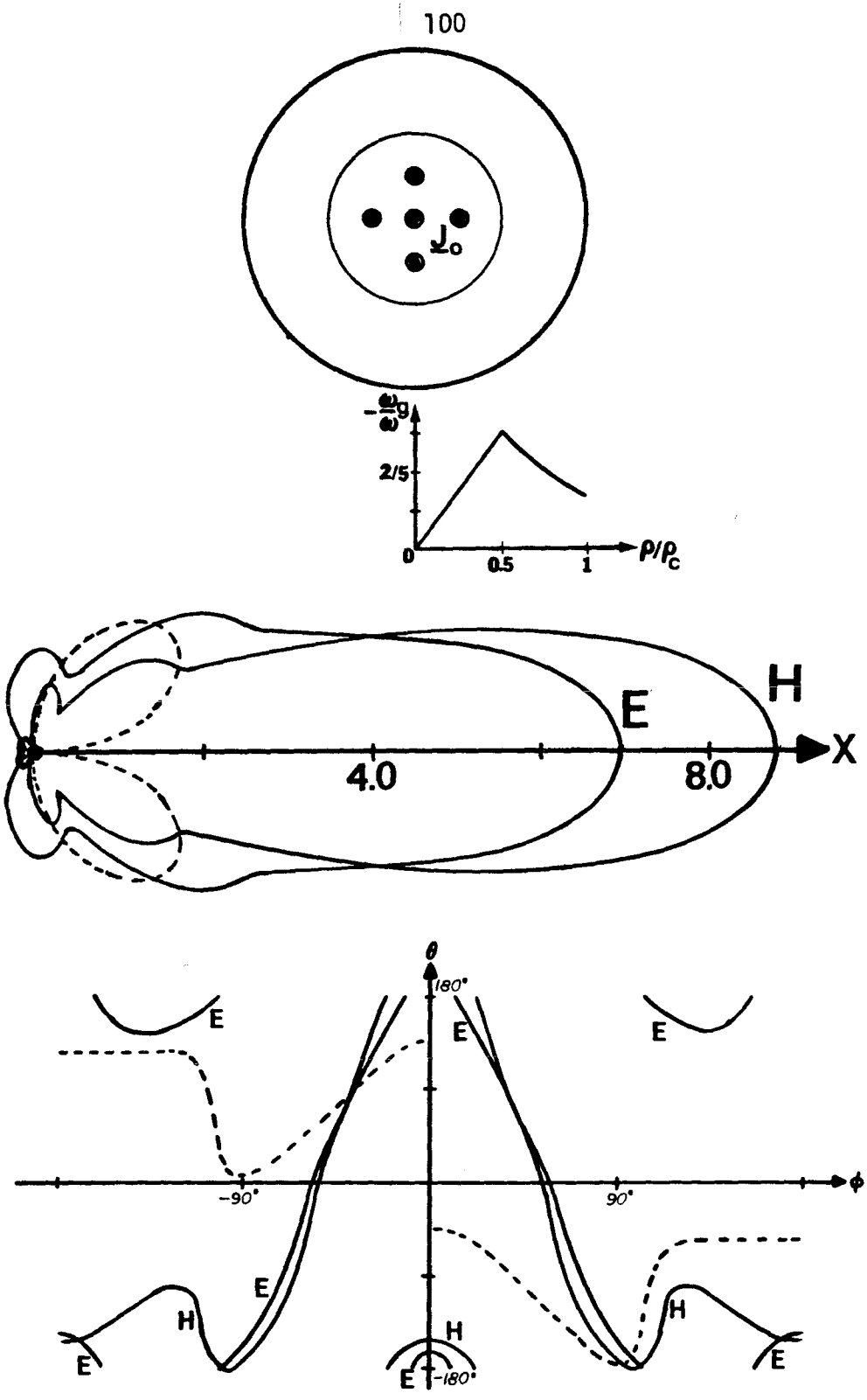

Fig. 18. A case of uniform current density in the central portion of the column is compared with a "homogeneous" case. The behavior of $-\omega_g/\omega$ is shown. The other parameters are $\omega_p/\omega = 3/5$, $k_o\rho_c = 20/3$.
(a) Inhomogeneous

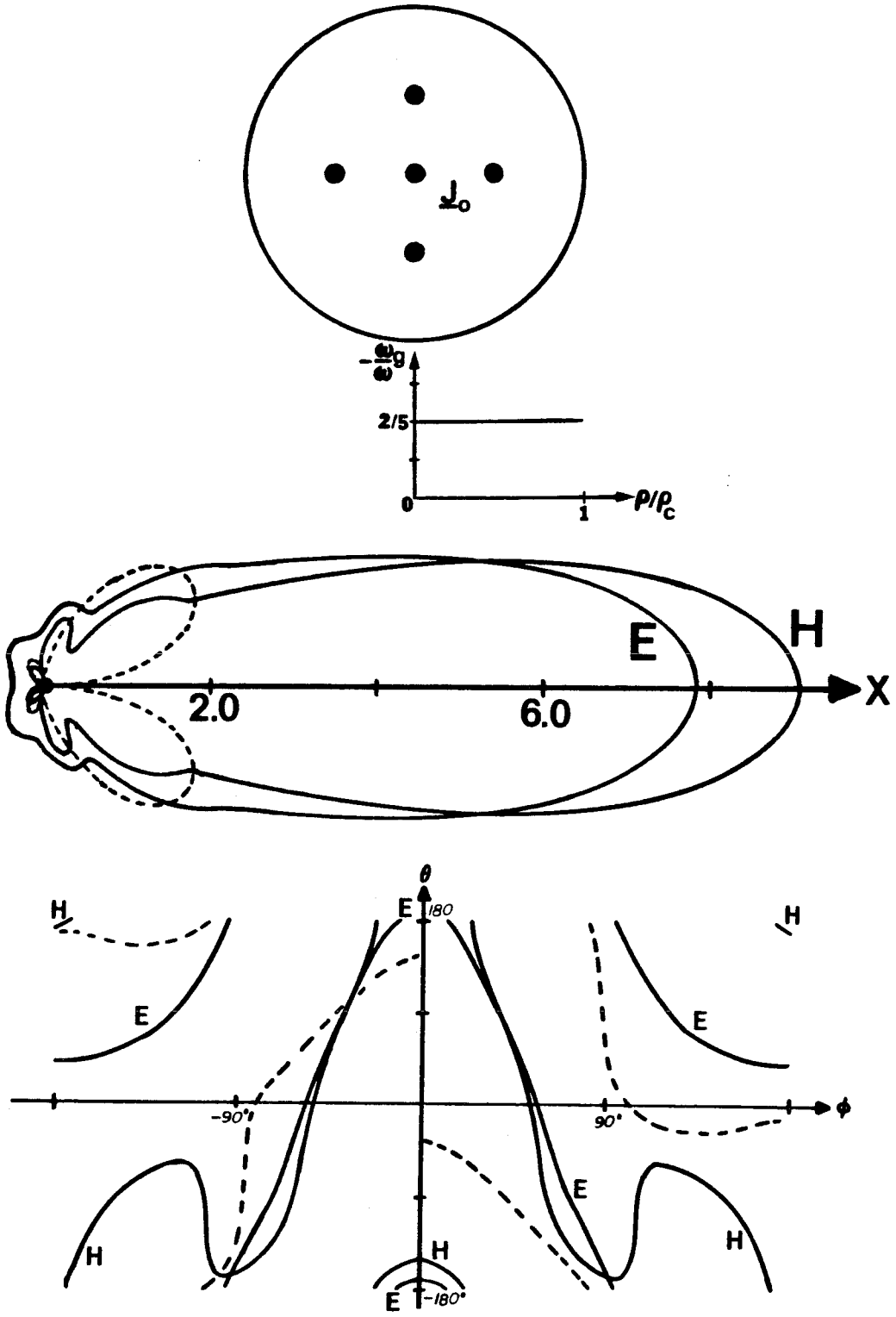

Fig. 18. (b) "Homogeneous"

We see from the above two examples that qualitatively the "homogeneous" solution has many of the characteristics of the inhomogeneous results.

The computer program used above was limited in two respects. First, special functions were not available to allow us to have $\omega < \omega_p$. Second, we did not incorporate the necessary asymptotic solutions to allow resonances (singularities occur in the coefficients when $\omega^2 = \omega_p^2 + \omega_g^2$). But the method can be used in these cases also.

CHAPTER 8

SUMMARY AND CONCLUSIONS

We have shown that the problem of an electric line source radiating into a homogeneous cold plasma containing an azimuthal biasing field, (generated by a large static current on the line source) can be formulated as a confluent form of Heun's differential equation. This differential equation can be solved by means of special function series analogous to the spheroidal wave equation. Reflection and transmission coefficients have been defined to describe the transmitted field amplitude at large radial distances and the reflected field amplitude in the vicinity of the line source. When the driving frequency is greater than the plasma frequency, and the plasma is unbounded the reflection coefficient is typically small and decreases with increasing static field or axial static current. The transmission coefficient decreases approximately exponentially with increasing static current as shown by the WKB approximation. These results are similar to the planar results when a resonance is present in the plasma. When the driving frequency is below the plasma frequency and the plasma is bounded, the transmission coefficient increases with increasing static current. The reflection coefficient decreases with increasing static current. These results are due to the fact that the magnetostatic field confines the motion of the plasma electrons near the wire. These results are accurately predicted by the WKB approximation.

The problem of scattering from a bounded column of plasma containing an azimuthal biasing field has also been treated. The problem has been formulated as a pair of coupled second order ordinary differential equations in the axial magnetic and electric fields. A matrix reflection coefficient has been defined which describes the scattered field amplitudes when a plane wave is normally incident. Using the method of invariant imbedding a matrix Riccati equation has been developed for this reflection coefficient. The solution of the scattering problem has thus been reduced to an initial value problem which can be integrated numerically.

The case of an axial static current density which is inversely proportional to radial distance leads to what has been labeled the "homogeneous" problem. The dielectric tensor in this case is independent of radial distance when the plasma is uniform. The coupled second order equations have only one finite singular point in this case. Their solution has been carried out by the method of Frobenius and by asymptotic methods. The connection between these two forms of solution has been related to the connection of solutions to Heun's equation which has been studied elsewhere.

The scattered fields contain a cross polarized component which has nulls on the axis defined by the incident wave. The scattered radiation is thus in general elliptically polarized. The scattered fields are directed forward when the column's radius increases. The scattered fields in the two "inhomogeneous" cases considered (where the axial current density was not inversely proportional to radius) computed via

the Riccati equation, resemble the "homogeneous" results.

The field behavior in the vicinity of the origin exhibits similarities to that encountered in wedges if the biasing field does not vanish at the origin. For example, under the simplifying assumption of infinite magnetostatic field, the electric field components transverse to the axial direction become infinite at the origin.

APPENDIX 1

Solution of Confluent Heun's Equation by Special Function Series

The solution of the equation

$$\frac{d^2E_z}{d\xi^2} + \frac{1}{\xi}\frac{dE_z}{d\xi} + \frac{\xi^2 - q^2}{\xi^2 - p^2} E_z = 0 \qquad (A1.1)$$

will now be determined. The new variable

$x = \xi^2/p^2$ transforms (A1.1) into

$$L_x E_z = x(1-x)\frac{d^2E_z}{dx^2} + (1-x)\frac{dE_z}{dx} + \frac{1}{4}(q^2 - p^2x)\,E_z = 0 \qquad (A1.2)$$

an equation with regular singular points at 0, 1, and an irregular singular point at ∞.

The exponents at a regular singular point can be determined by solving the indicial equation [33]. The pair of exponents at the origin of (A1.2) are 0, 0. The exponents at the point unity are 0, 1. The special functions selected for the series representation must have the same attributes as the solution at these singular points. Stated another way, they should be solutions of a simpler equation also having regular singular points at 0 and 1 with exponent pairs 0, 0, and 0, 1, respectively [10]. The functions selected must also have a singularity at infinity enabling a sum of them to emulate the essential singularity

of the solution. The hypergeometric functions can be selected to fit these requirements [22]. The solution to (A1.2) can be written as

$$E_z = EF(p, q, x) = \sum_{m=-\infty}^{\infty} c_m F(\Omega, -\Omega; 1; x) \qquad (A1.3)$$

where $\Omega = m + \nu$ and the notation EF is thus defined by this series. The constant ν is known as the characteristic exponent of the irregular singular point. The value of this exponent is determined by requiring convergence of the series. Operating on the hypergeometric function with L_x results in

$$L_x F = \left(\frac{q^2}{4} - \Omega^2 - \frac{p^2}{4} x\right) F \qquad (A1.4)$$

Two of the Gauss contiguous relations for the hypergeometric function $F(a, b; c; x)$ are

$$(b - a)F + a\, F(a + 1) - b\, F(b + 1) = 0 \qquad (A1.5)$$

$$(b - a)\,(1 - x)F - (c - a)\, F(a - 1) + (c - b)\, F(b - 1) = 0 \qquad (A1.6)$$

where only the incremented arguments of the hypergeometric functions are shown. These two relations can be used to eliminate the variable x in equation (A1.4) resulting in

$$L_x F = \left(\frac{1}{4} q^2 - \Omega^2 - \frac{1}{4} p^2 \frac{2\Omega^2 - 1}{4\Omega^2 - 1}\right) F(\Omega, -\Omega; 1; x)$$

$$+ \frac{p^2}{4} \frac{\Omega - 1}{2(2\Omega - 1)} F(\Omega - 1, 1 - \Omega; 1; x)$$

$$+ \frac{p^2}{4} \frac{\Omega + 1}{2(2\Omega + 1)} F(\Omega + 1, -1 - \Omega; 1; x) \qquad \text{(A1.7)}$$

use of (A1.7) in (A1.3) gives

$$L_x E_z = \sum_{m=-\infty}^{\infty} L_m c_m F(\Omega, -\Omega; 1; x) \qquad \text{(A1.8)}$$

where L_m is a second order difference operator

$$L_m c_m = c_{m+1} \frac{p^2}{4} \frac{\Omega}{2(2\Omega + 1)} + \left(\frac{1}{4} q^2 - \Omega^2 - \frac{1}{4} p^2 \frac{2\Omega^2 - 1}{4\Omega^2 - 1}\right) c_m$$

$$+ \frac{p^2}{4} \frac{\Omega}{2(2\Omega - 1)} c_{m-1} \qquad \text{(A1.9)}$$

Setting (A1.9) equal to zero gives the recurrence relation among the coefficients c_m. Convergence of the series (A1.3) hinges on the behavior of the coefficients c_m for large m. The equation

$$L_m C_m = 0 \qquad \text{(A1.10)}$$

is a three term difference equation and it thus has two linearly independent solutions. Let us define

$$v_m = \frac{c_{m+1}}{c_m} = 1/v'_m \tag{A1.11}$$

and from (A1.10) we obtain

$$v_{m-1} = \frac{\gamma_m^{(-)}}{1 - \delta_m - \gamma_m^{(+)} v_m} \tag{A1.12}$$

$$v'_m = \frac{\gamma_m^{(+)}}{1 - \delta_m - \gamma_m^{(-)} v'_{m-1}} \tag{A1.13}$$

where $\delta_m = \frac{1}{4\Omega^2}\left(q^2 - p^2 \frac{2\Omega^2 - 1}{4\Omega^2 - 1}\right)$

$$\gamma_m^{(\pm)} = \frac{p^2}{8\Omega(2\Omega \pm 1)}$$

Equations (A1.12) and (A1.13) can be used to determine the asymptotic behaviors of v_m and v'_m as m becomes large

$$\begin{aligned} v_m &= O(\Omega^{\pm 2}) \qquad m \to +\infty \\ v'_m &= O(\Omega^{\pm 2}) \qquad m \to -\infty \end{aligned} \tag{A1.14}$$

where O is the conventional order symbol. The behavior with the minus sign in (A1.14) will result in convergence of the series (A1.3). We are free to impose the desired behavior of v_m (minus sign) in one direction, $m \to +\infty$, but the behavior of v'_m in the other direction, $m \to -\infty$, will in general be undesirable (plus sign). The characteristic exponent, ν, is chosen in such a way that the desirable solution in one direction connects to the desirable solution in the other direction. The transcendental equation determining ν is found by iterating (A1.12) and (A1.13) to give the infinite continued fractions

$$v_m = \frac{\gamma_{m+1}^{(-)}}{1 - \delta_{m+1}} - \frac{\gamma_{m+1}^{(+)}\gamma_{m+2}^{(-)}}{1 - \delta_{m+2}} - \cdots \tag{A1.15}$$

$$v'_m = \frac{\gamma_m^{(+)}}{1 - \delta_m} - \frac{\gamma_m^{(-)}\gamma_{m-1}^{(+)}}{1 - \delta_{m-1}} - \cdots \tag{A1.16}$$

where the second term of the sequence is in the denominator of the first term, etc. Equations (A1.15) and (A1.16) give values which do not in general satisfy the definition (A1.11) of v_m and v'_m unless the characteristic exponent ν is chosen correctly. Thus (A1.11) together with (A1.15) and (A1.16) determine the value of ν. The value of m in these equations may be set conveniently. A general consideration of the differential equation (A1.2), which is identical to that used on the spheroidal wave equation, shows that if ν is a solution then so are $\nu \pm$ any integer [10]. Thus we may take the real part of ν to be between zero and one half. The above calculation of ν also determines v_m and v'_m

and therefore determines all coefficients, c_m, aside from an overall scaling factor. We make the solution definite by taking $c_o = 1$. Appendix 2 shows that the series (A1.3) with appropriate choice of ν converges for all x such that $|x| < \infty$.

The differential equation (A1.2) is second order and has two linearly independent solutions. The second solution can be represented as

$$E_z = EG(p, q, x) = \sum_{m=-\infty}^{\infty} c_m G(\Omega, -\Omega; 1; x) \qquad (A1.17)$$

where $G(\Omega, -\Omega; 1; x) = (1 - x) F(1 + \Omega, 1 - \Omega; 2; 1 - x)\Gamma(1 + \Omega)\Gamma(1 - \Omega)$ is a linearly independent solution of the hypergeometric equation. Using the above procedure and the contiguous relations (A1.5) and (A1.6) we can show that the coefficients c_m in (A1.17) are the same as in (A1.3). Appendix 2 shows that (A1.17) converges for all x such that $|x| < \infty$.

The representations (A1.3) and (A1.17) provide the general solution to (A1.2) for all x. Yet since the terms of these series grow like positive powers of x for large $|x|$, they do not provide the asymptotic form of the solution for large $|x|$. These series furthermore become slowly convergent as x becomes large. As in the case of the spheroidal wave equation [10], two other series representations will supplement (A1.3) and (A1.17). The functions used in these additional series possess the same essential singular behavior as the solution to (A1.2) at the point of infinity. They will therefore provide useful solutions for large x as well as the asymptotic form of the solution for large x. They are

$$E_z = EJ(p, q, \xi) = \sum_{m=-\infty}^{\infty} \frac{c_m}{\Omega} J_{2\Omega}(\xi) \qquad (A1.18)$$

$$E_z = EY(p, q, \xi) = \sum_{m=-\infty}^{\infty} \frac{c_m}{\Omega} Y_{2\Omega}(\xi) \qquad (A1.19)$$

The differential equation for E_z in terms of ξ is (A1.1) which can be written as

$$L_\xi E_z = (\xi^2 - p^2) \frac{d^2E_z}{d\xi^2} + \left(\xi - \frac{p^2}{\xi}\right)\frac{dE_z}{d\xi} + (\xi^2 - q^2) E_z = o \qquad (A1.20)$$

where L_ξ is a linear differential operator.

Operating on the Bessel function with L_ξ results in

$$L_\xi J = \left(4\Omega^2 - q^2 + p^2 - p^2 \frac{4\Omega^2}{\xi^2}\right) J \qquad (A1.21)$$

The variable ξ can be eliminated by repeated use of the relation

$$\frac{4\Omega}{\xi} J_{2\Omega}(\xi) = J_{2\Omega-1}(\xi) + J_{2\Omega+1}(\xi) \qquad (A1.22)$$

we obtain

$$L_\xi J = \left(4\Omega^2 - q^2 + p^2 \frac{2\Omega^2 - 1}{4\Omega^2 - 1}\right) J_{2\Omega}(\xi) - \frac{p^2\Omega}{2(2\Omega - 1)} J_{2\Omega-2}(\xi) - \frac{p^2\Omega}{2(2\Omega + 1)} J_{2\Omega+2}(\xi) \qquad (A1.23)$$

which when combined with (A1.17) gives

$$L_\xi E_z = -4 \sum_{m=-\infty}^{\infty} \frac{1}{\Omega} L_m c_m J_{2\Omega}(\xi) \qquad \text{(A1.24)}$$

where L_m is the same difference operator as defined in (A1.9). Thus the recurrence relation among the coefficients is identical to those obtained previously (A1.10).

This is also true of the Bessel function of the second kind, $Y_{2\Omega}(\xi)$, since it satisfies both the Bessel differential equation and relation (A1.22). Therefore the coefficients c_m are the same as in (A1.3). Appendix 2 shows that these series only converge for $|\xi| > p$ (or in terms of the variable $x = \xi^2/p^2$ for $|x| > 1$).

The connection between the solutions (A1.3), (A1.17) and the solutions (A1.18), (A1.19) is now determined. It will be assumed that the characteristic exponent, ν, is not an integer or half odd integer. Making use of the power series expansions of the Bessel functions we can write

$$EJ(p, q, px^{\frac{1}{2}}) = x^{\nu} EJ^{(+)}(p, q, x) \qquad \text{(A1.25)}$$

$$EY(p, q, px^{\frac{1}{2}}) = x^{\nu} EJ^{(+)}(p, q, x)\cot(2\pi\nu) - x^{-\nu} EJ^{(-)}(p, q, x)\csc(2\pi\nu) \qquad \text{(A1.26)}$$

where the denoted functions on the right are single valued and possess the Laurent series expansions

$$EJ^{(\pm)}(p, q, x) = \sum_{m=-\infty}^{\infty} j_m^{(\pm)} x^m \qquad \text{(A1.27)}$$

where the $j_m^{(+)}$, $j_m^{(-)}$ are known coefficients involving sums of the coefficients c_m, and the series are convergent in the region $1 < |x| < \infty$. The values of $j_m^{(\pm)}$ are given in Appendix 3.

The power series representation of the hypergeometric function convergent in the domain $1 < |x| < \infty$ can be obtained by using the linear transformation formulas for the hypergeometric functions (Appendix 3). Making use of this power series expansion allows us to write

$$EF(p, q, x) = e^{i\pi\nu} x^{-\nu} EF^{(-)}(p, q, x) + e^{-i\pi\nu} x^{\nu} EF^{(+)}(p, q, x) \tag{A1.28}$$

$$EG(p, q, x) = \pi \csc \pi\nu \left[x^{-\nu} EF^{(-)}(p, q, x) - x^{\nu} EF^{(+)}(p, q, x) \right] \tag{A1.29}$$

where the denoted functions on the right are single valued and possess the Laurent series expansions

$$EF^{(\pm)}(p, q, x) = \sum_{m=-\infty}^{\infty} f_m^{(\pm)} x^m \tag{A1.30}$$

where $f_m^{(+)}$, $f_m^{(-)}$ are known coefficients involving sums of the coefficients c_m, and the series are convergent in the region $1 < |x| < \infty$. The values of $f_m^{(\pm)}$ are given in Appendix 3. The solutions EJ, EY can be written as linear combinations of the solutions EF, EG. But since the functions $EJ^{(\pm)}$ and $EF^{(\pm)}$ are single valued in the annulus $1 < |x| < \infty$ we must have

$$EJ^{(\pm)}(p, q, x) = c^{(\pm)} EF^{(\pm)}(p, q, x) \tag{A1.31}$$

where $c^{(+)}$, $c^{(-)}$ are unknown coefficients of proportionality. However since the functions in equations (A1.31) are analytic in the annulus $1 < |x| < \infty$, the coefficients in their Laurent series expansions must be identical,

$$j_m^{(\pm)} = c^{(\pm)} f_m^{(\pm)} \tag{A1.32}$$

which determine the constants of proportionality $c^{(+)}$ and $c^{(-)}$. The index m may be set conveniently. Finally we may write

$$\begin{aligned} EJ &= x^{\nu}\, EJ^{(+)} = x^{\nu}\, c^{(+)}\, EF^{(+)} \\ &= c^{(+)}\, (EF - e^{i\pi\nu} \sin \pi\nu\, EG/\pi)/2 \cos \pi\nu \end{aligned} \tag{A1.33}$$

And we have

$$EY = \cot 2\pi\nu\, EJ - c^{(-)} \csc 2\pi\nu\, (EF + e^{i\pi\nu} \sin \pi\nu\, EG/\pi)/2 \cos \pi\nu \tag{A1.34}$$

The procedure used above to obtain the connection between solutions parallels that used on the spheroidal wave equation [10].

APPENDIX 2

Convergence of the Series Representations Given in Appendix 1

To discuss the convergence of the hypergeometric function series we must use asymptotic forms of these functions for large parameters. From the asymptotic form of $F(a + \lambda, b - \lambda; c; \frac{1}{2} - \frac{1}{2} z)$ for large λ given in [37] we deduce

$$\frac{F(\Omega \pm 1, -\Omega \mp 1; 1; x)}{F(\Omega, -\Omega; 1; x)} \sim - \frac{1 + \left(1 - \frac{1}{x}\right)^{\frac{1}{2}}}{1 - \left(1 - \frac{1}{x}\right)^{\frac{1}{2}}} \quad ; \; m \to \pm \infty \tag{A2.1}$$

and

$$\frac{G(\Omega \pm 1, -\Omega \mp 1; 1; x)}{G(\Omega, -\Omega; 1; x)} \sim \frac{1 + \left(1 - \frac{1}{x}\right)^{\frac{1}{2}}}{1 - \left(1 - \frac{1}{x}\right)^{\frac{1}{2}}} \quad , \; m \to \pm \infty \tag{A2.2}$$

where $G(\Omega, -\Omega; 1; x) = (1 - x) F(1 + \Omega, 1 - \Omega; 2; 1 - x) \Gamma(1 - \Omega) \Gamma(1 + \Omega)$ and $\Omega = m + \nu$.

From (A1.12) and (A1.13) the ratio of coefficients in the series expansions are given by

$$v_m = \frac{c_{m+1}}{c_m} \sim \frac{p^2}{16m^2} \quad , \quad m \to + \infty \tag{A2.3}$$

$$v_m' = \frac{c_m}{c_{m+1}} \sim \frac{p^2}{16m^2} \quad , \quad m \to - \infty \tag{A2.4}$$

where as discussed in Appendix 1 the characteristic exponent is chosen properly so that v_m and v'_m decrease as m becomes large in the positive and negative direction, respectively. The ratio test therefore shows that the series EF (A1.3) and EG (A1.17) converge for all finite values of x.

From the asymptotic form of the Bessel functions for large order [22] we can deduce that

$$\frac{J_{2\Omega \pm 2}(\xi)}{J_{2\Omega}(\xi)} \sim \begin{cases} \dfrac{\xi^2}{16m^2}, & m \to +\infty \\ \dfrac{16m^2}{\xi^2}, & m \to -\infty \end{cases} \tag{A2.5}$$

$$\frac{Y_{2\Omega \pm 2}(\xi)}{Y_{2\Omega}(\xi)} \sim \frac{16m^2}{\xi^2}, \quad m \to \pm\infty \tag{A2.6}$$

The ratio test therefore shows that the series EJ (A1.18) and EY (A1.19) converge only for $|\xi| > p$.

APPENDIX 3

Connection of the Series Representations Given in Appendix 1

Two linear transformation formulas of the hypergeometric function will be used [22].

$$F(a, b; c; x) = \frac{\Gamma(c)\,\Gamma(b-a)}{\Gamma(b)\,\Gamma(c-a)}(-x)^{-a} F\left(a, 1-c+a; 1-b+a; \frac{1}{x}\right)$$

$$+ \frac{\Gamma(c)\,\Gamma(a-b)}{\Gamma(a)\,\Gamma(c-b)}(-x)^{-b} F\left(b, 1-c+b; 1-a+b; \frac{1}{x}\right) \qquad (A3.1)$$

$$(|\arg(1-x)| < \pi)$$

$$F(a, b; c; x) = (1-x)^{-a} \frac{\Gamma(c)\,\Gamma(b-a)}{\Gamma(b)\,\Gamma(c-a)} F\left(a, c-b; a-b+1; \frac{1}{1-x}\right)$$

$$+ (1-x)^{-b} \frac{\Gamma(c)\,\Gamma(a-b)}{\Gamma(a)\,\Gamma(c-b)} F\left(b, c-a; b-a+1; \frac{1}{1-x}\right) \qquad (A3.2)$$

$$(|\arg(1-x)| < \pi)$$

These two formulas are used to obtain the analytic continuation of the series expansions given in Appendix 1. The formula (A3.1) gives

$$F(\Omega, -\Omega; 1; x) = \frac{\Gamma(-2\Omega)}{\Gamma(-\Omega)\,\Gamma(1-\Omega)}(-x)^{-\Omega} F\left(\Omega, \Omega; 1+2\Omega; \frac{1}{x}\right)$$

$$+ \frac{\Gamma(2\Omega)}{\Gamma(\Omega)\,\Gamma(1+\Omega)}(-x)^{\Omega} F\left(-\Omega, -\Omega; 1-2\Omega; \frac{1}{x}\right) \qquad \text{(A3.3)}$$

and (A3.2) gives

$$G(\Omega, -\Omega; 1; x) = \left(\frac{1}{x} - 1\right)\left[\frac{\Gamma(-2\Omega)\,\Gamma(1+\Omega)}{\Gamma(1-\Omega)} x^{-\Omega} F\left(1+\Omega, 1+\Omega; 1+2\Omega; \frac{1}{x}\right)\right.$$

$$\left. + \frac{\Gamma(2\Omega)\,\Gamma(1-\Omega)}{\Gamma(1+\Omega)} x^{\Omega} F\left(1-\Omega, 1-\Omega; 1-2\Omega; \frac{1}{x}\right)\right] \qquad \text{(A3.4)}$$

where $\Omega = m + \nu$, $G(\Omega, -\Omega; 1; x) = (1 - x)\, F(1 + \Omega, 1 - \Omega; 2; 1 - x)$ $\Gamma(1 - \Omega)\,\Gamma(1 + \Omega)$ and Γ is the gamma function. The identity $F(a, b; c, x) = (1 - x)^{c-a-b} F(c - a, c - b; c; x)$ and the reflection formula for the gamma function $\Gamma(1 - z)\,\Gamma(z) = \pi \csc \pi z$ allows (A3.4) to be written as

$$G(\Omega, -\Omega; 1; x) = \pi \csc \pi\Omega\left[\frac{\Gamma(-2\Omega)}{\Gamma(-\Omega)\,\Gamma(1-\Omega)} x^{-\Omega} F\left(\Omega, \Omega; 1+2\Omega; \frac{1}{x}\right)\right.$$

$$\left. - \frac{\Gamma(2\Omega)}{\Gamma(\Omega)\,\Gamma(1+\Omega)} x^{\Omega} F\left(-\Omega, -\Omega; 1-2\Omega; \frac{1}{x}\right)\right] \qquad \text{(A3.5)}$$

We take the branch cut for the hypergeometric function $G(\Omega, -\Omega; 1; x)$ along the positive real axis. This definition allows us to match the hypergeometric series solutions with the Bessel series solutions since both will have branch cuts along the positive real x axis.

The solution, E_z, of differential equation (A1.1) has branch points in general at $k_1\rho = \xi = 0, \pm p(x = \xi^2/p^2 = 0, 1)$. If we allow the collision frequency ω_{eff} to take on small positive values we find from the definition of k_1

$$k_1 \simeq k_o \sqrt{1 - \frac{\omega_p^2}{\omega^2}} \left[1 + \frac{i}{2} \frac{\omega_{eff}\, \omega_p^2/\omega^3}{1 - \omega_p^2/\omega^2}\right] \tag{A3.6}$$

$$p \simeq \frac{\eta}{c}(1 - i\, \omega_{eff}/\omega)$$

so for $\omega > \omega_p$ k_1 has a small positive imaginary component and p has a small negative imaginary component. The singularity of E_z at $\rho = p/k_1$ thus lies slightly below the positive real axis. The branch cut at $\rho = p/k_1$ must be taken to lie slightly below the positive real axis to avoid discontinuities in the solution for physical values of ρ. This branch point in the ξ plane lies at the point $\xi = p$ below the real positive axis for $\omega > \omega_p$. Physical values of ξ however now lie just above the positive real axis. This branch point singularity in the x plane lies at $x = 1$. Physical values of x for $\omega > \omega_p$ thus also lie just above the positive real axis, $\arg x = 0^+$.

The case of $\omega < \omega_p$ does not involve singularities along the physical axis. We may take k_1, and thus ξ, to be positive imaginary and x to be negative real with $\arg x = \pi$ (the parameter q in this case will be negative imaginary).

We use the relation

$$(-x)^{\pm\Omega} = e^{\mp i\pi\Omega}\, x^{\pm\Omega} \tag{A3.7}$$

where $0 < \arg x < 2\pi$

in equation (A3.3).

We now define the functions

$$F^{(\pm)}(\Omega, -\Omega; 1; x) = \frac{\Gamma(\pm 2\Omega)}{\Gamma(\pm\Omega)\,\Gamma(1 \pm \Omega)}\, x^{\pm m}\, F\left(\mp\Omega, \mp\Omega; 1 \mp 2\Omega; \frac{1}{x}\right) \tag{A3.8}$$

in terms of which (A3.3) and (A3.5) become

$$F(\Omega, -\Omega; 1; x) = (-1)^m \left[e^{i\pi\nu}\, x^{-\nu}\, F^{(-)}(\Omega, -\Omega; 1; x) + e^{-i\pi\nu} x^{\nu} F^{(+)}(\Omega, -\Omega; 1; x)\right] \tag{A3.9}$$

and

$$G(\Omega, -\Omega; 1; x) = (-1)^m\, \pi \csc \pi\nu \left[x^{-\nu} F^{(-)}(\Omega, -\Omega; 1; x) - x^{\nu} F^{(+)}(\Omega, -\Omega; 1; x)\right] \tag{A3.10}$$

The hypergeometric function series solutions EF (A1.3) and EG (A1.17) can therefore be written as

$$EF(p, x, x) = e^{i\pi\nu}\, x^{-\nu}\, EF^{(-)}(p, q, x) + e^{-i\pi\nu}\, x^{\nu}\, EF^{(+)}(p, q, x) \tag{A3.11}$$

$$EG(p, q, x) = \pi \csc \pi\nu \left[x^{-\nu}\, EF^{(-)}(p, q, x) - x^{\nu}\, EF^{(+)}(p, q, x)\right] \tag{A3.12}$$

where the functions denoted on the right are given by

$$EF^{(\pm)}(p, q, x) = \sum_{m=-\infty}^{\infty} (-1)^m c_m F^{(\pm)}(\Omega, -\Omega; 1; x) \tag{A3.13}$$

Substituting the power series representation of the hypergeometric function

$$F(a, b; c; x) = \sum_{m=0}^{\infty} \frac{(a)_m (b)_m}{(c)_m \, m!} x^m \tag{A3.14}$$

where

$$(a)_m = a(a + 1) \ldots (a + m - 1), \quad (a_0) = 1$$

into (A3.8) allows (A3.13) to be written as

$$EF^{(\pm)}(p, q, x) = \sum_{m=-\infty}^{\infty} f_m^{(\pm)} x^m \tag{A3.15}$$

where

$$f_m^{(\pm)} = \sum_{\ell=0}^{\infty} c_{\pm(\ell+m)} \frac{\Gamma(2\Omega_\pm)}{\Gamma(\Omega_\pm)\,\Gamma(1 + \Omega_\pm)} \frac{(-\Omega_\pm)_\ell^2 \, (-1)^{\ell+m}}{(1 - 2\Omega_\pm)_\ell \, \ell!} \tag{A3.16}$$

and $\Omega_\pm = \ell + m \pm \nu$. The recurrence properties of the gamma function can be used to cast (A3.16) into a form more useful for computation

$$f_m^{(\pm)} = \frac{\Gamma(2m \pm 2\nu)\,(-1)^m}{\Gamma^2(1 + m \pm \nu)} \sum_{\ell=0}^{\infty} c_{\pm(\ell+m)} \frac{(\ell + m \pm \nu)\,(2m \pm 2\nu)_\ell}{\ell!} \tag{A3.17}$$

The Bessel series solutions EJ (A1.18) and EY (A1.19), using $\xi = px^{\frac{1}{2}}$, can be written as

$$EJ(p, q, px^{\frac{1}{2}}) = x^{\nu}\, EJ^{(+)}(p, q, x) \tag{A3.18}$$

and

$$EY(p, q, px^{\frac{1}{2}}) = x^{\nu}\, EJ^{(+)}(p, q, x)\, \cot 2\pi\nu \; - x^{-\nu}\, EJ^{(-)}(p, q, x) \csc 2\pi\nu \tag{A3.19}$$

Using the series expansion for the Bessel function

$$J_{\mu}(\xi) = \left(\frac{1}{2}\xi\right)^{\mu} \sum_{m=0}^{\infty} \frac{\left(-\frac{1}{4}\xi^2\right)^m}{m!\, \Gamma(m + \mu + 1)} \tag{A3.20}$$

and the definition of the Bessel function of the second kind

$$Y_{\mu}(\xi) = J_{\mu}(\xi) \cot \pi\mu - J_{-\mu}(\xi) \csc \pi\mu \tag{A3.21}$$

the functions on the right of (A3.18) and (A3.19) can be written as

$$EJ^{(\pm)}(p, q, x) = \sum_{m=-\infty}^{\infty} j_m^{(\pm)}\, x^m \tag{A3.22}$$

where

$$j_m^{(\pm)} = \pm\left(\frac{p^2}{4}\right)^{m \pm \nu} \sum_{\ell=0}^{\infty} \frac{(-1)^{\ell}\; c_{\pm}(m-\ell)}{\ell!\, \Gamma(2m - \ell \pm 2\nu + 1)(m - \ell \pm \nu)} \tag{A3.23}$$

The recurrence properties of the gamma function give

$$j_m^{(\pm)} = \pm \frac{\left(\frac{p^2}{4}\right)^{m\pm\nu}}{\Gamma(2m \pm 2\nu + 1)} \sum_{\ell = 0}^{\infty} \frac{(-2m \mp 2\nu)_\ell}{\ell!\ (m - \ell \pm \nu)}\ c_{\pm(m-\ell)} \qquad \text{(A3.24)}$$

which is simpler for computation.

APPENDIX 4

Limiting Forms of Solutions

The behavior of the solutions EF (A1.3) and EG (A1.17) as x tends to zero will be determined. Since we know

$$F(\Omega, -\Omega; 1; 0) = 1$$

it immediately follows that

$$EF(p, q, x) \sim S_2 \ , \ x \to 0 \tag{A4.1}$$

where we define $S_2 = \sum_{m=-\infty}^{\infty} c_m$

The analytic continuation of the function $G(\Omega, -\Omega; 1; x)$ to the origin is carried out with the linear transformation formula

$$F(a, b, a+b; x) = \frac{\Gamma(a+b)}{\Gamma(a)\,\Gamma(b)} \sum_{m=0}^{\infty} \frac{(a)_m (b)_m}{(m!)^2} \Big[2\psi(m+1) - \psi(a+m) - \psi(b+m) - \ell n(1-x) \Big] (1-x)^m, (|\arg(1-x)| < \pi, \ |1-x| < 1) \tag{A4.2}$$

where ψ is the digamma function. The series expansion for G near the origin is therefore

$$G(\Omega, -\Omega; 1; x) = -F(\Omega, -\Omega; 1; x)\, \ell n x - \sum_{\ell=0}^{\infty} \frac{(\Omega)_\ell \, (-\Omega)_\ell}{(\ell!)^2} \Big[\psi(\ell+\Omega) + \psi(\ell-\Omega) - 2\psi(\ell+1) \Big] x^\ell \tag{A4.3}$$

The asymptotic form of EG is therefore

$$EG(p, q, x) \sim -(2\gamma + \ell n x)S_2 - \sum_{m=-\infty}^{\infty} c_m[\psi(\Omega) + \psi(-\Omega)] \qquad (A4.4)$$

where γ is Euler's constant

We define the sum

$$S_3 = -2\gamma\, S_2 - \sum_{m=-\infty}^{\infty} c_m[\psi(\Omega) + \psi(-\Omega)] \qquad (A4.5)$$

and using the recurrence properties of the digamma function this can be written as

$$S_3 = -\left[2\gamma + \pi \cot \pi\nu + 2\psi(\nu)\right] S_2 - \sum_{m=0}^{\infty} c_m \left[\frac{1}{m+\nu} + 2 \sum_{k=0}^{m-1} \frac{1}{k+\nu}\right]$$

$$- \sum_{m=1}^{\infty} c_{-m}\left[\frac{1}{m-\nu} + 2 \sum_{k=1}^{m-1} \frac{1}{k-\nu}\right] \qquad (A4.6)$$

where the last sum is defined to be zero if m equals zero.

The asymptotic behavior of the solution

$$EH(p, q, \xi) = \sum_{m=-\infty}^{\infty} \frac{c_m}{\Omega} H_{2\Omega}^{(1)}(\xi) \qquad (A4.7)$$

as ξ tends to infinity will now be determined. The asymptotic form of the Hankel function is

$$H_{2\Omega}^{(1)}(\xi) \sim \sqrt{\frac{2}{\pi\xi}}\, e^{i\left(\xi - \pi\Omega - \frac{\pi}{4}\right)}, \quad \xi \to \infty \tag{A4.8}$$

Therefore the expansion of (A4.7) is

$$EH(p, q, \xi) \sim \sqrt{\frac{2}{\pi\xi}}\, e^{i\left(\xi - \frac{\pi}{4}\right)}\, e^{-i\pi\nu}\, S_1 \tag{A4.9}$$

where

$$S_1 = \sum_{m=-\infty}^{\infty} \frac{c_m}{\Omega} (-1)^m \tag{A4.10}$$

We note from (A4.8) that the Hankel function of zeroth order has the same asymptotic form as the initial two factors in (A4.9). The replacement of these two factors by $H_0^{(1)}(\xi)$ in Chapter 3 is only done as a notational convenience and is not meant to indicate higher accuracy.

APPENDIX 5

WKB Solution to Radiation Problem

The differential equation to be solved is (3C.2) in the case where $\omega > \omega_p$. Defining a new dependent variable by

$$E_z = \xi'^{-\frac{1}{2}} u \tag{A5.1}$$

transforms (3C.2) into

$$\frac{d^2u}{d\xi'^2} = - p^2 \left[Q_o^2(\xi') + \frac{1}{4p^2\xi'^2} \right] u \tag{A5.2}$$

where

$$Q_o^2(\xi') = \frac{\xi'^2 - \alpha^2}{\xi'^2 - 1}$$

To apply the WKB method the positive real ξ' axis is split into six regions. The approximate solution in each region is

$$u \sim \xi'^{\frac{1}{2}} \left[H_o^{(1)}(\alpha p \xi') + R H_o^{(2)}(\alpha p \xi') \right] , \; 0 < \xi' << 1 \tag{A5.3}$$

$$u \sim a_6 \, Q_o^{-\frac{1}{2}}(\xi') \left[e^{ip\zeta'} + a_7 \, e^{-ip\zeta'} \right] , \; p^{-1} << \xi' < 1 \tag{A5.4}$$

$$(\xi' - 1) >> p^{-2}$$

where $\zeta' = \int_0^{\xi'} Q_0(t)dt$

$$u \sim a_4 y_1^{\frac{1}{2}} \left[I_1\left(2y_1^{\frac{1}{2}}\right) + a_5 K_1\left(2y_1^{\frac{1}{2}}\right) \right] , \quad (\xi' - 1) \ll 1 \tag{A5.5}$$

where $y_1 = p^2 \frac{\alpha^2 - 1}{2} (\xi' - 1)$ and I_1, K_1 are modified Bessel functions,

$$u \sim a_2 Q_0^{-\frac{1}{2}}(\xi') \left[e^{ip\zeta} + a_3 e^{-ip\zeta} \right] , \quad 1 < \xi' < \alpha, \tag{A5.6}$$

$$(\xi' - 1) \gg p^{-2}, \ (\xi' - \alpha) \gg p^{-2/3}$$

where $\zeta = \int_\alpha^{\xi'} Q_0(t)dt$

$$u \sim a_1 \left[Bi(-y_2) + i\, Ai(-y_2) \right] , \quad (\xi' - \alpha) \ll 1 \tag{A5.7}$$

where $y_2 = \left(p^2 \frac{2\alpha}{\alpha^2 - 1} \right)^{1/3} (\xi' - \alpha)$

$$u \sim T \sqrt{\frac{2}{\pi p}}\, e^{-i(p P_1 + \pi/4)}\, Q_0^{-\frac{1}{2}}(\xi')\, e^{ip\zeta} , \quad \xi' > \alpha, \tag{A5.8}$$

$$(\xi' - \alpha) \gg p^{-2/3}$$

where $P_1 = \int_\alpha^\infty [Q_0(t) - 1]\, dt - \alpha$

and the multiplicative factor in (A5.8) has been chosen so that this solution agrees with the asymptotic form of (2B.4). The matching of (A5.3) to (A5.8) in the regions of overlap determines the transmission and reflection coefficients T and R. To first order these are

$$R = \frac{1}{2} e^{-2p\zeta_o + i2pP_o} \tag{A5.9}$$

where $\zeta_o = \int_1^{\alpha} \sqrt{\frac{\alpha^2 - t^2}{t^2 - 1}}\, dt$

$$P_o = \int_o^{1} \sqrt{\frac{t^2 - \alpha^2}{t^2 - 1}}\, dt$$

and

$$T = e^{-p\zeta_o} \tag{A5.10}$$

The $\omega < \omega_p$ problem deals with equation (3C.5). The boundary is placed at

$$\tilde{\xi}_o = - i\xi_o/p = - ik_1\rho_o/p \tag{A5.11}$$

where $\tilde{\xi}_o$ is a real quantity. The boundary conditions (2B.7) and (2B.8) can be written as

$$E_z = T\, H_o^{(1)}(\tilde{\alpha} p \tilde{\xi}_o) \tag{A5.12}$$

$$\frac{dE_z}{d\tilde{\xi}} = - T\, p\, \tilde{\alpha}\, H_1^{(1)}(\tilde{\alpha} p \tilde{\xi}_o) \tag{A5.13}$$

The transformation

$$E_z = \tilde{\xi}^{-\frac{1}{2}} u \tag{A5.14}$$

transforms (3C.5) into

$$\frac{d^2u}{d\tilde{\xi}^2} = p^2\left[Q_1^2(\tilde{\xi}) - \frac{1}{4p^2\tilde{\xi}^2}\right]u \tag{A5.15}$$

where $Q_1^2(\tilde{\xi}) = \frac{\tilde{\xi}^2 - \tilde{\alpha}^2}{\tilde{\xi}^2 + 1}$ and $\arg Q_1(\tilde{\xi}) = \frac{\pi}{2}$ for $\tilde{\xi} < \tilde{\alpha}$

We assume that the quantity $\tilde{\alpha}$ is order unity and to further simplify matters that

$$\tilde{\alpha}\, p\, \tilde{\xi}_o >> 1 \tag{A5.16}$$

which allows the approximation of the boundary conditions (A5.12) and (A5.13) [38] as

$$u \sim T\sqrt{\frac{2}{\pi\tilde{\alpha}p}}\; e^{i(\tilde{\alpha}\, p\, \tilde{\xi}_o - \pi/4)} \tag{A5.17}$$

$$\frac{du}{d\tilde{\xi}} \sim T\, i\, \tilde{\alpha}\, p\sqrt{\frac{2}{\pi\tilde{\alpha}p}}\; e^{i(\tilde{\alpha}\, p\, \tilde{\xi}_o - \pi/4)} \tag{A5.18}$$

Making use of the Langer transform [39] we can write the asymptotic solution to (A5.15) as

$$u \sim d_1\, T\, Q_1^{-\frac{1}{2}}(\tilde{\xi})\,\psi^{\frac{1}{4}}\,[Ai(\psi) + d_2\, Bi(\psi)] \tag{A5.19}$$

where $\psi = \left[\frac{3p}{2}\int_{\tilde{\alpha}}^{\tilde{\xi}} Q_1(t)\, dt\right]^{2/3}$

and $\arg\psi = \pi$ if $\tilde{\xi} < \tilde{\alpha}$

Ai and Bi are the Airy functions and d_1 and d_2 are arbitrary constants. The boundary conditions (A5.17) and (A5.18) determine the values of d_1 and d_2 as

$$d_2 = \frac{i\,\tilde{\alpha}\,\psi_0^{\frac{1}{2}}\,Ai(\psi_0) - Ai'(\psi_0)\,Q_1(\tilde{\xi}_0)}{Bi'(\psi_0)\,Q_1(\tilde{\xi}_0) - i\,\tilde{\alpha}\,\psi_0^{\frac{1}{2}}\,Bi(\psi_0)} \tag{A5.20}$$

$$d_1 = \frac{\sqrt{\frac{2}{\pi\tilde{\alpha}p}}\,Q_1^{\frac{1}{2}}(\tilde{\xi}_0)\,\psi_0^{-\frac{1}{4}}\,e^{i(\tilde{\alpha}\,p\,\tilde{\xi}_0 - \pi/4)}}{Ai(\psi_0) + d_2\,Bi(\psi_0)} \tag{A5.21}$$

where $\psi_0 = \psi(\tilde{\xi}_0)$ and the prime denotes differentiation with respect to ψ. In the overlap region $1 >> \tilde{\xi} >> 1/p$ the boundary condition (2B.2) becomes

$$u \sim \sqrt{\frac{2}{\pi\tilde{\alpha}p}}\left[e^{i(\tilde{\alpha}\,p\,\tilde{\xi} - \pi/4)} + R\,e^{-i(\tilde{\alpha}\,p\,\tilde{\xi} - \pi/4)}\right] \tag{A5.22}$$

which when matched to (A5.19) determines R and T as

$$R = \frac{1 + i\,d_2}{-1 + i\,d_2}\,e^{i2p\zeta_3} \tag{A5.23}$$

$$T = \frac{2\sqrt{\frac{2}{p}}\,e^{ip\zeta_3}}{(i + d_2)\,d_1} \tag{A5.24}$$

where $\zeta_3 = \int_0^{\tilde{\alpha}} Q_2(t)\, dt$

and $Q_2(t) = - i\, Q_1(t)$

APPENDIX 6

Integral Representations and Connection of Solutions to Modal Equations

The modal equations given in Section 6B are

$$\frac{d^2h}{d\xi^2} + \frac{1}{\xi}\frac{dh}{d\xi} + \left(1 - \frac{\nu^2}{\xi^2}\right)h = i\frac{\beta}{\xi}e \tag{A6.1}$$

$$\frac{d^2e}{d\xi^2} + \frac{1}{\xi}\frac{de}{d\xi} + \left(k^2 - \frac{n^2}{\xi^2}\right)e = -i\frac{\beta}{\xi}h \tag{A6.2}$$

Series solutions were derived by the method of Frobenius in Section 6B. These are designated as $h_{\pm}^{(1)}$, $e_{\pm}^{(1)}$ and $h_{\pm}^{(2)}$, $e_{\pm}^{(2)}$. Asymptotic solutions for large ξ were also found. These are designated as $h_{\pm}^{(3)}$, $e_{\pm}^{(3)}$ and $h_{\pm}^{(4)}$, $e_{\pm}^{(4)}$. We wish now to find the connections which exist between the series and asymptotic solutions.

The connection problem can be related to one which has been studied previously, namely, the second order equation with four regular singular points (Heun's equation). To show this we assume a solution of the form

$$h = \int_c A(\lambda)\, J_\nu(\lambda\xi)\, d\lambda \tag{A6.3}$$

$$e = \int_c B(\lambda)\, \xi\, J_\nu(\lambda\xi)\, d\lambda \tag{A6.4}$$

where c is a suitably chosen contour. Inserting this trial solution into (A6.1) yields the relation

$$(1 - \lambda^2)\, A(\lambda) = i\, \beta\, B(\lambda) \tag{A6.5}$$

Inserting this trial solution into (A6.2) and using (A6.5) gives

$$\int_C B(\lambda)\, L_\nu\, J_\nu(\lambda\xi)\, d\lambda = 0 \tag{A6.6}$$

where L_ν represents the differential operator

$$L_\nu = (\lambda^2 - k^2) \frac{d^2}{d\lambda^2} + \left(3\lambda - \frac{k^2}{\lambda}\right) \frac{d}{d\lambda} + \frac{k^2\nu^2}{\lambda^2} - n^2 + 1 + \frac{\beta^2}{\lambda^2 - 1}$$

Successive integrations by parts give

$$\int_C J_\nu(\lambda\xi)\, M_\nu\, B(\lambda)\, d\lambda + Q_\nu(B) = 0 \tag{A6.7}$$

where M_ν is the adjoint to L_ν given by

$$M_\nu = (\lambda^2 - k^2) \frac{d^2}{d\lambda^2} + \left(\lambda + \frac{k^2}{\lambda}\right) \frac{d}{d\lambda} + \frac{k^2(\nu^2 - 1)}{\lambda^2} - n^2 + \frac{\beta^2}{\lambda^2 - 1}$$

and Q_ν represents the boundary terms resulting from integration by parts

$$Q_\nu(B) = \left[B(\lambda) \left\{ (\lambda^2 - k^2) \frac{d}{d\lambda} + 3\lambda - \frac{k^2}{\lambda} \right\} J_\nu(\lambda\xi)\right]_C$$

$$- \left[J_\nu(\lambda\xi) \left\{ (\lambda^2 - k^2) \frac{d}{d\lambda} + 2\lambda \right\} B(\lambda)\right]_C$$

where the notation $[\ ]_c$ indicates the quantity within the brackets is to be evaluated at the end points of the contour c. The integral representation (A6.4) for e will yield a solution to the modal equations if we take

$$M_\nu B = 0 \tag{A6.8}$$

and choose the contour appropriately so that the boundary terms $Q_\nu(B)$ vanish.

By making the change of variables

$$z = \lambda^2/k^2$$
$$B(\lambda) = z^{(1-\nu)/2}\, w(z) \tag{A6.9}$$

equation (A6.8) becomes

$$\frac{d^2w}{dz^2} + \left(\frac{\gamma_o}{z} + \frac{\delta_o}{z-1} + \frac{\varepsilon_o}{z-a}\right)\frac{dw}{dz} + \frac{\alpha_o\beta_o(z-q_o)}{z(z-1)(z-a)}\, w = 0 \tag{A6.10}$$

where $\gamma_o = 1 - \nu$ $\qquad \alpha_o = (1 - \nu - n)/2$

$\delta_o = 1$ $\qquad \beta_o = (1 - \nu + n)/2$

$\varepsilon_o = o$ $\qquad q_o = a - \dfrac{\beta^2 a}{(1-\nu)^2 - n^2}$

$a = 1/k^2$ $\qquad \alpha_o + \beta_o + 1 = \gamma_o + \delta_o + \varepsilon_o$

Equation (A6.10) is a second order ordinary differential equation with four regular singular points known as Heun's equation. The solution which is analytic at the origin is designated [16] by

$$w = Hu(a, q_o; \alpha_o, \beta_o, \gamma_o, \delta_o; z) \tag{A6.11}$$

where γ_o is not equal to zero or a negative integer. This solution has the series expansion

$$Hu(a, q_o; \alpha_o, \beta_o, \gamma_o, \delta_o; z) = \sum_{m=o}^{\infty} g_m(q_o)\, z^m \tag{A6.12}$$

where the $g_m(q_o)$ satisfy the three term recurrence relation

$$a(m+1)(m+\gamma_o)\, g_{m+1}(q_o) - [m^2(1+a) + m\{a(\gamma_o + \delta_o - 1) + \gamma_o + \varepsilon_o - 1\} + \alpha_o\beta_o\, q_o]\, g_m(q_o) + (m + \alpha_o - 1)(m + \beta_o - 1)\, g_{m-1}(q_o) = 0 \tag{A6.13}$$

with $g_o(q_o) = 1$ and $g_{-1}(q_o) = 0$. The series expansion (A6.12) only converges out to the nearer of the two singular points 1 or a. Solutions of (A6.10) near $z = \infty$ can be written as

$$w = z^{-\alpha_o} Hu\left(\frac{1}{a}, q_\infty; \alpha_o, \alpha_o - \gamma_o + 1, \alpha_o - \beta_o + 1, \delta_o; \frac{1}{z}\right) \tag{A6.14}$$

$$w = z^{-\beta_o} Hu\left(\frac{1}{a}, \tilde{q}_\infty; \beta_o, \beta_o - \gamma_o + 1, \beta_o - \alpha_o + 1, \delta_o; \frac{1}{z}\right) \tag{A6.15}$$

where

$$\alpha_o\beta_o q_o = a\,\alpha_o(\alpha_o - \gamma_o + 1)q_\infty + \alpha_o[\beta_o(1 + a) - \delta_o - \varepsilon_o\, a]$$

$$\alpha_o\beta_o q_o = a\,\beta_o(\beta_o - \gamma_o + 1)\,\tilde{q}_\infty + \beta_o[\alpha_o(1 + a) - \delta_o - \varepsilon_o a]$$

In our case the exponents at infinity, α_o and β_o, differ by an integer, n. Thus only the solution (A6.15) is valid. The equation (A6.14) must be modified by the inclusion of log terms. At present let us take (A6.15) as the desired solution of (A6.10). The integral representation for e now becomes

$$\frac{e}{\xi} = \int_c \left(\frac{\lambda}{k}\right)^{-n} Hu\left(\frac{1}{a}\,,\ \tilde{q}_\infty\ ;\ \beta_o,\ \beta_o - \gamma_o + 1,\ \beta_o - \alpha_o + 1,\ \delta_o;\ \frac{k^2}{\lambda^2}\right) J_\nu(\lambda\xi)\,d\lambda \tag{A6.16}$$

We will assume for simplicity that k is real and between 0 and 1. We further assume that ξ is positive real. This represents a typical case. The contour c is shown in Fig. 19. The boundary terms, $Q_\nu(B)$, vanish at the end points provided $n \geq 2$. Thus (A6.16) represents a solution to the modal equations for $n \geq 2$.

The series expansion for e may be extracted from (A6.16) by deforming the contour as shown in Fig. 20. We may now replace the solution of Heun's equation with its series representation about the point $\lambda = \infty$.

$$Hu\left(\frac{1}{a}\,,\ \tilde{q}_\infty\ ;\ \beta_o,\ \beta_o - \gamma_o + 1,\ \beta_o - \alpha_o + 1,\ \delta_o\ ;\ \frac{k^2}{\lambda^2}\right) = \sum_{m\,=\,o}^{\infty} g_m(\tilde{q}_\infty)\left(\frac{k^2}{\lambda^2}\right)^m \tag{A6.17}$$

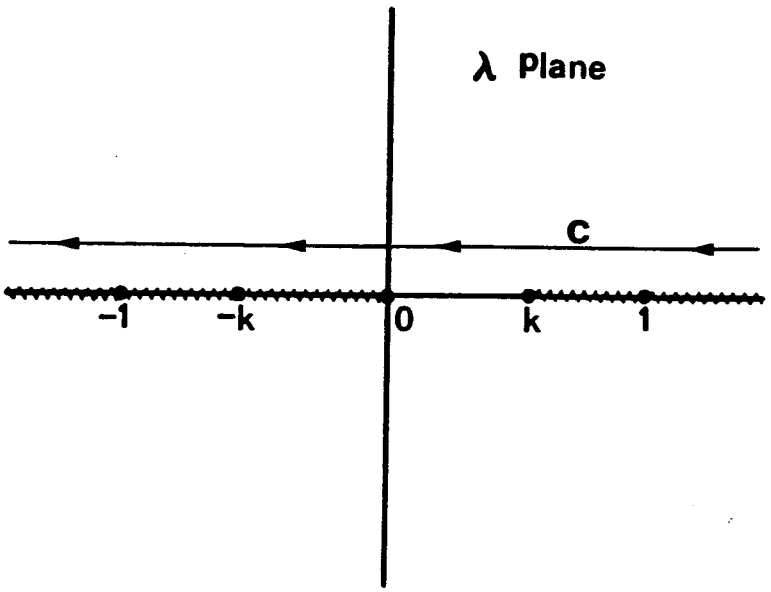

Fig. 19. Contour for the Hankel transform in the λ plane.

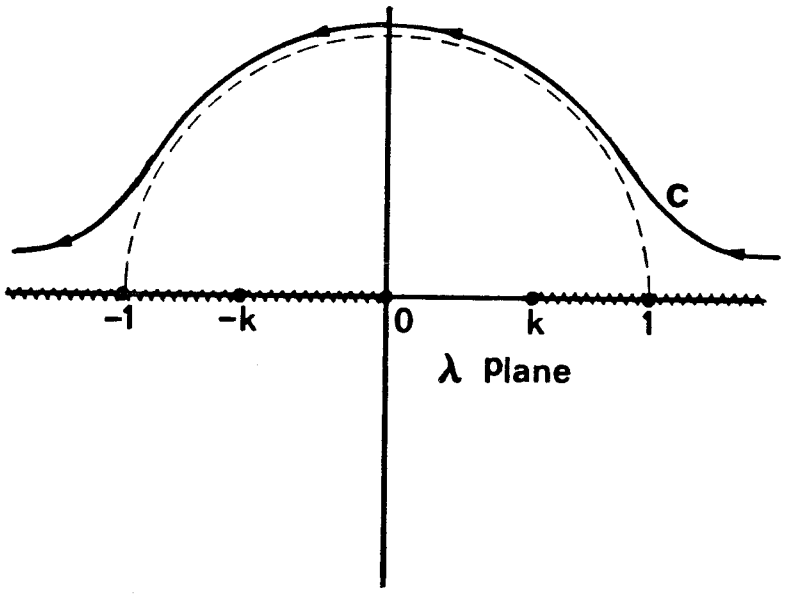

Fig. 20. Deformed contour for the evaluation of the Hankel transform as a power series.

where $g_m(\tilde{q}_\infty)$ satisfies recurrence relation (A6.13) with the parameters as indicated in the above expression. Since (A6.17) is uniformly convergent on the deformed contour c we may interchange the order of summation and integration

$$\frac{e}{\xi} = \sum_{m=0}^{\infty} g_m(\tilde{q}_\infty)\, k^{2m-n} \int_c \lambda^{-n-2m} J_\nu(\lambda\xi)\, d\lambda \tag{A6.18}$$

or

$$e = \sum_{m=0}^{\infty} g_m(\tilde{q}_\infty)\, k^{2m-n}\, \xi^{2m+n} \int_c \lambda^{-n-2m} J_\nu(\lambda)\, d\lambda \tag{A6.19}$$

By use of the Poisson integral representation for the Bessel function we obtain the identity [40]

$$\int_c \lambda^{\mu-\nu-1} J_\nu(\lambda)\, d\lambda = \frac{2i \sin\frac{\pi}{2}\mu\, \Gamma\left(\frac{\mu}{2}\right) e^{i\frac{\pi}{2}\mu}}{2^{\nu-\mu+1}\, \Gamma\left(\nu - \frac{\mu}{2} + 1\right)} \tag{A6.20}$$

$$\mathrm{Re}(\mu - \nu - 1) < \frac{1}{2}$$

Use of (A6.20) in (A6.19) along with the reflection formula of the gamma function yields

$$e = -\frac{\pi e^{i\frac{\pi}{2}(\nu-n)}}{2^{n-1} k^n} \sum_{m=0}^{\infty} \frac{g_m(\tilde{q}_\infty)(k/2)^{2m}(-1)^m}{\Gamma\left(\frac{n+2m+1+\nu}{2}\right)\Gamma\left(\frac{n+2m+1-\nu}{2}\right)} \xi^{2m+n} \tag{A6.21}$$

By transforming the recurrence relation (A6.13) we find that the coefficient

$$c_m = \frac{g_m(\tilde{q}_\infty)\ (k/2)^{2m}(-1)^m}{\Gamma\left(\frac{n + 2m + 1 + \nu}{2}\right)\Gamma\left(\frac{n + 2m + 1 - \nu}{2}\right)}$$

satisfies the recurrence relation

$$\left\{(2m + n + 1)^2 - \nu^2\right\}\left\{(2m + n + 2)^2 - n^2\right\} c_{m+1} +$$

$$+ \left[k^2\left\{(2m + n + 1)^2 - \nu^2\right\} + (2m + n)^2 - n^2 - \beta^2\right] c_m + k^2 c_{m-1} = 0 \qquad \text{(A6.22)}$$

the same recurrence relation satisfied by $b_m^{(2)+}$ in (6B.6). Therefore

$$e = -\frac{\pi\, e^{i\frac{\pi}{2}(\nu-n)}}{2^{n-1}\, k^n\, \Gamma\left(\frac{n + 1 + \nu}{2}\right)\Gamma\left(\frac{n + 1 - \nu}{2}\right)}\ e_+^{(2)} \qquad \text{(A6.23)}$$

We now wish to determine the asymptotic form of e from the integral representation (A6.16). First we transform the integral to the z plane.

$$\frac{e}{\xi} = \frac{k}{2}\int_c z^{-\beta_0}\, Hu\left(\frac{1}{a}, \tilde{q}_\infty; \beta_0, \beta_0 - \gamma_0 + 1, \beta_0 - \alpha_0 + 1, \delta_0; \frac{1}{z}\right)$$

$$z^{-\nu/2}\, J_\nu(k\xi z^{1/2})dz \qquad \text{(A6.24)}$$

where the contour in the z plane is shown in Fig. 21 . We have chosen the origin branch cut to lie along the positive real axis rather than its typical definition. The contour is deformed as shown in Fig. 22 . We label the circular contour about the origin c_a, the top contour c_b, and the bottom contour c_c. Now let us define

$$w(z) = z^{-\beta_o} \, Hu\left(\frac{1}{a}, \tilde{q}_\infty; \beta_o; \beta_o - \gamma_o + 1, \delta_o; \frac{1}{z}\right) \tag{A6.25}$$

and in terms of this we can write

$$I_a = \int_{c_a} w(z) \, z^{-\nu/2} \, J_\nu(k\xi z^{1/2}) dz, \quad 0 < \arg z < 2\pi \tag{A6.26}$$

$$I_b = \int_{c_b} w(z) \, z^{-\nu/2} \, J_\nu(k\xi z^{1/2}) dz, \quad \arg z = 0 \tag{A6.27}$$

$$I_c = \int_{c_c} w(ze^{i2\pi}) \, z^{-\nu/2} \, J_\nu(k\xi z^{1/2}) dz, \quad \arg z = 0 \tag{A6.28}$$

and $\frac{2}{k} e/\xi = I_a + I_b + I_c$

we need to consider the form taken by w(z) in the vicinity of the origin. The analytic continuation is

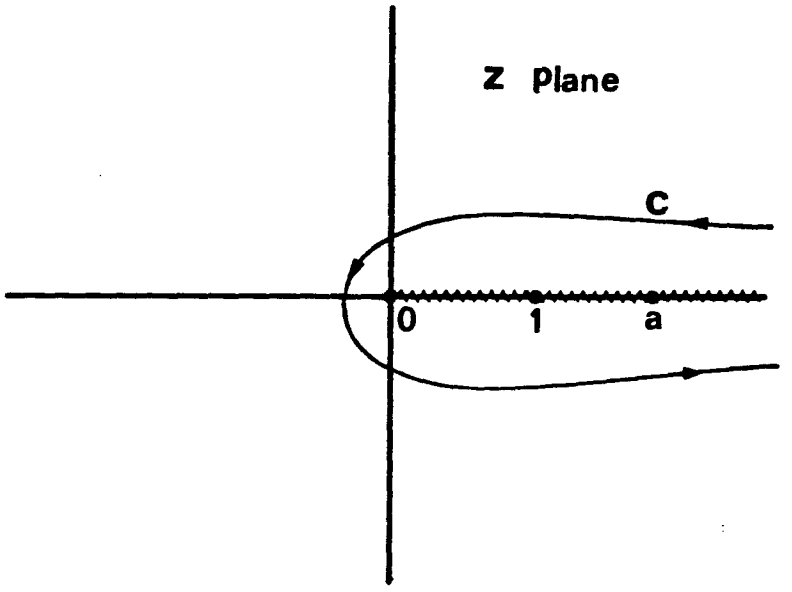

Fig. 21. Contour for the Hankel transform in the z plane.

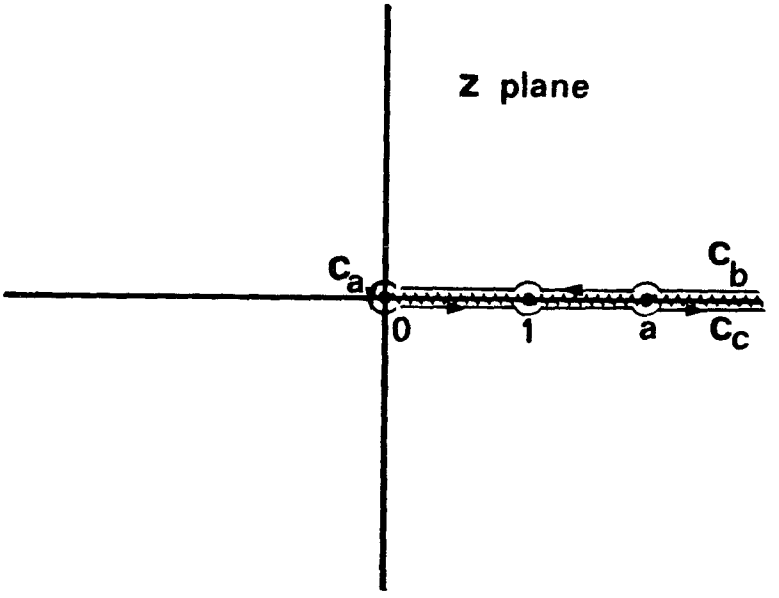

Fig. 22. Deformed contour for asymptotic evaluation of the Hankel transform.

$$w(z) = c_{\infty 2}^{o1}\, Hu(a, q_o; \alpha_o, \beta_o, \gamma_o, \delta_o; z) +$$

$$+ c_{\infty 2}^{o2}\; z^{1-\gamma_o}\, Hu(a, \tilde{q}_o; \alpha_o - \gamma_o + 1, \beta_o - \gamma_o + 1, 2 - \gamma_o, \delta_o; z) =$$

$$= c_{\infty 2}^{o1}\; w_{o1} + c_{\infty 2}^{o2}\; w_{o2} \qquad \text{(A6.29)}$$

where $c_{\infty 2}^{o1}$ and $c_{\infty 2}^{o2}$ are connecting constants for Heun's equation. The equation (A6.29) thus connects the 2nd solution at ∞, (A6.25), with the two solutions near the origin. From the form of w(z) given in (A6.29) and the value of γ_o given below (A6.10) we see that I_a vanishes as the radius of the contour c_a approaches zero. Using the identity

$$J_\nu(k\xi z^{1/2}) = \frac{1}{2}\left[H_\nu^{(1)}(k\xi z^{1/2}) + H_\nu^{(2)}(k\xi z^{1/2})\right] \qquad \text{(A6.30)}$$

we write I_b and I_c each as the sum of six integrals.

$$I_b = I_{b1} + I_{b2} + I_{b3} + I_{b4} + I_{b5} + I_{b6} \qquad \text{(A6.31)}$$

where

$$I_{b1} = \frac{1}{2}\int_{c_{b1}} w(z)\, z^{-\nu/2}\, H_\nu^{(1)}(k\xi z^{1/2})dz, \quad \arg z = \pi$$

$$I_{b2} = \frac{1}{2}\int_{c_{b2}} w(z)\, z^{-\nu/2}\, H_\nu^{(1)}(k\xi z^{1/2})dz, \quad 0 < \arg z < \pi$$

$$I_{b3} = \frac{1}{2} \int_{C_{b3}} w(z)\, z^{-\nu/2}\, H_\nu^{(2)}(k\xi z^{1/2})dz, \quad \arg z = -\pi$$

$$I_{b4} = \frac{1}{2} \int_{C_{b4}} w(z)\, z^{-\nu/2}\, H_\nu^{(2)}(k\xi z^{1/2})dz, \quad -\pi < \arg z < 0$$

$$I_{b5} = \frac{1}{2} \int_{C_{b5}} w(z)\, z^{-\nu/2}\, H_\nu^{(2)}(k\xi z^{1/2})dz, \quad \begin{matrix} -\pi < \arg z < 0 \\ -\frac{3\pi}{2} < \arg(1 - z) < \frac{\pi}{2} \end{matrix}$$

$$I_{b6} = \frac{1}{2} \int_{C_{b6}} w(z)\, z^{-\nu/2}\, H_\nu^{(2)}(k\xi z^{1/2})dz, \quad \begin{matrix} -\pi < \arg z < 0 \\ -\frac{3\pi}{2} < \arg(a - z) < \frac{\pi}{2} \end{matrix}$$

The various contours are shown in Fig. 23. Similarly,

$$I_c = I_{c1} + I_{c2} + I_{c3} + I_{c4} + I_{c5} + I_{c6} \tag{A6.32}$$

where

$$I_{c1} = \frac{1}{2} \int_{C_{c1}} w(ze^{i2\pi})\, z^{-\nu/2}\, H_\nu^{(2)}(k\xi z^{1/2})dz, \quad \arg z = -\pi$$

$$I_{c2} = \frac{1}{2} \int_{C_{c2}} w(ze^{i2\pi})\, z^{-\nu/2}\, H_\nu^{(2)}(k\xi z^{1/2})dz, \quad -\pi < \arg z < 0$$

$$I_{c3} = \frac{1}{2} \int_{C_{c3}} w(ze^{i2\pi})\, z^{-\nu/2}\, H_\nu^{(1)}(k\xi z^{1/2})dz, \quad \arg z = \pi$$

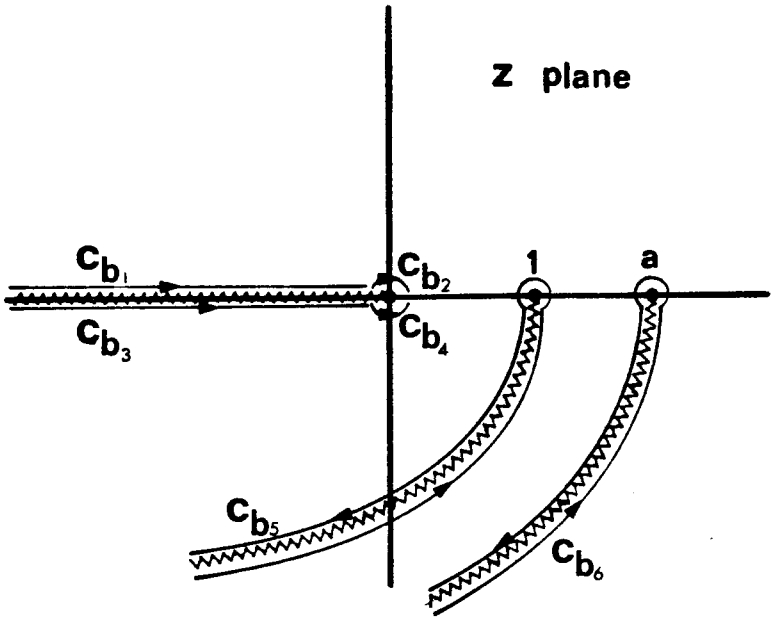

Fig. 23. Contour c_b further broken up for asymptotic evaluation of the Hankel transform.

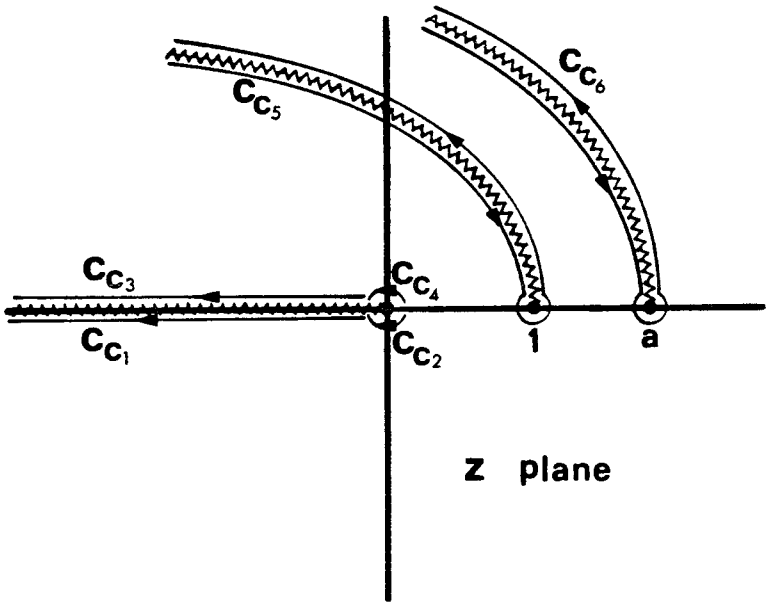

Fig. 24. Contour c_C further broken up for asymptotic evaluation of the Hankel transform.

$$I_{c4} = \frac{1}{2} \int_{C_{c4}} w(ze^{i2\pi})\, z^{-\nu/2}\, H_\nu^{(1)}(k\xi z^{1/2})dz, \quad 0 < \arg z < \pi$$

$$I_{c5} = \frac{1}{2} \int_{C_{c5}} w(ze^{i2\pi})\, z^{-\nu/2}\, H_\nu^{(1)}(k\xi z^{1/2})dz, \quad \begin{matrix} 0 < \arg z < \pi \\ -\frac{\pi}{2} < \arg(1 - z) < \frac{3\pi}{2} \end{matrix}$$

$$I_{c6} = \frac{1}{2} \int_{C_{c6}} w(ze^{i2\pi})\, z^{-\nu/2}\, H_\nu^{(1)}(k\xi z^{1/2})dz, \quad \begin{matrix} 0 < \arg z < \pi \\ -\frac{\pi}{2} < \arg(a - z) < \frac{3\pi}{2} \end{matrix}$$

where the various contours are shown in Fig. 24. The contribution to I_{b2}, I_{b4}, I_{c2}, and I_{c4} from the w_{o2} component of $w(z)$ vanish as the radii of these circular contours approach zero. Furthermore, since $w_{o1}(z)$ is analytic at the origin $w_{o1}(ze^{i2\pi}) = w_{o1}(z)$ and therefore

$$I_{b2} = - I_{c4}$$

$$I_{b4} = - I_{c2}$$

Thus the contribution from the circular contours near the origin cancel. The analyticity of $w_{o1}(z)$ at the origin also means that

$$I'_{b1} = - I'_{c3}$$

$$I'_{b3} = - I'_{c1}$$

where the superscript 1 indicates the w_{o1} component. We are therefore left to consider I^2_{b1}, I^2_{b3}, I^2_{c1}, and I^2_{c3}, the w_{o2} components. We note that

$$w_{o2}(ze^{-i\pi}) = e^{-i2\pi\nu}\, w_{o2}(ze^{i\pi})$$

and therefore

$$I^2_{b1} = -\, I^2_{b3} = -\,\frac{i}{\pi}\, e^{-i\pi\nu}\, c^{o2}_{\infty 2} \int_0^\infty w_{o2}(ze^{i\pi})\, z^{-\nu/2}\, K_\nu(k\xi z^{1/2})dz$$

and similarly

$$I^2_{c1} = -\, I^2_{c3} = -\,\frac{i}{\pi}\, e^{i\pi\nu}\, c^{o2}_{\infty 2} \int_0^\infty w_{o2}(ze^{i\pi})\, z^{-\nu/2}\, K_\nu(k\xi z^{1/2})dz$$

where K_ν represents the modified Bessel function.

The integrals near the origin therefore all cancel and we are left with

$$\frac{2}{k}\;\frac{e}{\xi} = I_{b5} + I_{b6} + I_{c5} + I_{c6} \qquad \text{(A6.33)}$$

We will now perform an asymptotic evaluation of the integrals in (A6.33). However, we must first discuss the analytic continuation of w(z) to the vicinity of the points z = 1 and z = a. Since the exponent differences at each of these points are integers log terms will appear. Near z = 1

we have

$$w(z) = c_{\infty 2}^{11} \; w_{11} + c_{\infty 2}^{12} \; w_{12} \tag{A6.34}$$

where

$$w_{11} = F_1(z) + \ell n\,(1 - z)\, w_{12}$$

$$w_{12} = Hu(1 - a, \tilde{q}_1; \alpha_o, \beta_o, 1, \gamma_o; 1 - z)$$

$$\delta_o = 1$$

and

$$\tilde{q}_1 = 1 - q_o$$

The function $F_1(z)$ is analytic at $z = 1$. The constants $c_{\infty 2}^{11}$ and $c_{\infty 2}^{12}$ connect the solution at $z = \infty$ to those at $z = 1$. The precise form of the function $F_1(z)$ does not concern us since only the log term will contribute to the integral.

Near $z = a$ we have

$$w(z) = c_{\infty 2}^{a1} \; w_{a1} + c_{\infty 2}^{a2} \; w_{a2} \tag{A6.35}$$

where

$$w_{a1} = F_a(z) + \ell n \left(1 - \frac{z}{a}\right) w_{a2}$$

$$w_{a2} = \left(1 - \frac{z}{a}\right) Hu\left(\frac{a - 1}{a}, \tilde{q}_a; \alpha_o + 1, \beta_o + 1, 2, \gamma_o ; 1 - \frac{z}{a}\right)$$

$$\varepsilon_o = 0$$

and

$$\alpha_o \beta_o q_o = a(\alpha_o + 1)(\beta_o + 1)(1 - \tilde{q}_a) - \gamma_o$$

The function $F_a(z)$ is analytic at $z = a$. The constants $c_{\infty 2}^{a1}$ and $c_{\infty 2}^{a2}$ connect the solution at $z = \infty$ to those at $z = a$.

The asymptotic form of the integrals in (A6.33) can now be obtained. We are only interested in leading order results since these will provide the connection we are seeking. The circular parts of the contours will not contribute as a result of the behavior of $w(z)$ near $z = 1$ and $z = a$. Near the point $z = a$ we deform the path c_{b6} so that it proceeds vertically downward. Let us take

$$z = a(1 - ix)$$

and expanding the Hankel function we obtain

$$I_{b6} \sim \frac{1}{2}\left[i\frac{\pi}{2} - \left(-i\frac{3\pi}{2}\right)\right] c_{\infty 2}^{a1} \sqrt{\frac{2}{\pi k \xi a^{1/2}}}\, e^{-i\left(ka^{1/2}\xi - \frac{1}{2}\nu\pi - \frac{\pi}{4}\right)} a^{-\nu/2}$$

$$\int_0^\infty i\, x\, e^{-\frac{\xi x}{2} ka^{\frac{1}{2}}} (-ia)dx, \quad \xi \to \infty$$

noting that $a = 1/k^2$

$$I_{b6} \sim ik^{\nu}\, c_{\infty 2}^{a1} \sqrt{\frac{2\pi}{\xi}} \left(\frac{2}{k\xi}\right)^2 e^{-i\left(\xi - \frac{1}{2}\nu\pi - \frac{\pi}{4}\right)}, \quad \xi \to \infty \tag{A6.36}$$

similarly deforming the contour c_{b5} near $z = 1$ and letting $z = 1 - ix$ we obtain

$$I_{b5} \sim c_{\infty 2}^{11} \sqrt{\frac{2\pi}{k\xi}} \left(\frac{2}{\xi}\right) e^{-i\left(k\xi - \frac{1}{2}\nu\pi - \frac{\pi}{4}\right)}, \quad \xi \to \infty \tag{A6.37}$$

we must next find the asymptotic expansion of I_{c5} and I_{c6}. To find these we must know the form of $w(ze^{i2\pi})$ in the vicinity of $z = 1$ and $z = a$. Near $z = a$ $w(ze^{i2\pi})$ signifies a counterclockwise circuit (positive sense) of $z = 0$ and $z = 1$. This is equivalent to circuits of $z = \infty$ and $z = a$ in the negative sense. Thus

$$w(ze^{i2\pi}) = e^{-i2\pi\beta_o}\left[c_{\infty 2}^{a1}\left\{w_{a1}(z) - i2\pi\, w_{a2}(z)\right\} + c_{\infty 2}^{a2}\, w_{a2}(z)\right] \tag{A6.38}$$

Near the point unity we write

$$w(ze^{i2\pi}) = \tilde{c}_{\infty 2}^{11}\; w_{11} + \tilde{c}_{\infty 2}^{12}\; w_{12} \tag{A6.39}$$

where the new constants $\tilde{c}_{\infty 2}^{11}$ and $\tilde{c}_{\infty 2}^{12}$ must be determined by making a rotation about the origin in the positive sense with (A6.34). We deform the contour I_{c6} vertically upward near $z = a$ and let $z = a(1 + ix)$

resulting in

$$I_{c6} \sim -ik^{\nu}\, c_{\infty 2}^{a1} \sqrt{\frac{2\pi}{\xi}} \left(\frac{2}{k\xi}\right)^2 e^{i\left(\xi - \frac{1}{2}n\pi - \frac{\pi}{4}\right)} e^{i\frac{\pi}{2}(\nu-n)}, \quad \xi \to \infty \tag{A6.40}$$

similarly for I_{c5} let $z = 1 + ix$ resulting in

$$I_{c5} \sim -\tilde{c}_{\infty 2}^{11} \sqrt{\frac{2\pi}{k\xi}} \left(\frac{2}{\xi}\right) e^{i\left(k\xi - \frac{1}{2}\nu\pi - \frac{\pi}{4}\right)}, \quad \xi \to \infty \tag{A6.41}$$

Therefore the asymptotic form of e is given by

$$e \sim k^{\nu-1} c_{\infty 2}^{a1} \sqrt{\frac{2\pi}{\xi}} \frac{4}{\xi} e^{i\frac{\pi}{2}(\nu-n)} \sin\left(\xi - \frac{1}{2}n\pi - \frac{\pi}{4}\right) +$$

$$+ \sqrt{\frac{2\pi k}{\xi}} \left[-\tilde{c}_{\infty 2}^{11} e^{i\left(k\xi - \frac{1}{2}\nu\pi - \frac{\pi}{4}\right)} + c_{\infty 2}^{11} e^{-i\left(k\xi - \frac{1}{2}\nu\pi - \frac{\pi}{4}\right)}\right] \tag{A6.42}$$

which furnishes the connection between the series $e_{+}^{(2)}$ and the asymptotic expansions $e_{\underline{+}}^{(3)}$ and $e_{\underline{+}}^{(4)}$. Equation (A6.42) contains three constants which represent connecting constants of solutions to Heun's equation. We have therefore determined the connection of the solutions to the modal equations in terms of the connection of solutions to Heun's equation. The connection of solution to Heun's equation has been studied previously. Using difference equation methods [41], the connecting constants can be found as the sum of factorial series [16,35].

We have thus related the connection problem of the solution $e_{\pm}^{(2)}$ to Heun's equation. The next question is how can the other solutions be constructed in the form of an integral representation such as (A6.16). The trial solution pair

$$h = \int_c \tilde{A}(\lambda)\, \xi\, J_n(\lambda\xi)\, d\lambda \tag{A6.43}$$

$$e = \int_c \tilde{B}(\lambda)\, J_n(\lambda\xi)\, d\lambda \tag{A6.44}$$

when substituted into the modal equations (A6.1) and (A6.2) results in the relation

$$(k^2 - \lambda^2)\, \tilde{B}(\lambda) = -i\beta\, \tilde{A}(\lambda) \tag{A6.45}$$

and subsequently in the equation

$$\int_c \tilde{A}(\lambda)\, L_n\, J_n(\lambda\xi)\, d\lambda = 0 \tag{A6.46}$$

where L_n is the operator

$$L_n = (\lambda^2 - 1)\frac{d^2}{d\lambda^2} + \left(3\lambda - \frac{1}{\lambda}\right)\frac{d}{d\lambda} + \frac{n^2}{\lambda^2} - \nu^2 + 1 + \frac{\beta^2}{\lambda^2 - k^2}$$

Repeated integration by parts yields

$$\int_C J_n(\lambda\xi)\, M_n\, \tilde{A}(\lambda)\, d\lambda + Q_n\,(\tilde{A}) = 0 \qquad \text{(A6.47)}$$

where M_n is the adjoint

$$M_n = (\lambda^2 - 1)\frac{d^2}{d\lambda^2} + \left(\lambda + \frac{1}{\lambda}\right)\frac{d}{d\lambda} + \frac{n^2 - 1}{\lambda^2} - \nu^2 + \frac{\beta^2}{\lambda^2 - k^2}$$

and Q_n represents the boundary terms

$$Q_n(\tilde{A}) = \left[\tilde{A}(\lambda)\left\{(\lambda^2 - 1)\frac{d}{d\lambda} + 3\lambda - \frac{1}{\lambda}\right\} J_n(\lambda\xi)\right]_C$$

$$- \left[J_n(\lambda\xi)\left\{(\lambda^2 - 1)\frac{d}{d\lambda} + 2\lambda\right\}\tilde{A}(\lambda)\right]_C$$

The integral representation (A6.43) for h will yield a solution to the modal equations if we take

$$M_n\,\tilde{A} = 0 \qquad \text{(A6.48)}$$

and choose the contour so that $Q_n(\tilde{A})$ vanishes.

By making the change of variables

$$z = \lambda^2/k^2$$

$$\tilde{A}(\lambda) = z^{(1-n)/2}\,\tilde{w}(z) \qquad \text{(A6.49)}$$

one finds that $\tilde{w}(z)$ satisfies Heun's equation (A6.10) with the parameters

$$\gamma_o = 1 - n \qquad \alpha_o = (1 - n - \nu)/2$$
$$\delta_o = 0 \qquad \beta_o = (1 - n + \nu)/2$$
$$\varepsilon_o = 1 \qquad q_o = 1 - \frac{\beta^2 a}{(1 - n)^2 - \nu^2}$$
$$a = 1/k^2$$

(Note that the differential equation (A6.10) with the above set of parameters is identical to the differential equation (A6.10) with the original set of parameters under the transformation $x = a/z$ and $x^{\alpha_o} w(x) = \tilde{w}(z)$). The solutions near $z = \infty$ (A6.14) and (A6.15) both have meaning since the exponent difference at this point is no longer an integer. The choice (A6.15) and the previously discussed contour leads to an integral representation for $h_+^{(1)}$ when $R_e(\nu) > \frac{3}{2}$. The manipulations required to extract the asymptotic expansion are the same as those previously used. The exponent difference at the origin now is an integer giving rise to log terms. But once again the integrals in the vicinity of the origin cancel.

We still must construct the remaining two solutions. Furthermore, we need to extend the above solutions to cover the cases $0 < R_e(\nu) \leq \frac{3}{2}$ and $n = 1$. If we look back at the identity (A6.20) we find a clue useful in achieving these two goals. The right hand side of (A6.20) is an entire function of μ and ν. But the integral on the left only converges

for $\mathrm{Re}(\mu - \nu - 1) < \frac{1}{2}$. Can we generalize the integral on the left, so that it remains valid regardless of the values of μ and ν, but coincides with this integral when $\mathrm{Re}(\mu - \nu - 1) < \frac{1}{2}$? Let us define

$$I = \int_C \lambda^{\mu-\nu-1} J_\nu(\lambda)\, d\lambda \tag{A6.50}$$

Now we write

$$I = \int_{C_1} \lambda^{\mu-\nu-1} J_\nu(\lambda)\, d\lambda + \frac{1}{2}\int_{C_2} \lambda^{\mu-\nu-1} H_\nu^{(1)}(\lambda)\, d\lambda +$$

$$+ \frac{1}{2}\int_{C_3} \lambda^{\mu-\nu-1} H_\nu^{(2)}(\lambda)\, d\lambda + \frac{e^{i\pi\nu}}{2}\int_{C_4} H_\nu^{(1)}(\lambda e^{-i\pi})\, \lambda^{\mu-\nu-1}\, d\lambda +$$

$$+ \frac{e^{i\pi\nu}}{2}\int_{C_5} H_\nu^{(2)}(\lambda e^{-i\pi})\, \lambda^{\mu-\nu-1}\, d\lambda \tag{A6.51}$$

where the contours are as shown in Fig. 25. When the condition $\mathrm{Re}\,(\mu - \nu - 1) < \frac{1}{2}$ is satisfied the contours C_2 and C_3 can be deformed to the positive real axis and the contours C_4 and C_5 can be deformed to the negative real axis. Thus the quantity I in (A6.51) becomes that in (A6.50). However, the integrals (A6.51) remain convergent regardless of the values of μ and ν and are equal to the right hand side of (A6.20). This generalization can now be used on the integral representations (A6.4) and (A6.43). The boundary terms $Q_\nu(B)$ or $Q_n(\tilde{A})$ will now vanish regardless of the values of n or ν. In terms of this generalized definition we may also make use of the other linearly independent solution

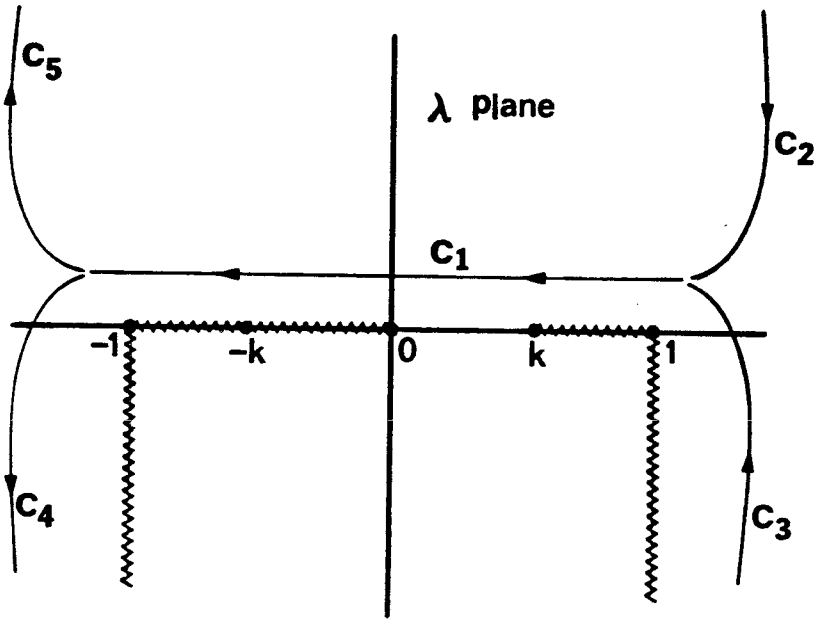

Fig. 25. Contours for the generalized definition of the Hankel transform.

of Heun's equation at $z = \infty$. For example, use of the solution (A6.14) in the integrand of (A6.43) yields an integral representation for $\underline{h}^{(1)}$. Use of the log solution at infinity in the integrand (A6.4) yields an integral representation for $\underline{e}^{(2)}$. The latter case involves the integration of a logarithm, times a power, times a Bessel function, which can be handled by differentiating the identity (A6.20) or its extended definition (A6.51) with respect to μ.

APPENDIX 7

Bessel Function Solutions to Inhomogeneous Modal Equations

The solutions

$$W = \begin{pmatrix} \sqrt{\frac{\mu_o}{\varepsilon_o}}\, x_1 J_n(\gamma_1 \rho) & y_1 J_n(\gamma_1 \rho) \\ \sqrt{\frac{\mu_o}{\varepsilon_o}}\, x_2 J_n(\gamma_2 \rho) & y_2 J_n(\gamma_2 \rho) \end{pmatrix} \tag{A7.1}$$

$$V = \begin{pmatrix} \sqrt{\frac{\mu_o}{\varepsilon_o}}\, x_1 H_n^{(1)}(\gamma_1 \rho) & y_1 H_n^{(1)}(\gamma_1 \rho) \\ \sqrt{\frac{\mu_o}{\varepsilon_o}}\, x_2 H_n^{(1)}(\gamma_2 \rho) & y_2 H_n^{(1)}(\gamma_2 \rho) \end{pmatrix} \tag{A7.2}$$

introduced in section 6C have two drawbacks. First it is possible under certain circumstances for γ_1 to become equal to γ_2 at a certain position in the dielectric profile. The solutions represented by each row of W (or V) become identical in such a situation. Second if γ_1 or γ_2 should vanish at a given position, the solution V becomes singular. Both problems occur due to the fact that the actual solutions of the modal equations no longer have the form (A7.1) and (A7.2).

The following solutions were used instead

$$W = \frac{\gamma_o^n}{1 - xy}\begin{pmatrix} \sqrt{\frac{\mu_o}{\varepsilon_o}}(\gamma_1^{-n} J_n(\gamma_1\rho) - xy\,\gamma_2^{-n} J_n(\gamma_2\rho)) & y(\gamma_1^{-n} J_n(\gamma_1\rho) - \gamma_2^{-n} J_n(\gamma_2\rho)) \\ \sqrt{\frac{\mu_o}{\varepsilon_o}}\, x(\gamma_2^{-n} J_n(\gamma_2\rho) - \gamma_1^{-n} J_n(\gamma_1\rho)) & \gamma_2^{-n} J_n(\gamma_2\rho) - xy\,\gamma_2^{-n} J_n(\gamma_1\rho) \end{pmatrix} \tag{A7.3}$$

$$V = \frac{\gamma_o^{-n}}{1 - xy}\begin{pmatrix} \sqrt{\frac{\mu_o}{\varepsilon_o}}(\gamma_1^{n} H_n(\gamma_1\rho) - xy\,\gamma_2^{n} H_n(\gamma_2\rho)) & y(\gamma_1^{n} H_n^{(1)}(\gamma_1\rho) - \gamma_2^{n} H_n^{(1)}(\gamma_2\rho)) \\ \sqrt{\frac{\mu_o}{\varepsilon_o}}\, x(\gamma_2^{n} H_n^{(1)}(\gamma_2\rho) - \gamma_1^{n} H_n^{(1)}(\gamma_1\rho)) & \gamma_2^{n} H_n^{(1)}(\gamma_2\rho) - xy\,\gamma_1^{n} H_n^{(1)}(\gamma_1\rho) \end{pmatrix} \tag{A7.4}$$

where $(\hat{k}_1^2 - \gamma_1^2) = i\hat{\beta}_1 y$

$(\hat{k}_2^2 - \gamma_2^2) = i\hat{\beta}_2 x$

and γ_o = external medium wave number.

The limiting forms of (A7.3) and (A7.4) in both the cases $\gamma_1 \to \gamma_2$ and (γ_1 or γ_2) $\to 0$ are well behaved solutions of the modal equations. Furthermore, when the medium becomes homogeneous and isotropic (and let us take $\gamma_1 = \gamma_2 = \gamma_o$) (A7.3) and (A7.4) reduce to

$$W = \begin{pmatrix} \sqrt{\frac{\mu_o}{\varepsilon_o}}\, J_n(\gamma_o \rho) & 0 \\ 0 & J_n(\gamma_o \rho) \end{pmatrix} \tag{A7.5}$$

$$V = \begin{pmatrix} \sqrt{\frac{\mu_o}{\varepsilon_o}}\, H_n^{(1)}(\gamma_o \rho) & 0 \\ 0 & H_n^{(1)}(\gamma_o \rho) \end{pmatrix} \tag{A7.6}$$

which match the external solutions as desired. We note that in terms of the incident and scattered solutions (A7.3) and (A7.4) it is not clear that R will remain a bounded quantity. This is the case since spontaneous singularities may occur in a Riccati equation. However in the event that R becomes large we may switch to R^{-1}, which also satisfies a Riccati equation, and continue the numerical integration.

REFERENCES

1. Budden, K. G., Radio Waves in the Ionosphere, Cambridge University Press, London (1961).
2. Ginzburg, V. L., The Propagation of Electromagnetic Waves in Plasmas, Pergamon Press, Oxford (1970).
3. Platzman, P. M. and H. T. Ozaki, "Scattering of Electromagnetic Waves from an Infinitely Long Magnetized Cylindrical Plasma," Journal of Applied Physics, 31 (9), 1597-1601 (1960).
4. Nagelburg, E. R., "Microwave Interaction with Bounded Gyroelectric Plasmas," Caltech Antenna Lab Report No. 31 (1964).
5. Yeh, C. and W. V. T. Rusch, "Interaction of Microwaves with an Inhomogeneous and Anisotropic Plasma Column," Journal of Applied Physics, 36 (7), 2302-2306 (1965).
6. Westcott, B. S., "Exact Solutions for Transverse Electromagnetic Wave Propagation in a Cylindrically Stratified Axially Magnetized Plasma," Proc. Camb. Phil. Soc., 66, 129-143 (1969).
7. Papas, C. H., Theory of Electromagnetic Wave Propagation, Chapter 6, McGraw Hill, New York (1965).
8. Erdelyi, A., et al, Bateman Manuscript Project: Higher Transcendental Functions, Volume III, Section 15.3, McGraw-Hill, New York (1955).
9. Van Duin, C. A. and P. W. Sluijter, "Refractive Index Profiles with a Local Resonance Based on Heun's Equation," Radio Science, 15 (1), 95-103 (1980).
10. Arscott, F. M., Periodic Differential Equations, Chapter 8, Macmillan, New York (1964).

11. Nordgard, J. D., "A Martian Entry Propagation Study," Radio Science, 11 (11), 947-957 (1976).

12. Uman, M. A., Lightning, McGraw-Hill, New York (1969).

13. Krall, N. A. and A. W. Trivelpiece, Principles of Plasma Physics, McGraw-Hill, New York (1973).

14. Bellman, R. and G. M. Wing, An Introduction to Invariant Imbedding, Wiley, New York (1975).

15. Latham, R. W., "Electromagnetic Scattering from Cylindrically and Spherically Stratified Bodies," Caltech Antenna Lab Report No. 42 (1967).

16. Sleeman, B. D., "Integral Representations for Solutions of Heun's Equation," Proc. Camb. Phil. Soc. 65, 447-459 (1969).

17. Morse, P. M. and H. Feshbach, Methods of Theoretical Physics: Part 1, Chapter 5, McGraw-Hill, New York (1953).

18. Dingle, R. B., Asymptotic Expansions: Their Derivation and Interpretation, Chapter 1, Academic Press, New York (1973).

19. Bender, C. M. and S. A. Orszag, Advanced Mathematical Methods for Scientists and Engineers, Chapter 10, McGraw-Hill, New York (1978).

20. Olver, F. W. J., Asymptotics and Special Functions, Chapters 7, 10, 11, 12, Academic Press, New York (1974).

21. Felson, L. B. and N. Marcuvitz, Radiation and Scattering of Waves, Section 3.5, Prentice Hall, Englewood Cliffs (1973).

22. Abromowitz, M. and I. A. Stegun, Handbook of Mathematical Functions, Dover, New York (1972).

23. Brekhovskikh, L. M., Waves in Layered Media, 229-230, Academic Press, New York (1960).

24. Chen, F. F., Plasma Physics, Section 4.9, Plenum Press, New York (1974).

25. Chen, H. C., Theory of Electromagnetic Waves: A Coordinate Free Approach, Section 2.6, McGraw-Hill, New York (1983).

26. Meixner, J., "The Behavior of Electromagnetic Fields at Edges," IEEE Trans. Antennas and Prop., AP-20 (4), 442-446 (1972).

27. Felson, L. B., op. cit. Section 7.4.

28. Hurd, R. A., "The Edge Condition in Electromagnetics," IEEE Trans. Antennas and Prop., AP-24 (1), 70-73 (1976).

29. Von Hippel, A. R., Dielectric Materials and Applications, Wiley, New York (1954).

30. Hurd, R. A., "On the Possibility of Intrinsic Loss Occurring at the Edges of Ferrites," Canadian J. of Phys., 40, 1067-1076 (1962).

31. Hurd, R. A., "Intrinsic Loss at the Edges of Anisotropic Plasmas," Canadian J. of Phys., 41, 1554-1562 (1963).

32. Lee, S. W. and R. Mittra, "Edge Condition and Intrinsic Loss in Uniaxial Plasma," Canadian J. of Phys., 46, 111-120 (1968).

33. Ince, E. L., Ordinary Differential Equations, Chapter 16, Dover, New York (1956).

34. Bender, C., op. cit. Chapter 3.

35. Ford, W. B., The Asymptotic Developments of Functions Defined by Maclaurin Series, Chelsea, New York (1960).

36. Van Bladel, J., Electromagnetic Fields, Section 8.7, McGraw-Hill, New York (1964).

37. Watson, G. N., "Asymptotic Expansions of Hypergeometric Functions," Trans. Cambridge Phil. Soc., 22, 277-308 (1918).

38. Adams, M. J., An Introduction to Optical Wave Guides, Section 5.2, Wiley, New York (1981).

39. Nayfeh, A. H., Introduction to Perturbation Techniques, Section 14.6, Wiley, New York (1981).

40. Watson, G. N., A Treatise on the Theory of Bessel Functions, 24, 25, 391-392, Cambridge University Press (1966).

41. Milne-Thomson, L. M., The Calculus of Finite Differences, Chapter 15, Chelsea, New York (1981).